

Copyright Warning & Restrictions

The copyright law of the United States (Title 17, United States Code) governs the making of photocopies or other reproductions of copyrighted material.

Under certain conditions specified in the law, libraries and archives are authorized to furnish a photocopy or other reproduction. One of these specified conditions is that the photocopy or reproduction is not to be “used for any purpose other than private study, scholarship, or research.” If a user makes a request for, or later uses, a photocopy or reproduction for purposes in excess of “fair use” that user may be liable for copyright infringement,

This institution reserves the right to refuse to accept a copying order if, in its judgment, fulfillment of the order would involve violation of copyright law.

Please Note: The author retains the copyright while the New Jersey Institute of Technology reserves the right to distribute this thesis or dissertation

Printing note: If you do not wish to print this page, then select “Pages from: first page # to: last page #” on the print dialog screen

The Van Houten library has removed some of the personal information and all signatures from the approval page and biographical sketches of theses and dissertations in order to protect the identity of NJIT graduates and faculty.

INFORMATION TO USERS

This dissertation was produced from a microfilm copy of the original document. While the most advanced technological means to photograph and reproduce this document have been used, the quality is heavily dependent upon the quality of the original submitted.

The following explanation of techniques is provided to help you understand markings or patterns which may appear on this reproduction.

1. The sign or "target" for pages apparently lacking from the document photographed is "Missing Page(s)". If it was possible to obtain the missing page(s) or section, they are spliced into the film along with adjacent pages. This may have necessitated cutting thru an image and duplicating adjacent pages to insure you complete continuity.
2. When an image on the film is obliterated with a large round black mark, it is an indication that the photographer suspected that the copy may have moved during exposure and thus cause a blurred image. You will find a good image of the page in the adjacent frame.
3. When a map, drawing or chart, etc., was part of the material being photographed the photographer followed a definite method in "sectioning" the material. It is customary to begin photoing at the upper left hand corner of a large sheet and to continue photoing from left to right in equal sections with a small overlap. If necessary, sectioning is continued again — beginning below the first row and continuing on until complete.
4. The majority of users indicate that the textual content is of greatest value, however, a somewhat higher quality reproduction could be made from "photographs" if essential to the understanding of the dissertation. Silver prints of "photographs" may be ordered at additional charge by writing the Order Department, giving the catalog number, title, author and specific pages you wish reproduced.

University Microfilms

300 North Zeeb Road
Ann Arbor, Michigan 48106
A Xerox Education Company

72-26,334

KOKTA, Milan R., 1941-
STRUCTURE AND MAGNETIC PROPERTIES OF RARE EARTH
GARNETS.

Newark College of Engineering, D.Eng.Sc., 1972
Engineering, chemical

University Microfilms, A XEROX Company, Ann Arbor, Michigan

PLEASE NOTE:

Some pages may have
indistinct print.

Filmed as received.

University Microfilms, A Xerox Education Company

STRUCTURE AND MAGNETIC PROPERTIES OF RARE EARTH GARNETS

BY

MILAN R. KOKTA

A DISSERTATION

PRESENTED IN PARTIAL FULFILLMENT

OF THE REQUIREMENTS FOR THE DEGREE

OF

DOCTOR OF ENGINEERING SCIENCE

AT

NEWARK COLLEGE OF ENGINEERING

This thesis is to be used only with due regard to the rights of the author(s). Bibliographical references may be noted, but passages must not be copied without permission of the College and without credit being given in subsequent written or published work.

NEWARK, N.J.
1972

APPROVAL OF DISSERTATION
STRUCTURE AND MAGNETIC PROPERTIES
OF RARE EARTH GARNETS

BY

MILAN KOKTA

FOR

DEPARTMENT OF CHEMICAL ENGINEERING
NEWARK COLLEGE OF ENGINEERING

BY

FACULTY COMMITTEE

APPROVED:

CHAIRMAN

NEWARK, NEW JERSEY

PREFACE

The project which is the subject of this work originated in the laboratory of Prof. L. Suchow at Newark College of Engineering from preliminary experiments of Prof. L. Suchow and V. Flynn in 1968. The author started his experimental work in January, 1969, and completed it in October, 1971. Some additional data were obtained in the laboratory of Prof. A. Wold at Brown University, Providence, R.I., and at Bell Telephone Laboratories, Murray Hill, N.J., as mentioned in the text. This work has been supported by National Science Foundation Grants GP-7100 and GP-11527.

The author wishes to express great appreciation for all kinds of help, valuable advice, and kind supervision received from Prof. L. Suchow, PhD, during the years of work.

The author also wishes to thank Dean A. Bedrosian and the staff of the Graduate Division of NCE for financial support and help with which he was provided, and acknowledge the cooperation of Prof. A. Wold and Messrs. J. De Luca, T. Catalano and H. Nahagian at Brown University, and Mr. R. C. Sherwood at Bell Telephone Laboratories.

ABSTRACT

This study deals with preparation and magnetic properties of garnet compounds containing rare earth ions and scandium ions on two crystallographic sites: the dodecahedral and the octahedral. A number of compounds of the types $\{R_{3-y}r_y\} [r_x \text{ Ga}_{2-x}] (\text{Ga}_3) \text{O}_{12}$, $\{R_3\} [\text{Sc}_2] (\text{Fe}_z \text{ Ga}_{3-z}) \text{O}_{12}$, $\{R_{3-y} \text{ Sc}_y\} [\text{Sc}_2] (\text{Fe}_3) \text{O}_{12}$, and $\{R_{3-y} r_y\} [r_2] (\text{Fe}_z \text{ Ga}_{3-z}) \text{O}_{12}$, where R stands for large rare earth ions such as Nd^{3+} and Pr^{3+} , r stands for small rare earth ions such as Lu^{3+} , Yb^{3+} , Tm^{3+} , Er^{3+} , Ho^{3+} , and Dy^{3+} , was prepared. Distribution of rare earth ions was studied in rare earth gallium garnets in order to determine limits of existence of gallium garnets with both dodecahedral and octahedral sites fully occupied by rare earth ions. Attempts were made to replace tetrahedrally coordinated gallium in such compounds by trivalent iron ions. In addition, attempts were made to prepare rare earth iron garnet compounds with iron fully replaced by scandium on the octahedral sites.

All preparations were made by solid state reactions among oxides of pertinent ions at elevated temperatures. The results of reactions were checked by X-ray diffraction. Compositions of reactant mixtures were varied until single phase compounds were obtained. Single phase compounds were subjected to magnetic measurements. Magnetic susceptibilities as functions of temperature were measured with a Faraday apparatus, and Curie constants were calculated and compared with theoretical values.

In studies of ionic distribution, it has been found that the placement of large rare earth ions such as Nd^{3+} or Pr^{3+} on the dodecahedral sites opens up the lattice so that small rare earth ions may enter the octahedral sites. For cases where the small rare earth was Lu, single phase garnets $\left\{ \text{R}_3 \right\} \left[\text{r}_2 \right] \left(\text{Ga}_3 \right) \text{O}_{12}$ were prepared. To prepare single phase compounds with r ions larger than Lu^{3+} , it was necessary to place simultaneously determined minimum amounts of r in the dodecahedral positions according to the general formula $\left\{ \text{R}_{3-y} \quad \text{r}_y \right\} \left[\text{r}_2 \right] \left(\text{Ga}_3 \right) \text{O}_{12}$. Required minimum value of y increases as the difference in ionic radii of ions occupying the dodecahedral and the octahedral sites decreases. Trends found in iron systems were consistent with these findings. The results of magnetic measurements indicate paramagnetic behavior for all garnets which do not contain iron ions. Results of measurements on garnet compounds where the tetrahedral sites contain iron at least to some extent show more complicated magnetic behavior where ferrimagnetic interactions are more likely to be expected.

IV

TABLE OF CONTENTS

	Page
I INTRODUCTION	1
1.1 Classification of Solid Substances	1
1.2 Classification of Magnetic Properties	3
1.3 The Garnet Structure	5
1.4 Synthetic Garnets	11
1.4.1 Silicate Garnets	11
1.4.2 Garnate Garnets	12
1.4.3 Garnets of the Type $\left\{ \text{Rare Earth}_3 \right\} \text{Me}_5 \text{O}_{12}$	14
1.5 Ferrimagnetic Garnets	15
1.5.1 Yttrium Iron Garnet, YIG	15
1.5.2 Magnetic Properties of Substituted YIG	17
1.5.3 Other than Octahedral - Tetrahedral Ion Interaction in the Garnet Structure	20
1.5.3.1 Direct c - a Interactions	20
1.5.3.2 Direct c - d Interactions	21
1.5.4 Rare Earth Iron Garnets	22
1.5.4.1 Ferrimagnetic Interactions in Rare Earth Garnets .	22
II EXPERIMENTAL STUDIES	27
II.1 Objectives	27
II.2 Experimental Approach	28
II.3 Preparations	29
II.4 X-Ray Diffraction Studies	29
II.5 Magnetic Measurements	31
III GARNET COMPOUNDS PREPARED	33
III.1 Gallium Garnets with Rare Earth on Both Octahedral and Dodecahedral Sites	33
III.1.1 Neodymium Systems	34
III.1.1.1 Preparation Conditions	34
III.1.1.2 Results	34
III.1.1.3 Discussion of Results	38

TABLE OF CONTENTS (Continued)

	Page	
III.1.2	Preseodymium Systems	51
III.1.2.1	Preparations	52
III.1.2.2	Results	52
III.1.2.3	Discussion of Results	54
III.2	Rare Earth Iron Garnet with the Octahedral Sites Completely Filled with Non-Magnetic Ions	62
III.2.1.1	Preparations	63
III.2.2.1	Gd - Sc Iron Garnet	63
III.2.2.2	Results	63
III.2.3	Related Compounds of General Formula $\left\{ R_{3-y} Sc_y \right\}$ $[Sc_2] (Fe_3) O_{12}$	66
III.2.4	Systems with Large Rare Earth on the Dodecahedral Sites	68
III.2.4.1	Neodymium Scandium Iron Garnet	69
III.2.4.2	Praseodymium Scandium Iron Garnet	70
III.2.4.3	Discussion of Results	70
III.3	Garnets with Rare Earth on the Octahedral and Dodecahedral Sites Containing Fe Ions on the Tetrahedral Sites	72
III.4	Garnet Compounds with Trivalent Vanadium	74
III.4.1	Substitution of V^{3+} in Iron Garnets	75
III.4.1.2	Preparation	75
III.4.1.3	Results and Discussion	75
III.4.2	Substitution of V^{3+} in Gallium Garnets	76
III.4.2.1	Preparation	76
III.4.2.2	Results and Discussion	77
IV	LATTICE CONSTANT CALCULATIONS	79
IV.1	Analytical Calculations	79
IV.2	Empirical Calculations	84
V	RESULTS OF MAGNETIC MEASUREMENTS	89
V.1	Preliminary Measurements	89
V.2	Measurements on Neodymium - Small Rare Earth Gallium Garnets	94

VI

TABLE OF CONTENTS (Continued)

	Page
V.3	Measurements on Praseodymium - Small Rare Earth Garnet Compounds 101
V.4	Magnetic Measurements on Iron - Containing Garnets 106
V.4.1	Magnetic Behavior of the Compounds $\left\{ \begin{matrix} R_{3-y} & Sc_y \end{matrix} \right\}$ $[Sc_2] (Fe_3) O_{12}$ 106
V.4.2	Magnetic Measurements on System $\left\{ R_3 \right\} [Sc_2]$ $(Ga_{3-z} Fe_z) O_{12}$ 107
V.4.3	Magnetic Measurements on Garnets $\left\{ \begin{matrix} Nd_{3-y} & Yb_y \end{matrix} \right\} [Yb_2]$ $(Ga_{3-z} Fe_z) O_{12}$ 110
VI	CRITICAL EVALUATIONS AND RECOMMENDATIONS 114
VI.1	Compounds with Rare Earth Ions on Both Dodecahedral and Octahedral Sites 114
VI.2	Compounds with Non-Magnetic Ions on the Octahedral Sites 115
VI.3	Garnet Compounds with Rare Earth on the Dodecahedral and Octahedral Sites and with Iron on the Tetrahedral Site. 115

VII

LIST OF FIGURES

FIGURES		PAGES
I.1	The Surroundings of an Oxygen Ion in Grossularite	7
I.2	Arrangement of Cations in c, a and d Sites in Four Octants of the Garnet Unit Cell	9
I.3	Magnetisation vs Composition x in $\{Y_x\} [Sc_x Fe_{2-x}] (Fe_3)_{012}$ and $\{Y_{3-2x} Ca_{2x}\} [Sb_x Fe_{2-x}] (Fe_3)_{012}$	19
I.4	Spontaneous magnetisation in Bohr Magnetons per Formula Unit vs Temperature of Tm, Yb and Lu Iron Garnets	23
I.5	Spontaneous Magnetization in Bohr Magnetons per Formula Unit vs Temperature of Gd, Tb, Dy, Ho and Er Iron Garnets	24
III.1	Lattice Constants vs y for $\{Nd_{3-y} Yb_y\} [Ga_2] (Ga_3)_{012}$	39
III.2	Lattice Constants vs Nominal x for Nominal $\{Nd_3\} [R_x Ga_{2-x}] (Ga_3)_{012}$ and vs Nominal y for Nominal $\{Nd_{3-y} R_y\} [R_2] (Ga_3)_{012}$	40
III.3	Lattice Constants vs Nominal x with Several Values of Nominal y for $\{Nd_{3-y} Yb_y\} [Yb_x Ga_{2-x}] (Ga_3)_{012}$	45
III.4	Lattice vs x for $\{Nd_{3-y} R_y\} [R_x Ga_{2-x}] (Ga_3)_{012}$	48
III.5	-y values Required to Yield Single-phase Garnets and Straight Lines in Fig. 4 vs Ionic Radii of Trivalent Rare Earth R	49
III.6	The Ternary System $Nd_2 O_3 - Ga_2 O_3 - Yb_2 O_3$	50
III.7	Lattice Constants vs Nominal x for Nominal $\{Pr_3\} [R_x Ga_{2-x}] (Ga_3)_{012}$	55
III.8	Lattice Constants vs Nominal x with Several Values of Nominal y for $\{Pr_{3-y} Yb_y\} [Yb_x Ga_{2-x}] (Ga_3)_{012}$	56
III.9	Lattice Constants Versus x for $\{Pr_{3-y} R_y\} [R_x Ga_{2-x}] (Ga_3)_{012}$	60
III.10	- y - Values Required to Yield Single-phase Garnets and Straight Lines in Fig. 9 (and Fig. 4) vs Ionic Radii of Trivalent Rare Earth, R	61
III.11	Lattice Constant vs x Nominal for Systems $\{Gd_3\} [Sc_x Fe_{2-x}] (Fe_3)_{012}$ and $\{Gd_{2.5} Sc_{0.5}\} [Sc_x Fe_{2-x}] (Fe_3)_{012}$	65
IV.1	Detail of Garnet Structure Along [001] Direction	

VIII

LIST OF FIGURES (Continued)

FIGURES		PAGE
V.1	Reciprocal Molar Susceptibilities vs Absolute Temperature for Garnet Compounds with Trivalent Rare Earth Ions on Either Dodecahedral or Octahedral Sites.	91
V.2	Reciprocal Molar Susceptibilities vs Absolute Temperature for Garnet Compounds and Solid Solutions with Trivalent Rare Earth Ions on Either Dodecahedral or Octahedral Sites.	92
V.3	Reciprocal Molar Susceptibilities vs Absolute Temperature for Garnets with Trivalent Rare Earth Ions on Both Dodecahedral and Octahedral Sites (R = Yb)	96
V.4	Reciprocal Molar Susceptibility vs Absolute Temperature for Garnets with Trivalent Rare Earth Ions on Both Dodecahedral and Octahedral Sites (R=Tm)	97
V.5	Reciprocal Molar Susceptibilities vs Absolute Temperature for Garnets with Trivalent Rare Earth Ions on both Dodecahedral and Octahedral Sites (R=Er, Ho, Dy)	98
V.6	Reciprocal Molar Susceptibilities vs Absolute Temperature for Pr Garnets with Rare Earth Ions on Both Dodecahedral and Octahedral Sites (R = Yb)	102
V.7	Reciprocal Molar Susceptibilities vs Absolute Temperature for Pr Garnets with Rare Earth Ions on Both Dodecahedral and Octahedral Sites (R = Tm)	103
V.8	Reciprocal Molar Susceptibilities vs Absolute Temperature for Pr Garnets with Rare Earth Ions on Both Dodecahedral and Octahedral Sites R = Er	104
V.9	Reciprocal Molar Susceptibilities vs Absolute Temperature for Garnets $\{R_{3-y} Sc_y\} [Sc_2] (Fe_3) O_{12}$ R = Gd, Dy, Ho, Er and Tm	108
V.10	Molar Susceptibilities χ_M vs Absolute Temperature for Garnets $\{R_{3-y} Sc_y\} [Sc_2] (Fe_3) O_{12}$ R = Gd, Dy, Ho, Er and Tm	109
V.11	Reciprocal Molar Susceptibilities vs Absolute Temperature for Garnets $\{R_3\} [Sc_2] (Fe_z Ga_{3-z}) O_{12}$ R = Nd, Pr	111
V.12	Reciprocal Molar Susceptibilities vs Absolute Temperature for Garnets $\{Nd_{3-y} Yb_y\} [Yb_2] (Fe_z Ga_{3-z}) O_{12}$	113

IX

LIST OF TABLES

TABLE		PAGE
I.1	Crystalline Structures Yielding Magnetic Materials	3
I.2	Description of Garnet Structure	6
I.3	End Member Silicate Garnets	12
I.4	End Member Germanate Garnets	13
I.5	Lattice Constants of Rare Earth Garnets	14 & 15
I.6	Magnetic and Crystallographic Properties of Garnets	26
II.1	Indexed X-Ray Pattern of $\text{Nd}_3 \text{Ga}_5 \text{O}_{12}$	30 & 31
III.1	System $\{ \text{Nd}_{3-y} \text{Yb}_y \} [\text{Yb}_x \text{Ga}_{2-x}] (\text{Ga}_3)_0_{12}$	35
III.2	System $\{ \text{Nd}_3 \} [\text{Lu}_x \text{Ga}_{2-x}] (\text{Ga}_3)_0_{12}$	35
III.3	System $\{ \text{Nd}_{3-y} \text{Tm}_y \} [\text{Tm}_x \text{Ga}_{2-x}] (\text{Ga}_3)_0_{12}$	36
III.4	System $\{ \text{Nd}_{3-y} \text{Er}_y \} [\text{Er}_x \text{Ga}_{2-x}] (\text{Ga}_3)_0_{12}$	36
III.5	System $\{ \text{Nd}_{3-y} \text{Ho}_y \} [\text{Ho}_x \text{Ga}_{2-x}] (\text{Ga}_3)_0_{12}$	37
III.6	System $\{ \text{Nd}_{3-y} \text{Dy}_y \} [\text{Dy}_x \text{Ga}_{2-x}] (\text{Ga}_3)_0_{12}$	37
III.7	System $\{ \text{Nd}_{3-y} \text{Yb}_y \} [\text{Ga}_2] (\text{Ga}_3)_0_{12}$	38
III.8	System $\{ \text{Nd}_{2.8} \text{Yb}_{0.2} \} [\text{Yb}_x \text{Ga}_{2-x}] (\text{Ga}_3)_0_{12}$	43
III.9	System $\{ \text{Nd}_{2.7} \text{Yb}_{0.3} \} [\text{Yb}_x \text{Ga}_{2-x}] (\text{Ga}_3)_0_{12}$	43
III.10	System $\{ \text{Nd}_{2.4} \text{Yb}_{0.6} \} [\text{Tm}_x \text{Ga}_{2-x}] (\text{Ga}_3)_0_{12}$	46
III.11	System $\{ \text{Nd}_{1.9} \text{Er}_{1.1} \} [\text{Er}_x \text{Ga}_{2-x}] (\text{Ga}_3)_0_{12}$	46
III.12	System $\{ \text{Pr}_3 \} [\text{Yb}_x \text{Ga}_{2-x}] (\text{Ga}_3)_0_{12}$	53
III.13	System $\{ \text{Pr}_3 \} [\text{Tm}_x \text{Ga}_{2-x}] (\text{Ga}_3)_0_{12}$	53
III.14	System $\{ \text{Pr}_3 \} [\text{Er}_x \text{Ga}_{2-x}] (\text{Ga}_3)_0_{12}$	54
III.15	System $\{ \text{Pr}_{2.8} \text{Yb}_{0.2} \} [\text{Yb}_x \text{Ga}_{2-x}] (\text{Ga}_3)_0_{12}$	57
III.16	System $\{ \text{Pr}_{2.5} \text{Yb}_{0.5} \} [\text{Yb}_x \text{Ga}_{2-x}] (\text{Ga}_3)_0_{12}$	57
III.17	System $\{ \text{Pr}_{2.2} \text{Tm}_{0.8} \} [\text{Tm}_x \text{Ga}_{2-x}] (\text{Ga}_3)_0_{12}$	58
III.18	System $\{ \text{Pr}_{1.85} \text{Er}_{1.15} \} [\text{Er}_x \text{Ga}_{2-x}] (\text{Ga}_3)_0_{12}$	58
III.19	Calculated average radii for dodecahedral site containing Nd^{3+} or Pr^{3+} and minimum y value amounts of small rare earth R.	62
III.20	System $\{ \text{Gd}_3 \} [\text{Sc}_x \text{Fe}_{2-x}] (\text{Fe}_3)_0_{12}$	64
III.21	System $\{ \text{Gd}_{2.5} \text{Sc}_{0.5} \} [\text{Sc}_x \text{Fe}_{2-x}] (\text{Fe}_3)_0_{12}$	66
III.22	Compounds $\{ \text{R}_{3-y} \text{Sc}_y \} [\text{Sc}_2] (\text{Fe}_3)_0_{12}$ R = Tm, Er, Ho, and Dy	67

X

LIST OF TABLES (Continued)

TABLES		PAGES
III.23		71
III.24	System $\{ \text{Nd}_{3-y} \text{Yb}_y \} [\text{Yb}_2] (\text{Ga}_{3-z} \text{Fe}_z) \text{O}_{12}$	74
III.25	Experimental and Calculated Lattice Constants of Vanadium Substituted Rare Earth Gallium Garnets	77
IV.1	The Length of d_{80} of for Rare Earth Gallium Garnets	82
IV.2	Calculated and Experimental Values of Lattice Constants of Rare Earth Gallium Garnets	83
IV.3	Observed and Calculated Lattice Constants of Neodymium-Gallium Garnets	86
IV.4	Observed and Calculated Lattice Constants of Some Other Rare Earth Gallium Garnets.	87
IV.5	Observed and Calculated Lattice Constants of Praseodymium Gallium Garnets	88
V.1	Experimental and Calculated Molar Curie Constants (C_M) of Garnets with Trivalent Rare Earth Ions on Either Dodecahedral or Octahedral Sites	93
V.2	Individual Gram-Atom Curie Constants (C_{ind})	94
V.3	Experimental and Calculated Molar Curie Constants of Garnets with Two Rare Earth Ions on Dodecahedral Sites and Ga and/or Rare Earth Ions on Octahedral Sites	99
V.4	Experimental and Calculated Molar Curie Constants of Pr Small Rare Earth Garnet Solid Solutions	105
V.5	Experimental and Theoretical Curie Constants and Weiss Constants Obtained by Extrapolation of $1/X_m$	110
V.6	Experimental, Theoretical, and Weiss Constants for Garnet Compounds $\{ \text{Nd}_{3-y} \text{Yb}_y \} [\text{Yb}_2] (\text{Ga}_{3-z} \text{Fe}_z) \text{O}_{12}$	112

I. INTRODUCTION

I.1 Classification of Solid Substances

Solids in crystalline form can be simply classified on the basis of the symmetries of their crystal structures. In the case of an ideal crystal without any defects which would be formed by the repetition of the basic cell of atoms or ions, there always exist points and directions which are equivalent. Symmetry operations which transform points or directions, and by so doing the crystal is transformed into itself, define the "space group" of a crystal. There exist 230 such groups for classification of crystals.

Very often, physical properties of the crystal are related to definite directions in the crystals. Using symmetry elements excluding translations, symmetry "point groups" which define 32 crystallographic classes are developed. Determination of the crystallographic class and assignment of one of the 230 space groups to the crystal is of basic importance because it allows a systematic classification of solid matters and it creates a defined system of them (1).

When the atoms or ions in the crystal possess a magnetic moment and when these moments are ordered in some definite manner, the magnetic structure of such a crystal can be defined (2). The periodicity of the magnetic structure generally may not be the same as the periodicity of the crystal lattice, and therefore the crystallographic and magnetic unit cells may or may not be identical. By analogy with the crystallographic structure, the magnetic structure also has

symmetry elements which form a group. However, due to the vector character of the magnetic moment, the number of possible symmetry elements of magnetic structures is much greater than in case of crystallographic structures. The great number of symmetry elements leads to a greater number of possible "magnetic groups", 1651 in all (3).

Such a large number of groups is hardly practical for use in classification. It is more practical to base the classification of solids on physical properties, such as type of bonding, electric or magnetic properties, even if it is too broad and inaccurate. The combination of the second way of classification of solids with crystal structure classification gives grounds for analyses of physical properties with regard to symmetry and the crystal structure type in any particular case.

As an example of this approach, extensive studies conducted on magnetic oxides can be cited here. Some collective phenomena such as ferri, antiferri, and ferri-magnetism are of interest in studies of magnetic oxides. Excluding ferro-magnetism which is scarce in oxide systems, there is one necessary condition for these phenomena to occur, and that is the presence of sublattices in the crystal structure. However, ferromagnetism can also occur in the crystal structure containing only one type of equivalent positions as, for instance, in the NaCl structure. On analyzing those cases more closely, it was found that long distance order of different ions on these positions, i.e., a "super structure", is needed to yield ferromagnetism.

The different structures yielding magnetic materials can be generally summarized in Table I.1 taken from (4).

Table I.1

Structure Type	Number of Non-equivalent Sublattices	Coordination Number of Sublattices	Magnetic Structure
NaCl	1	6	AF,F,Fi
Perovskite	2	6,12	AF,F,WF,Fi
Spinel	2	4,6	Fi,F,AF
Magnetoplumbite	More than 3	4,5,6, (12)	Fi
Ilmenite	1	6	WF,AF,Fi
Garnet	3	4,6,8	Fi,AF

F - Ferromagnetism
 Fi - Ferrimagnetism
 WF - Weak Ferromagnetism
 AF - Antiferromagnetism

The garnet structure is in some respects different from the others in the above table. This structure is not based on close-packed oxide ions, and this fact imposes some difficulties in mathematical description of relations of lattice constants to ionic radii of pertinent ions. On the other hand, the presence of three nonequivalent types of cation positions introduces a great flexibility in varying physical properties of the garnets by changing ionic distribution among the different sublattices.

I.2 Classification of Magnetic Properties

From the macroscopic point of view, magnetic properties of a compound are classified by means of behavior of a compound in a magnetic field. The magnetic field causes magnetization of a compound which results in magnetic moment. This macroscopic moment is

related to the presence of elementary moments in matter. Such elementary magnetic moments are either induced by the magnetic field, or else are permanent and independent of the outer magnetic field.

If the induced magnetic moments are oriented in a direction opposite to that of the applied magnetic field, and the latter is weakened by their effect, the behavior is called diamagnetism. Diamagnetism is common to all compounds or elements and diamagnetic moment is very weak.

If the permanent dipoles are aligned in a direction parallel to the applied outer field, this behavior (depending on circumstances) can result in paramagnetism, ferromagnetism, antiferromagnetism, or ferrimagnetism.

The existence of paramagnetism, and even more ferromagnetism and ferrimagnetism, is restricted to certain groups of matter only. There can exist two types of permanent elementary magnetic moments in matter: the magnetic moment of an atomic nucleus and the moment of an electron.

The magnetism of a nucleus is very weak in comparison to magnetism originating from the magnetic moments of electrons, and in the total magnetic moment its effect is negligible.

In a ferromagnetic substance, the atomic moments are ordered in the crystal lattice with all moments aligned in parallel direction at absolute zero. The effect of increasing temperature is to reduce the ordering. When the temperature reaches Curie temperature and

above, the ordering is completely destroyed, and the system becomes paramagnetic. In the case where the magnetic moments are antiparallel to each other, the net moment is zero and the substance is called antiferromagnetic. Most magnetic oxide systems are ferrimagnetic below the Curie temperature. Ferrimagnetism is a special case of antiferromagnetism where the antiparallel moments are unequal so that there is a net overall magnetization.

1.3 The Garnet Structure

The garnet structure was originally determined by Menzer (5,6) for the naturally occurring garnets such as grossularite $\text{Ca}_3 \text{Al}_2 (\text{SiO}_4)_3$, spessartite $\text{Mn}_3 \text{Al}_2 (\text{SiO}_4)_3$, or pyrope $\text{Mg}_{1.6} \text{Fe}_{1.2} \text{Ca}_{.2} \text{Al}_2 (\text{SiO}_4)_3$. The technological importance of the naturally occurring garnets was limited to that of abrasives, and some of the silicate garnets are semiprecious stones used in jewelry. It was about thirty years before the importance of the garnet structure for magnetic materials was recognized. The first clue was given by the Neel theory (7) which points to those crystal structures in which ferrimagnetism might exist.

The garnet structure is cubic but not derived from the cubic close packed structure, and it belongs to the space group $\text{Ia}\bar{3}\text{d}$. All of the cations are in special positions with no degrees of freedom, while the oxygen atoms are in the general position h with 3 degrees of freedom. Each oxygen is at the corners of four polyhedra: one tetrahedron surrounding a "d" ion (see Table 2), one octahedron surrounding an "a" ion, and two dodecahedras surrounding "c" ions.

Table I.2 (From (8)): Description of Garnet Structure.

Point Symmetry	222	3	4	1
Space Group Position	24c	16a	24d	96h
Typical Ideal Formula	$\{Ca_3\}$	$[Al_2]$	(Si_3)	O_{12}
Coordination to Oxygen	8	6	4	
Type Polyhedron	Dodecahedron Distorted Cube	Octahedron	Tetrahedron	

The use of different types of brackets has been adopted in the description of the garnet structures: the curly brackets indicate eight-fold dodecahedral coordination (a distorted cube), the square brackets indicate six-fold octahedral coordination, and the parentheses indicate four-fold tetrahedral coordination.

Figure I.1 shows the arrangement of different types of polyhedra in the garnet structure. Unfortunately, the drawing fails to show that the tetrahedron shares two edges with dodecahedra and two edges with octahedra.

FIG. I-1

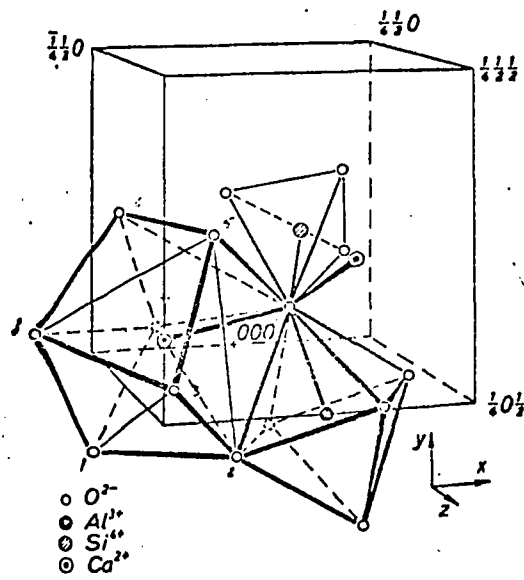


Fig. 1. Coordination about an oxygen ion in grossularite (after ABRAHAM and GELLER¹⁷)

Another fact that cannot be seen from the drawing is that no two tetrahedra have common corners. The octahedron shares one half of its edges with dodecahedra and the second half with octahedra. The positions of the oxygen ions in the structures are defined by three general parameters: x , y , and z . The values of these parameters change with the chemical composition of garnets, and they depend first of all on the radii of cations. When oxide ions are shifted from ideal positions, distortion of polyhedra results. The distortion changes the lengths of the polyhedra edges. However, the distances between the center and the corners of polyhedra are given by cation-oxygen radii in the tetrahedron and octahedron cases. The distortion phenomenon arises therefore from the fact that the lengths of three different polyhedra must match in the structure. The coordinates of cations are given as fractions of the length of the unit cell in three directions and their arrangement results in overall cubic symmetry.¹

Figure I.2 shows the arrangement of cations in the garnet structure (9).

¹ This statement does not appear to be quite correct because of the existence of ferrimagnetic garnets. Magnetic materials cannot truly be cubic because spontaneous magnetization appears in only one direction in a given domain. However, measurements such as X-ray diffraction which are insensitive to spontaneous magnetization, may not reveal deviation from the cubic symmetry.

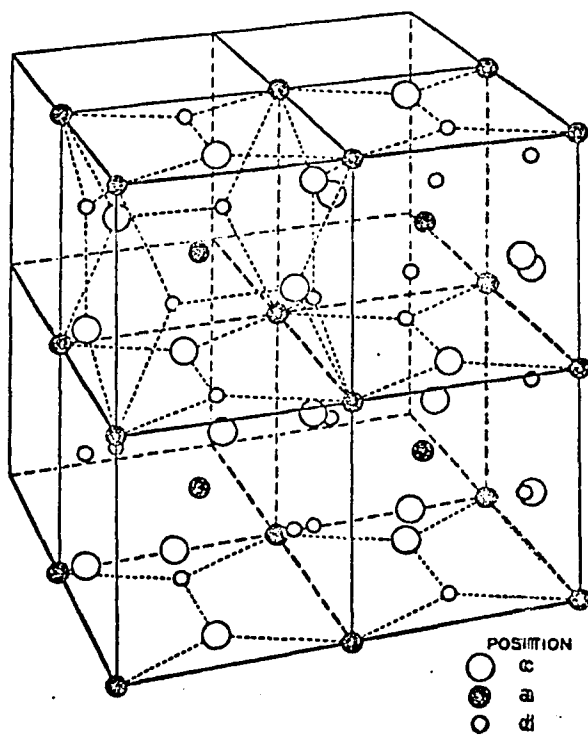


Fig. 1 — Arrangement of cations in *c*, *a*, and *d* sites in four octants of the garnet unit cell.

Limitations in the extent of distortions which are probably different for different electronic configurations of cations and the requirement for the overall cubic symmetry are the cause of relatively high selectivity of the garnet structure. They are also the ruling factors for distribution of ions among the sublattices, and they place limits on possible formation of the garnet structure. The summary of general rules, for ionic distribution and site preference are to be found in reference (8):

1. The octahedral and tetrahedral sites appear to prefer exclusively ions with spherical or pseudo-spherical electronic configuration. The dodecahedral sites are not selective in this regard.
2. Site preferences depend on relative ionic sizes:
 - a) If an ion has a spherical electronic configuration in both octahedral and tetrahedral crystal fields, the larger the ion, the greater will be its preference for the octahedral site. The dodecahedral sites are usually occupied by the largest metal ions present.
 - b) The substitution of one ion for another in some particular garnet is limited by relative sizes of all of the ions involved.

However, in the light of the latest discoveries, these rules appear not quite correct.

I.4 Synthetic Garnets

A new era for scientific and technological exploration of the garnets was opened by discovery of ferrimagnetic yttrium iron garnet $\left\{Y_3\right\} \left[Fe_2\right] \left(Fe_3\right) O_{12}$, abbreviated YIG. The discovery had been made independently by two groups of investigators: by Bertaut and Forrat (11) at Grenoble, and by Gilleo and Geller (12) at Bell Telephone Laboratories; the latter discovery was published one year later than that of Bertaut and Forrat.

The ferrimagnetic garnets became important because of their use in modern electronic devices. Important optical properties of other groups of garnets have been found suitable for preparation of good laser materials (13, 14, 15). More recently, iron garnets with mixed rare earth on the dodecahedral site became important for magnetic bubble domain materials (16).

Basically, there are five groups of garnet compounds which have been studied:

Silicate Garnets

Germanium Garnets

Aluminum Garnets

Gallium Garnets

Iron Garnets

I.4.1 Silicate Garnets. All of the natural garnets fall into this group, and they were the first subject of structural refinements (17, 18, 19, 20, 21) made either on synthetic or natural materials. Those measurements revealed the distortions of polyhedra in the garnet

structure and contributed to better understanding of garnet crystal chemistry. A survey of the most important silicate garnets is given by Geller in (8).

Table I.3: End Member Silicate Garnets

A ²⁺	B ³⁺	a[Å]	References
Mg	Al	11.459	18,22,23
	Cr	Not Reported	22
	Fe	Not Reported	22
Ca	Al	11.851	23
	Sc	12.270	24
	V	12.09, 12.07	24, 25
	Cr	12.00, 11.999	
	Fe	12.048, 12.059	23, 27
	Ga	12.00	28
Mn	In	12.350	24
	Al	11.621	23, 29
	Fe	11.82	22, 30
Fe	Al	11.526	23
Co	Al	11.471	31

Most of the silicate garnets listed in Table I.3 have been prepared by hydrothermal techniques. Synthetic uvarovite $\{Ca_3\}[Cr_2](Si_3)O_{12}$ may be obtained by solid state reaction.

I.4.2 Germanate Garnets. There are many new garnets among the simple end-member germanates in Table I.4 according to Geller (8). Some of them involve trivalent yttrium or rare earth ion in the "a" sites and Ca²⁺ and Sr²⁺ ions in the "c" sites. All of these garnets may be prepared by solid state reaction (34).

Table I.4: End-Member Germanate Garnets

A ²⁺	B ³⁺	a [Å]	References
Ca	Al	12.120	35
	Sc	12.504	36
	V	12.350, 12.320	24
	Cr	12.265, 12.275	36, 37
	Mn	12.325	38
	Fe	12.320, 12.312	35, 36
	Ga	12.251	
	In	12.620, 12.590	38, 34
	Rh	12.350	38
	Y	12.805	34
	Dy	12.830	34
	Ho	12.810	34
	Er	12.785	34
	Tm	12.765	34
	Yb	12.740	34
	Lu	12.730	34
	Sr	Sc	12.785
In		12.870, 12.88	34
Y		13.085, 13,091	34
Ho		13.090	34
Er		13.065	34
Tm		13.040	34
Yb		13.03	34
Lu		13.01	34
Mn	Al	11.902, 11.901, 11.895	35, 36, 37
	V	12.125, 12.099	24
	Cr	12.027	35,36
	Fe	12.087	35, 36
	Ga	12.043	37
Cd	Al	12.077	37
	Sc	12.447	37
	V	12.290	24
	Cr	12.213	37
	Mn	12.270	38
	Fe	12.261	37
	Ga	12.191	37
	In	12.515	24
	Rh	12.285	38

The significance of the existence of such garnets is revealed when germanates are compared with other types of garnets. Such

comparison shows that there is greater variety of composition than in the case of other systems. Garnets containing relatively large rare earth ions on the octahedral sites are especially important in relation to the present work.

I.4.3 Garnets of the Type $\{ \text{Rare Earth}_3 \} \cdot \text{Me}_5 \cdot \text{O}_{12}$. These compounds belong to the group of the most intensively studied garnet compounds. Me stands for trivalent ions such as Al^{3+} , Ga^{3+} , and Fe^{3+} . The broad attention given to these groups originated from the discovery of ferrimagnetism in the case of iron garnets. The lattice parameters of compounds in this group were summarized by Geller (8), and are listed in Table I.5.

Table I.5:

A ³⁺	B ³⁺	a [Å]	References
Y	Al	12.01, 12.02, 12.00, 12.003	39, 40, 42, 43, 20
Gd		12.11, 12.113, 12.111	20, 42, 44
Tb		12.074	45
Dy		12.06, 12.042	42, 45
Ho		12.011	45
Er		11.98, 11.981	42, 45
Tm		11.957	44
Yb		11.929	44
Lu		11.912	44
Y	Fe	12.376	46, 12
La*		12.767	47
Pr*		12.646	47
Nd*		12.600, 12.596	46, 47, 48
Pm*		12.57, 12.561	46, 47
Sm		12.524, 12.530, 12.528, 12.529	46, 47, 48, 49
Eu		12.518, 12.498	46, 47
Gd		12.479, 12.472, 12.471	46, 47, 48

* Hypothetical

Table I.5 (Cont'd)

A ³⁺	B ³⁺	a [Å]	References
Tb		12.447,12.436	46,47
Dy		12.414,12.405	46,47
Ho		12.380,12.375	46,47
Er		12.349,12.347	46,48
Tm		12.325,12.323	46,47
Yb		12.291,12.302	46,47
Lu		12.277,12.283	46,47
Y	Ga	12.30,12.273,12.280,12.275,12.274	42,43,20,41,50
Pr		12.57	42
Nd		12.50,12.506	41,42
Sm		12.355,12.420,12.433	40,41,42
Eu		12.402	41
Gd		12.390,12.376	41,42
Tb		Not Reported	
Dy		12.320,12.307	41,42
Ho		12.282	41
Er		12.25,12.255	41,42
Tm		Not Reported 12.229	Our Value
Yb		12.204,12.200	20,41
Lu		12.188,12.183	20,41

I.5 Ferrimagnetic Garnets

I.5.1 Yttrium Iron Garnet, YIG. Néel (7) first proposed the explanation of magnetic properties of ferrites. He stated: "If two atoms of unlike spin are antiparallel, there can be a resultant magnetic moment, and the exchange coupling which favors an antiparallel short range order can lead to an outstanding magnetic moment," and he suggested the name ferrimagnetism for this behavior. Ferrimagnetism is thus a special kind of ferromagnetism and differs from antiferromagnetism in such a way that the oppositely aligned moments are of different magnitude and therefore do not exactly compensate. Antiferromagnetism originates from negative superexchange interaction (51). In all cases, the unit of interaction is a linkage of the M-O-M type. The

excited states of the oxide ions couple their spins through interaction with d-electrons or f-electrons of the cations. The coupling is expected to be greater the shorter the cation-oxygen distance, and the closer the M-O-M angle is to 180° .

Antiparallel short range order of ions with magnetic moments of different magnitude can exist in the structure with at least two nonequivalent sublattices which can provide linkage M-O-M. The garnet structure even offers three such nonequivalent sublattices.

YIG, which was the first ferrimagnetic garnet prepared, has a formula $\{Y_3\} [Fe_2] (Fe_3)O_{12}$. The presence of iron in two sublattices shows the origin of ferrimagnetic interactions. The ferrimagnetic moment of an ion is given by $M = gJ$ where g is gyromagnetic ratio and J is $L-S$ for ions with less than half filled shells, and $L+S$ for those with half or more than half filled shells. The word "shell" refers to "f" shells because for the ions of iron-like type with d-shell the formula for ferrimagnetic moments is simplified to $M = gS$, where g equals 2 and S is the spin quantum number. Therefore, one can determine the ferrimagnetic moment of one Fe^{3+} ion of configuration $3d^5$ to be $M = (2)(2.5) = 5\mu_B$ where μ_B is Bohr magneton of value $\mu_B = \frac{he}{4\pi mc}$, h is Planck's constant, e is the electronic charge, m is the electron mass, and c is the velocity of light.

For antiparallel alignment of "a" and "d" sublattices, the net magnetic moment per formula unit can be calculated:

$$m = 3m_c - (3m_d - 2m_a) , \quad (E-1)$$

where m_c is the moment of the dodecahedral sublattice, m_d is the

moment of the tetrahedral sublattice, and m_a is the moment of the octahedral sublattice. Then for $\{Y_3\} [Fe_2] (Fe_3) O_{12}$ where $m_c = 0$

$$m = 0 - (3 \times 5 - 2 \times 5) = -5\mu_B$$

The resulting moment can be taken as $5\mu_B$ because the sign only describes the arbitrary orientation with regard to the third sublattice. This theoretical calculation is in excellent agreement with all experimental measurements on this compound (11, 12).

1.5.2 Magnetic Properties of Substituted Yttrium-Iron Garnets.

The magnetic moment of YIG can be varied with composition by substituting nonmagnetic ions either on the octahedral site or tetrahedral site. The magnetic moment should rise with octahedral substitution of nonmagnetic ions and fall with tetrahedral substitution because the moment corresponds to the difference in the moments of the Fe^{3+} ions in the two octahedral sites and three tetrahedral sites per formula unit.

In order to study such behavior, a number of systems have been studied by Geller, Gilleo, and others (9, 10, 43). The nonmagnetic ions used in substitution were Sc^{3+} , In^{3+} , Cr^{3+} , Ga^{3+} , Al^{3+} , Zr^{4+} , Si^{4+} , Ge^{4+} , V^{5+} . The substitutions took place in some cases on the octahedral sites only, while in some cases the nonmagnetic ions were substituted into both "a" and "d" sites simultaneously, and in some cases on tetrahedral sites only. It has been found that the proposed behavior holds only for low concentrations of the nonmagnetic ions in garnet. The behavior of magnetic moments in the systems

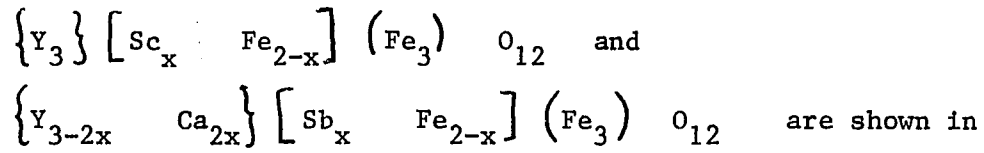


Figure I.3.

It can be seen that magnetic moments increase with increasing x ; however, the maximum moment is observed when x reaches a value about 0.8. The moments then fall sharply with increasing x . Also, the Curie temperature is decreased by the substitution of non-magnetic ions for iron. The decrease of the magnetic moment and Curie temperature is due to the decrease in the number of $\text{Fe}^{3+} - \text{O}^{2-} - \text{Fe}^{3+}$ interactions.

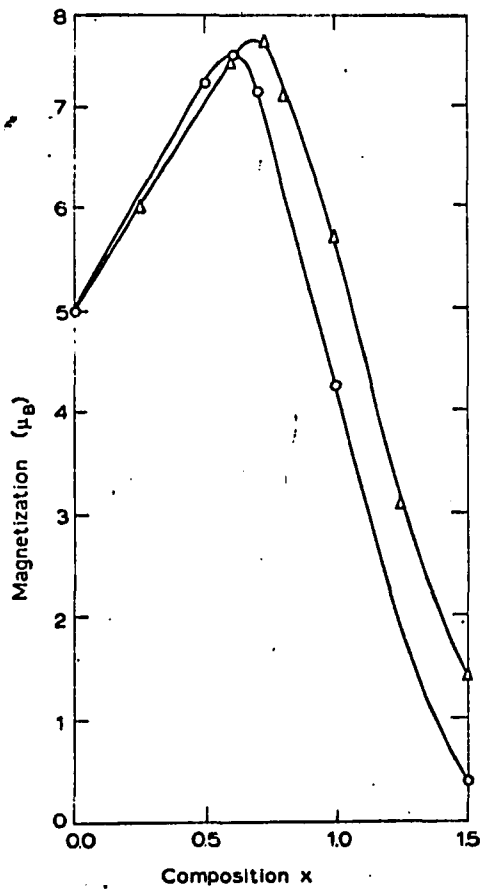


Fig. I-3. Magnetization versus composition x in $\{Y_3\}[Sc_xFe_{3-x}](Fe_3)O_{12}$ (Δ) and $\{Y_{3-2x}Ca_{2x}\}[Sb_xFe_{3-x}](Fe_3)O_{12}$ (O).

Geller et al. 1964b

Several theories have been proposed to explain the intrasub-lattice magnetic interactions (52, 53, 54, 55), for example the Gilleo theory and theories of Néel, Yafet and Kittel, and Anderson. The possibility of a quantitative theory which could predict the magnetic behavior of the substituted garnets is complicated by the various effects of substitution on the magnetic structure. It has been found (9) that different nonmagnetic ions in the same site may produce different magnetic behavior. This results from the effects on interaction geometry. Unfortunately, quantitative theory capable of such predictions has not been developed.

I.5.3. Other than Octahedral-Tetrahedral Ion Interaction in the Garnet Structure. Much of the work on synthetic garnets was an outgrowth of the desire to observe directly the interactions between magnetic ions in other than the octahedral a and tetrahedral d sites. As a matter of fact, a - d interactions have also been observed for mutually interacting iron ions only. The refinement of the structure of YIG indicated that the c - d interaction would be stronger than a c - a interaction, but the c - d direct interaction has not been studied yet, and it was only indirectly deduced from magnetic properties of iron garnets with dodecahedral c sites filled with rare earth ions.

I.5.3.1. Direct c - a Interaction. The anticipation of the possibility of obtaining a ferrimagnetic silicate was so exciting for some investigators (30, 22) that they expended considerable effort and disregarded the prediction of a very low Curie temperature for such a compound. Geller and others unsuccessfully tried to prepare

garnet $\{Mn_3\}[Fe_2](Si_3)O_{12}$. Coes (22) succeeded in preparing this at high pressure by the hydrothermal method. The magnetic measurements of this compound were disappointing at $0^\circ K$; the spontaneous magnetization was only $0.1 \mu_B$ (56). A number of germanium garnets including $\{Mn_3\}[Fe_2](Ge_3)O_{12}$ were discovered by Tauber et al (57). This garnet was found to be only antiferromagnetic at low temperatures. The structural refinements of this garnet were accomplished by Geller and Lind (58). The authors concluded on the basis of this refinement that the reason for such magnetic behavior is the unfavorable geometry or inherently weak interaction between Mn^{2+} and Fe^{3+} ions. However, they considered the last reason to be unlikely.

Gilleo and Geller (59) found garnets $\{M^{2+} Gd_2\}[Mn_2](Ge_3)O_{12}$, where $M = Mn$ and Ca to be ferrimagnetic at $6^\circ K$ or lower. They carried out more definite measurements on $\{Gd_3\}[Mn_2](GaGe_2)O_{12}$, which was found to have a Curie temperature of $8^\circ K$ and at $0^\circ K$ a saturation magnetization of $9.6 \mu_B$ (theoretical value of $11 \mu_B$). The fact that the $Gd - O - Mn$ interaction is stronger than $Mn - O - Fe$ interaction is especially interesting because one might tend to consider rare earth ions to be less capable of ferrimagnetic interactions because the participating electrons of Gd^{3+} are in inner f - shells.

I.5.3.2 Direct c - d Interactions. Geller et al. (60) reported preparation of garnet $\{Gd Ca_2\}[Zr_2](Fe_3)O_{12}$ and the results of magnetic measurements. They observed a residual magnetic moment $0.2 \mu_B$, and an extrapolated Curie temperature about $6^\circ K$, and they deduced from the $\frac{1}{\chi}$ vs T curve that the sample is weakly ferromagnetic. This case is the only known example of direct c - d

interaction.

I.5.4 Rare Earth Iron Garnets.

I.5.4.1 Ferrimagnetic Interactions in Rare Earth Garnets.

The model of ferrimagnetic interactions involving the rare earth ions was developed from almost exhaustive studies (61) of this group. The moment of rare earth ions occupying c sites is combined with the net magnetic moment of iron sublattices. The most valuable information for the derivation of this model comes from measurements of the magnetic moment-temperature dependency. The results for such measurements are shown in Figures I.4 and 5.

The theoretical ferrimagnetic moment M of rare earth ions is gJ where J is $L - S$ for those with less than half filled f shells, and $L + S$ for those with more than half filled f shells. M is $L + 2S$ for the latter group and slightly smaller than $L - 2S$ for some of the ions of the former group.

In the garnet $\{Gd_3\} [Fe_2] (Fe_3) O_{12}$ where the Gd^{3+} ion partakes in super exchange interaction with the ferric ions, the c sublattice moment can be calculated and has a value of $21\mu_B$. At $0^\circ K$ the saturation magnetization observed (Figure I.5) is $16\mu_B$ per formula unit. This indicates that the spin moment ($L = 0$) of the c sublattice is antiparallel to the net moment of iron sublattices. The net moment of the iron sublattices is in the direction of the d sublattice. Equation (E.1) in I.5.1 is the mathematical expression for this relationship.

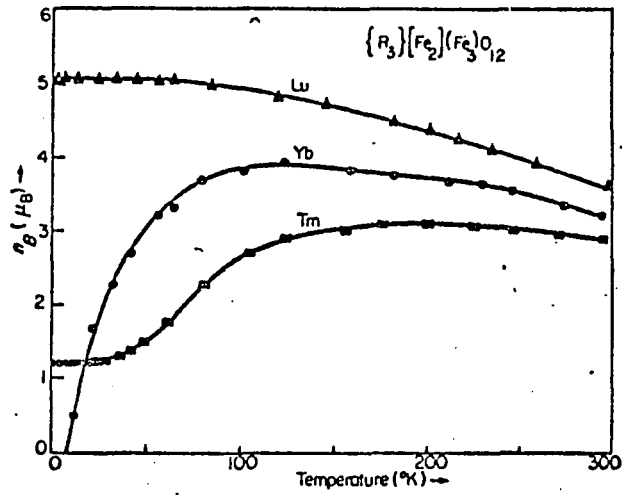


Figure I-4 Spontaneous magnetization in Bohr magnetons per formula unit vs. temperature of Tm, Yb and Lu iron garnets (Geller *et al.*, 1964).

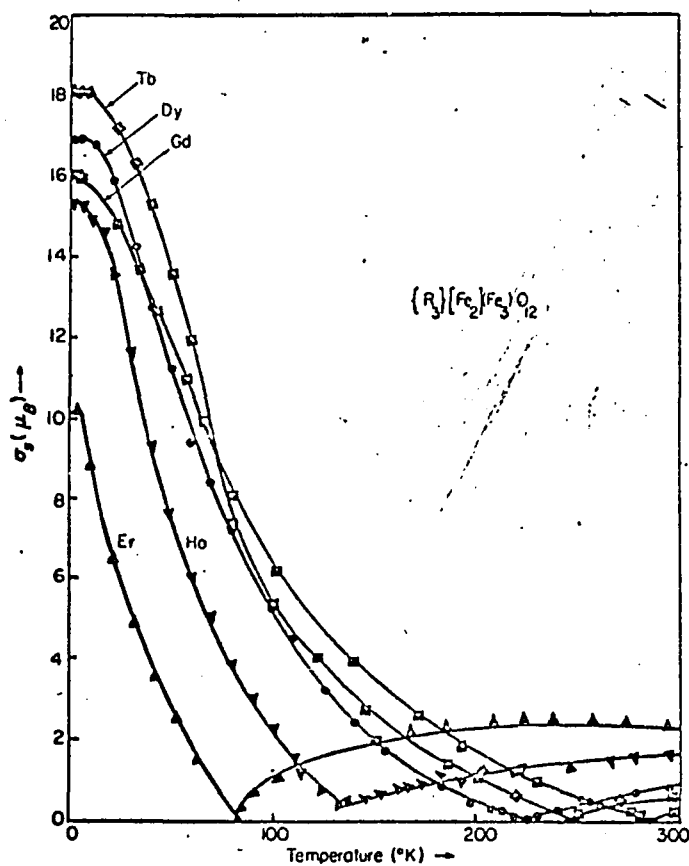


Figure ■ Spontaneous magnetization in Bohr magnetons per formula unit vs. temperature of Gd, Tb, Dy, Ho and Er iron garnets (Geller *et al.*, 1964).

Because $\text{Nd}_3 \text{Fe}_5 \text{O}_{12}$ does not exist, the behavior of Nd^{3+} in the c site can be observed in compounds prepared by substitution of Nd^{3+} for Y^{3+} in YIG. Such substitution results in an increase in the net ferrimagnetic moment (Figure I.4) because $L = 6$ and $S = \frac{3}{2}$ so that the moment due to the orbital momentum is greater and opposite in direction to that due to the spin; as a result, there is a net additional moment parallel to the tetrahedral sublattice. The direction of this moment is antiparallel to the octahedral sublattice, because the a and d sublattices are antiparallel.

Only $\text{Gd}_3 \text{Fe}_5 \text{O}_{12}$ exhibits precise agreement with this simple model; the moment of other rare earth iron garnets are found to be lower than predicted on the basis of this model. The characteristics of rare earth garnets of the type $\text{M}_3 \text{Fe}_5 \text{O}_{12}$ where M is rare earth ion, and compiled in the Table I.6.

Figure I.5 illustrates another important property of substituted rare earth garnets; that is, the existence of "compensation point". The compensation point is the temperature of which the overall magnetic moment of a substance equals zero. The existence of compensation point is due to different rate of decreasing magnetic moments of rare earth and iron sublattices with increasing temperature. The magnetic moment of rare earth sublattice is usually greater than moment of iron sublattice, but it decreases more rapidly with increasing temperature than does the net moment of iron sublattices and thus at compensation point these two antiparallel moments are equal to each other, and therefore, the resulting net moment is zero. When the compensation point is overcome by further increasing the temperature the net moment of iron sublattices is overwhelming the moment of rare earth sublattice and the overall moment appears again and it continues to be present up to the Curie temperature of the compound.

Table I.6 Magnetic and Crystallographic Properties of Garnets. n is the magnetic moment

in Bohr magnetons per unit formula $M_3 Fe_5 O_{12}$ (results are sometimes given per unit formula $(3M_2 O_3)$ $(2Fe_2 O_3)$ $(3Fe_2 O_3)$, i.e. $M_3 Fe_5 O_{12}$, giving twice n). The information in brackets is extrapolated from substituted compounds (Espinosa, 1962; Geller et al., 1964b, 1965a, b).

Ion M	a (Å)	Density	No. of 4f Electrons	L	2S	3m-5 M=L+2S	3m-5 m=2S	n at 0°K	I_s e.m.u.cm ⁻³ (20°C)	Compens. Curie Temp
Y	12.376	5.17	0	0	0	-5	-5	5.01	139	
La	(12.767)	(5.67)	0	0	0	-5	-5	(5.0)		
Pr	(12.646)	(5.87)	2	5	2	4	1	(9.8)		
Nd	(12.600)	6.00	3	6	3	4	4	(8.7)		
Sm	12.529	6.23	5	5	5	0	10	5.43	135	578
Eu	12.498	6.31	6	3	6	4	13	2.78	93	566
Gd	12.471	6.46	7	0	7	16	16	16.0	135	564
Tb	12.436	6.55	8	3	6	22	13	18.2	4	286
Dy	12.405	6.61	9	5	5	25	10	16.9	43	246
Ho	12.375	6.77	10	6	4	25	7	15.2	78	226
Er	12.347	6.87	11	6	3	22	4	10.2	103	137
Tm	12.323	6.94	12	5	2	16	1	1.2	110	83
Yb	12.302	7.06	13	3	1	7	-2	0.0	130	None
Lu	12.283	7.14	14	0	0	-5	-5	5.07	140	0-6

II. EXPERIMENTAL STUDIES

II.1 Objectives

The preceding literature survey of research accomplished on garnets is far from complete but it suggests general lines which are to be followed in further investigations.

The present work was oriented toward the magnetic properties of garnets. Taking into account the existence of three non-equivalent sublattices, the garnet structure is almost ideal for studies of varying magnetic properties by means of changing ionic distribution among sublattices. Reviewing compositions of prepared synthetic garnets, it is seen that their number is rather small in comparison with the number of possibilities offered with regard to the number of transition elements and the available sublattices. The reason is the high selectivity of the garnet structure. From the structural relations, it can be deduced that the selectivity originates from the fact that all polyhedra share edges with each other. Unfortunately there is not enough experimental data available to draw definite conclusions and develop rigorous rules governing substitutions in the garnet structure.

As a matter of fact, the preparation of new synthetic garnet compounds was based on more or less empirical assumptions. The first objective was to gather more experimental data with regard to ion distributions of rare earth ions in the garnet structure, and to prepare garnets with rare earth ions on two crystallographic sites, namely dodecahedral and octahedral sites. The simultaneous

occurrence of rare earth ions on more than one site in the given compound is quite interesting in itself, and from a view oriented toward magnetic properties, it would be an example of c - a interactions if they could exist between rare earth ions.

The second objective was to prepare compounds containing rare earth ions on the dodecahedral sites and magnetic ions on the tetrahedral sites, leaving the octahedral site filled with non-magnetic ions. Such a type of compound would be suitable for studies of direct c - d magnetic interactions.

The third objective was to show the possibility of preparing a garnet containing rare earth ions on the octahedral site and iron on the tetrahedral sites. The behavior of rare earth ions on the octahedral sites has not yet been studied, and it would be rather interesting to find out how the magnetic moments of rare earth ions in "a" sites are oriented when ferrimagnetic interaction with trivalent iron ions on the tetrahedral sites take place.

II.2 Experimental Approach

As mentioned above, the preparation of a new synthetic garnet has to be based on empirical assumptions because there is no theory which would allow one to make definite predictions. However, there are several empirical rules which help to draw conclusions about ion distributions. The most important one says that only ions with spherical or pseudo-spherical symmetry of electron shell can be tetrahedrally coordinated. Attempts were made to prepare compounds with desired ions on the crystallographic sites of the garnet

structure. The compounds were prepared in polycrystalline form and subjected to X-ray diffraction studies as the only method available for drawing conclusions about the purity of the garnet phase and ionic distribution. Measurements of magnetic properties of single phases were the last step.

II.3 Preparations

All preparations were made by solid state reaction among rare earth oxides at least 99.9% pure, Ga_2O_3 99.999% pure and Fe_2O_3 99.9% pure. Desired quantities of oxides were carefully weighed and intimately mixed by grinding with an agate mortar and pestle. Then the mixtures were heated for several hours at elevated temperature in open platinum crucibles in a muffle furnace. After this, the samples were reground and reheated under the same conditions. The conditions such as temperature and firing periods were different for the different systems studied, and they are given for each system. The procedure was repeated as many times as was needed for reaching equilibrium. It was decided from the results of the x-ray diffraction whether refiring was needed. Because of the limitation of the furnace used, 1500°C was the maximum temperature employed.

II.4 X-ray Diffraction Studies

The x-ray diffraction powder method using Norelco equipment with 57.3 mm radius powder cameras was the basic technique used to characterize the prepared compounds. X-ray patterns obtained were checked to see whether they contained only lines belonging to the garnet structure. The pattern of $\text{Nd}_3\text{Ga}_5\text{O}_{12}$ garnet was used as a reference. The reflections of this pattern are given in Table II.1.

The lattice constant, a , was the only measurable parameter which served as indication of the ionic distribution. The lattice constants were calculated according to the relationship for the cubic crystal structure.

$$a = d \sqrt{h^2 + k^2 + l^2}$$

where d is the spacing between planes in the unit cell, and h , k , and l are the Miller indexes of the planes. Four lines in the back reflection region of the powder pattern (i.e. (12 8 2), (12 6 6), (12 10 0), and (12 10 2)) were used for lattice constant calculations.

Table II.1 Indexed x - ray pattern of $\{\text{Nd}_3\}[\text{Ga}_2](\text{Ga}_3)_{12}\text{O}_{12}$. (75)

d (Å)	I/I_0	h	k	l	$h^2+k^2+l^2$	$\sqrt{h^2+k^2+l^2}$
5.11	16	2	1	1	6	2.449
4.42	6	2	2	0	8	2.828
3.342	12	3	2	1	14	3.741
3.128	30	4	0	0	16	4.000
2.796	100	4	2	0	20	4.472
2.669	2	3	3	2	22	4.690
2.553	45	4	2	2	24	4.898
2.452	4	4	3	1	26	5.099
2.283	12	5	2	1	30	5.477
2.211	4	4	4	0	32	5.656
2.029	14	6	1	1	38	6.164
1.977	2	6	2	0	40	6.324
1.843	4	6	3	1	46	6.782
1.805	16	4	4	4	48	6.928
1.735	30	6	4	0	52	7.211
1.701	6	7	2	1	54	7.348
1.6712	35	6	4	2	56	7.483
1.5883	10	7	3	2	62	7.874
1.563	16	8	0	0	64	8.000
1.3982	10	8	4	0	80	8.944
1.3646	20	8	4	2	84	9.165
1.3489	4	9	2	1	86	9.273
1.3333	8	6	6	4	88	9.380
1.2267	6	10	2	0	104	10.198
1.1923	4	10	3	1	110	10.488

Table II.1 (Cont'd)

d (Å)	I/I ₀	h	k	l	$h^2+k^2+l^2$	$\sqrt{h^2+k^2+l^2}$
1.1614	18	10	4	0	116	10.770
1.1513	2	10	3	3	118	10.862
1.1417	10	10	4	2	120	10.254
1.1143	4	11	2	1	126	11.224
1.105	10	8	8	0	128	11.313
1.0801	2	11	3	2	134	11.576
1.0422	8	12	0	0	144	12.000
1.0281	10	12	2	0	148	12.165
1.0212	6	11	5	2	150	12.247
1.0146	10	12	2	2	152	12.328
0.9707	4	11	6	3	166	12.884
0.9482	2	13	2	1	174	13.191
0.9425	8	12	4	4	176	13.266
0.9321	14	12	6	0	180	13.416
0.921		12	6	2	184	13.565
0.859		12	8	2	212	14.560*
0.8505		12	6	6	216	14.696*
0.8005		12	10	0	244	15.620*
0.794		12	10	2	248	15.748*

* Used for lattice constant calculations.

II.5 Magnetic Measurements

Magnetic susceptibilities were determined by the Faraday method with an apparatus consisting essentially of a 4-inch diameter Varian electromagnet with Faraday poles, along with a Cahn GRAM Electrobalance in a helium-filled glass chamber placed between the poles for measurement of the weight change of the sample upon application of the magnetic field. A Dewar flask filled with liquid nitrogen was used to cool the sample. Samples of different weights from about 3 to 5 mg were placed in a 5 mm diameter quartz pan at the end of a quartz fiber in a Vycor hangdown tube. Weighings were made first

without and then with the field applied. The field strength H in the vicinity of the sample was about 6 kG.

A Cu-constant and thermocouple close to the sample pan was employed to measure the temperature. All runs were started at about 78°K (which is the boiling temperature of liquid nitrogen). Then the coolant was slowly boiled away from the sample area, and after that the sample was heated up to room temperature. The heating was provided by a double-wound, insulated nichrome coil around the hangdown tube.

Magnetic susceptibilities were calculated by comparison with the results of weight change of the accepted standard using the same applied field strength. Mercury thiocyanatocobaltate II ($\text{Hg} \left[\text{Co} \left(\text{SCN} \right)_4 \right]$ (62) (Eastman Organic Chemicals # 8588) was used as a standard. Its gram susceptibility at 20°C is 16.44×10^{-6} . The apparatus is described in detail in (63).

III. GARNET COMPOUNDS PREPARED

III.1 Gallium Garnets with Rare Earth on Both Octahedral and Dodecahedral Sites

Rare earth ions have been observed to distribute themselves at least to some extent on two crystallographic sites in some garnets. Scheider, Roth and Waring (41) investigated the extent of garnet solid solution in garnet systems containing Ga_2O_3 with oxides of trivalent rare earth. Similar work was also done by Keith and Roy (40). The maximum solubility of rare earth on the dodecahedral sites was found at Tm^{3+} and fell off in both directions along the rare earth series. The formula of the composition with maximum Tm is $\{\text{Tm}_3\} [\text{Tm}_{.8} \text{Ga}_{1.2}] (\text{Ga}_3) \text{O}_{12}$. Schneider, Roth and Waring (41) found solubility of Y^{3+} on the octahedral site of yttrium gallium garnet about $\{\text{Y}_3\} [\text{Y}_{.74} \text{Ga}_{1.26}] (\text{Ga}_3) \text{O}_{12}$, a result very similar to that of Geller and Espinosa (8). Geller and Espinosa also observed linear increase of the lattice constant with increasing concentration of Y^{3+} in the garnet. Mill (34) prepared germanate garnets with alkaline earth ions on the dodecahedral sites and small trivalent rare earth ions on the octahedral sites.

Such results suggested that it might be possible to prepare gallium garnets with trivalent rare earth ions on both dodecahedral and octahedral sites, perhaps to exclusion of all other ions on the octahedral sites if the dodecahedral sites were filled with large rare earth ions.

III.1.1 The Neodymium Systems. At first, attempts were made to prepare solid solutions of $\{Nd_3\} [Ga_2] (Ga_3) O_{12}$ with the nominal compositions $\{Nd_3\} [R_2] (Ga_3) O_{12}$, and to determine the relationship between composition and the lattice constant. R stands for other rare earth ions: Lu^{3+} , Tm^{3+} , Yb^{3+} , Er^{3+} , Ho^{3+} , Dy^{3+} . The range of this system actually corresponds to the formula $\{Nd_3\} [Ga_{2-x} R_x] (Ga_3) O_{12}$ where the above formulas represent the end members for $x = 0$ and $x = 2$ respectively. Nd^{3+} was chosen for the first runs because of its radius which is among the largest found in the rare earths. Although it enters the dodecahedral sites of gallia garnets with ease, it will not enter the octahedral sites at all (Ref. 41; also confirmed in present studies).

III.1.1.1 Preparation Conditions. The temperature employed for the solid state reactions for Nd^{3+} system was $1500^\circ C$. Oxide mixtures were heated first for three hours and then reground and reheated for an additional five hours. This procedure was found to be sufficient for equilibrium to be reached in all cases.

III.1.1.2 Results. The results of the preparation according to the general formula $\{Nd_{3-y} R_y\} [R_x Ga_{2-x}] (Ga_3) O_{12}$ are compiled in Tables III.1 to III.7.

Table III.1 System $\{Nd_{3-y} Yb_y\} [Yb_x Ga_{2-x}] (Ga_3) O_{12}$

x	y	a (Å)	Purity
0.2	0	12.504	Slightly Impure
0.3	0	12.511	Slightly Impure
0.4	0	12.526	Impure
0.5	0	12.551	Impure
0.7	0	12.595	Very Impure
0.8	0	12.618	Very Impure
0.9	0	12.650	Impure
1.0	0	12.680	Impure
1.1	0	12.699	Impure
1.2	0	12.718	Slightly Impure
1.3	0	12.747	Slightly Impure
1.4	0	12.770	Slightly Impure
1.5	0	12.784	Slightly Impure
1.6	0	12.804	Slightly Impure
1.8	0	12.840	Impure
1.9	0	12.864	Impure
2.0	0	12.890	Impure
2.0	0.1	12.906	Impure
2.0	0.2	12.900	Slightly Impure
2.0	0.3	12.864	Pure
2.0	0.5	12.855	Pure

Table III.2 System $\{Nd_3\} [Lu_x Ga_{2-x}] (Ga_3) O_{12}$ y = 0

x	a (Å)	Purity
0.2	12.522	Very Slightly Impure
0.4	12.535	Slightly Impure
0.6	12.592	Impure
1.0	12.666	Slightly Impure
1.4	12.459	Slightly Impure
1.8	12.829	Pure
2.0	12.881	Pure

Table III.3 System $\left\{ \text{Nd}_{3-y} \text{ Tm}_y \right\} \left[\text{Tm}_x \text{ Ga}_{2-x} \right] (\text{Ga}_3) \text{O}_{12}$

X	Y	a (Å)	Purity
0.2	0	12.503	Impure
0.4	0	12.501	Impure
0.6	0	12.527	Impure
0.8	0	12.585	Impure
0.9	0	12.611	Impure
1.2	0	12.684	Slightly Impure
1.6	0	12.793	Impure
2.0	0	12.882	Impure
2.0	0.2	12.882	Impure
2.0	0.4	12.876	Slightly Impure
2.0	0.6	12.854	Pure

 Table III.4 System $\left\{ \text{Nd}_{3-y} \text{ Er}_y \right\} \left[\text{Er}_x \text{ Ga}_{2-x} \right] (\text{Ga}_3) \text{O}_{12}$

x	y	a (Å)	Purity
0.2	0	12.504	Impure
0.6	0	12.503	Impure
0.9	0	12.594	Impure
0.95	0	12.606	Impure
1.05	0	12.624	Impure
1.2	0	12.660	Impure
1.4	0	12.693	Impure
1.60	0	12.744	Impure
1.8	0	12.784	Impure
2.0	0	12.831	Impure
2.0	0.2	12.828	Impure
2.0	0.4	12.837	Impure
2.0	0.6	12.827	Impure

Table III.5 System $\left\{ \text{Nd}_{3-y} \text{Ho}_y \right\} \left[\text{Ho}_x \text{Ga}_{2-x} \right] (\text{Ga}_3) \text{O}_{12}$

x	y	a (Å)	Purity
0.2	0	12.502	Impure
0.4	0	12.492	Impure
0.8	0	12.522	Impure
1.0	0	12.553	Impure
1.2	0	12.569	Impure
1.4	0	12.605	Impure
1.8	0	12.640	Impure
2.0	0	12.652	Impure
2.0	0.2	12.657	Impure
2.0	0.4	12.662	Impure
2.0	0.6	12.643	Impure

Table III.6 System $\left\{ \text{Nd}_{3-y} \text{Dy}_y \right\} \left[\text{Dy}_x \text{Ga}_{2-x} \right] (\text{Ga}_3) \text{O}_{12}$

x	y	a (Å)	Purity
0.2	0	12.501	Impure
0.4	0	12.492	Impure
0.6	0	12.479	Impure
0.8	0	12.483	Impure
1.0	0	12.492	Impure
1.4	0	12.504	Impure
1.8	0	12.510	Impure
2.0	0	12.510	Impure
2.0	0.2	12.524	Impure
2.0	0.4	12.530	Impure
2.0	0.6	-	Impure*

* The x-ray pattern has very poor back reflections, and therefore the lattice constant cannot be determined with proper accuracy.

Table III.7 System $\left\{ \text{Nd}_{3-y} \text{ Yb}_y \right\} \left[\text{Ga}_2 \right] \left(\text{Ga}_3 \right) \text{O}_{12}$

y	a (Å)	Purity
0.5	12.465	Pure
1.0	12.431	Pure
2.0	12.314	Pure
3.0	12.203	Pure

III.1.1.3 Discussion of Results. When sufficient Ga^{3+} ion is present in an attempt to make a solid solution, it fills both the octahedral and tetrahedral sites, and all rare earths, whether Nd^{3+} or R^{3+} enter only dodecahedral positions. Data for solid solutions of the type $(\text{Nd}_3 \text{ Ga}_5 \text{ O}_{12} - \text{Yb}_3 \text{ Ga}_5 \text{ O}_{12})$ are given in Table III.7, and the plot of the lattice constants for this system which actually corresponds to $\left\{ \text{Nd}_{3-y} \text{ Yb}_y \right\} \left[\text{Ga}_2 \right] \left(\text{Ga}_3 \right) \text{O}_{12}$ is given in Figure III.1.

When attempting to prepare $\left\{ \text{Nd}_3 \right\} \left[\text{R}_2 \right] \left(\text{Ga}_3 \right) \text{O}_{12}$ compounds it was found that garnets were formed in all cases but except for $\left\{ \text{Nd}_3 \right\} \left[\text{Lu}_2 \right] \left(\text{Ga}_3 \right) \text{O}_{12}$, which contains the smallest of all rare earth ions, impurities were also present. However, the observed increases of the lattice constants prove that rare earth ions do enter the octahedral positions to an appreciable extent.

The results plotted in Figure III.2 indicate that Vegard's law is not obeyed; rather, each of the curves contains at least two segments with different slopes. The first segment with small additions of R (i.e., x small) have much lower slopes than the second segments

FIG. III -1

Lattice constants vs. y for $\{Nd_{3-y} Yb_y\} [Ca_2] (Ga_3) O_{12}$.

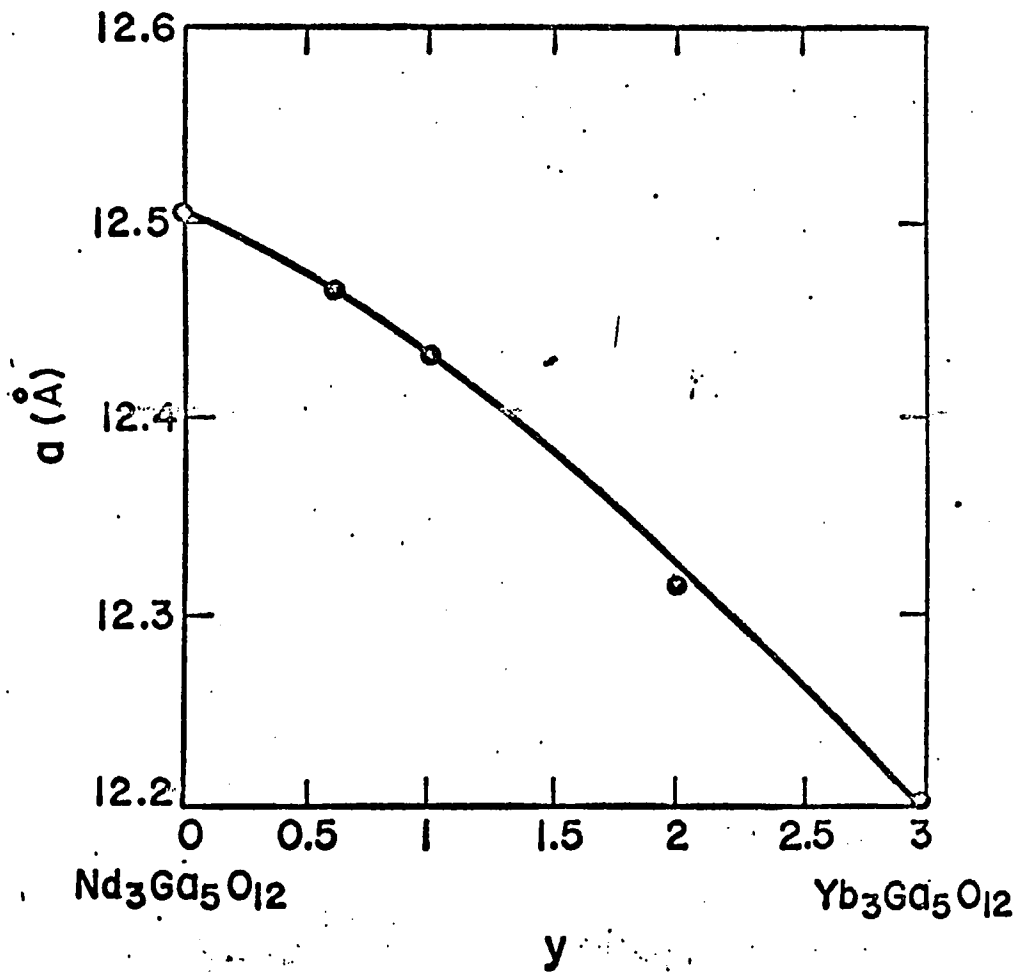
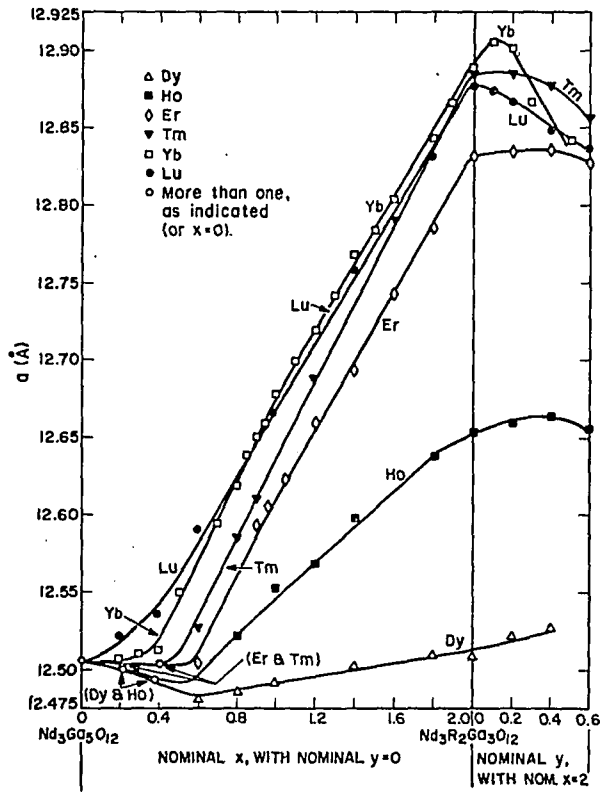


FIG. III - 2



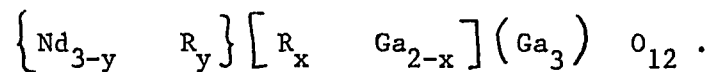
Lattice constants versus nominal x for nominal $\{Nd_3\}[R_xGa_{2-x}](Ga_3)O_{12}$ and versus nominal y for nominal $\{Nd_{3-y}R_y\}[R_2](Ga_3)O_{12}$.

where x is larger. Some of the first segment slopes are actually zero or negative. The logical explanation for this appears to be that of some of the small rare earth ion, R, was actually entering the dodecahedral positions along with the Nd, while simultaneously entering the octahedral positions. Since the first would decrease the lattice constant and the second would increase it, the net change would be small, which is precisely what was observed. In addition, with R entering the dodecahedral sites and Nd unable to enter the octahedral sites, there would be a surplus of Nd. This is in fact the case, for one impurity phase found was the perovskite, NdGaO_3 , when $x \approx 0.6$ for Lu, 1.2 for Yb, and Tm 1.8 for Er and 0-2 for Ho and Dy. Additional impurity phases found when $x = 1.1-2$ for Yb, 1-2 for Tm, 0.9-2 for Er, and 0.8-2 for Ho and Dy were not identified. The loss of Ga available to the garnet phase which results from the formation of perovskite also affects the amount, composition, and the lattice constant of the garnet formed. This is the reason that the abscissa in Fig. III.2 is labeled "Nominal x " which means the amount of R introduced into the mixture of reactants based on the expected ideal solid solution formation. The sharp rise of the second segments of the curves in Fig. III.2 indicate that, following partial filling of the dodecahedral positions with R, the octahedral positions fill up more exclusively.

The lower levels of the Er, Ho, and Dy curves indicate that the true maximum values of " x " attained in these nominal systems were lower than with the smaller ions Lu, Yb, and Tm.

If some of the small rare earth R enters the dodecahedral sites and thus leaves insufficient R for the octahedral sites, it could be expected that further addition of R actually results in expansion of the lattice, at least up to the point where a maximum value of x is reached. This should occur because such further addition would provide sufficient R both to satisfy the dodecahedral sites and to continue filling of the octahedral sites.

None of the rare earth ions will enter the tetrahedral sites in substitution for Ga. The formula which would better characterize the true situation can be written as



It is the nominal value of this y (with nominal x = 2) which is plotted in the right portion of Fig. III - 2. In the case of Lu where the composition $\left\{ \text{Nd}_3 \right\} \left[\text{Lu}_2 \right] (\text{Ga}_3) \text{O}_{12}$ is a single phase, one expects to find an immediate decrease in the value of a . In all other cases either an increase or a levelling off is observed. The maintenance of a constant value of a is also significant because a true increase in y in a single-phase material could only cause a decrease in the lattice constant.

Several systems were prepared with constant y values while changing x. The data obtained are compiled in Tables III - 8 through III - 9.

Table III-8 System $\left\{ \text{Nd}_{2.8} \text{ Yb}_{.2} \right\} \left[\text{Yb}_x \text{ Ga}_{2-x} \right] (\text{Ga}_3) \text{O}_{12}$
 $y=0.2$

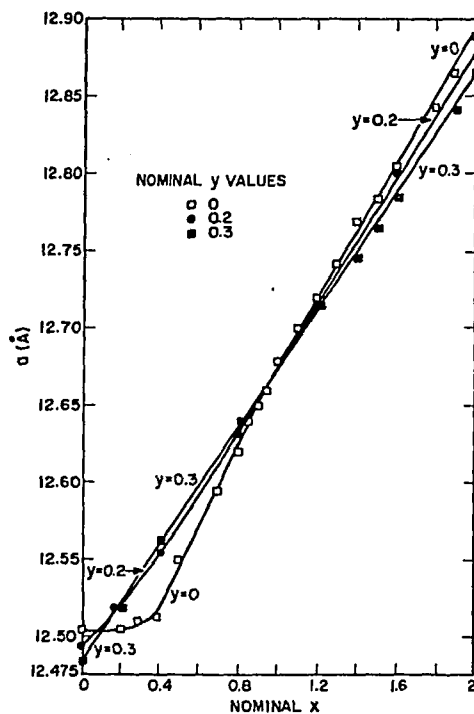
x	a (Å)	Purity
0.0	12.495	Pure
0.2	12.522	Slightly Impure
0.4	12.555	Slightly Impure
0.8	12.631	Slightly Impure
1.2	12.715	Almost Pure
1.6	12.800	Almost Pure
2.0	12.900	Almost Pure

Table III-9 System $\left\{ \text{Nd}_{2.7} \text{ Yb}_{.3} \right\} \left[\text{Yb}_x \text{ Ga}_{2-x} \right] (\text{Ga}_3) \text{O}_{12}$
 $y=0.3$

x	a (Å)	Purity
0.0	12.486	Pure
0.2	12.520	Pure
0.4	12.562	Pure
0.8	12.640	Pure
1.2	12.715	Pure
1.4	12.744	Pure
1.5	12.767	Pure
1.6	12.784	Pure
1.9	12.842	Pure
2.0	12.864	Pure

It was found that, as the value of y approached a certain required minimum, single-phase garnets were obtained. When approaching this minimum value, the plots of the lattice constants vs composition became more linear, and at the value of y which yields purity, it was linear. The linearity of such a plot means that the law of Vegard is obeyed. The progressive increase in linearity for the system $\left\{ \text{Nd}_{3-y} \quad \text{Yb}_y \right\} \left[\text{Yb}_x \quad \text{Ga}_{2-x} \right] (\text{Ga}_3)_{012}$ can be seen in Fig. III - 3.

The minimum required value of y for the Yb system was found to be 0.3. For the other systems, that is, those with the other small rare earths, the y - values were determined as follows: A nominal composition was chosen where the perovskite impurity lines in the x-ray diffraction powder method pattern were strongest, and the value of y was varied while x was held constant until a single phase compound was obtained. In the Lu system, this value of x was 0.5, while for the Tm and Er system, 0.8. The values of y determined were 0.6 for the Tm system, 0.2 for the Lu system, and 1.1 for the Er system. Data for those systems are compiled in the following tables.



Lattice constants versus nominal x with several values of nominal y for $\{Nd_{3-y}Yb_y\}[Yb_xGa_{2-x}](Ga_3)O_{12}$.

Table III-10 System $\{Nd_{2.4} Tm_{.6}\} [Tm_x Ga_{2-x}] (Ga_x)_0_{12}$
 $y = 0.6$

x	a (Å)	Purity
0.0	12.454	Pure
0.4	12.525	Pure
0.8	12.624	Pure
1.2	12.705	Pure
1.6	12.784	Pure
2.0	12.854	Pure

Table III-11 System $\{Nd_{1.9} Er_{1.1}\} [Er_x Ga_{2-x}] (Ga_3)_0_{12}$
 $y = 1.1$

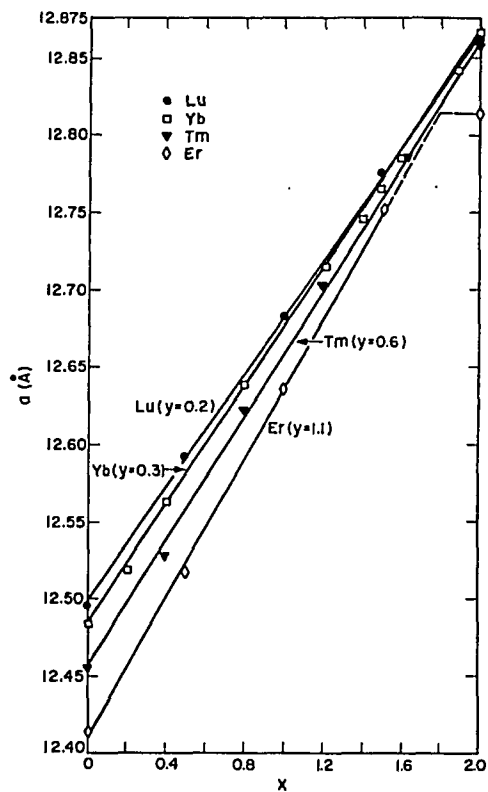
x	a (Å)	Purity
0.0	12.414	Pure
0.5	12.514	Pure
1.0	12.638	Pure
1.5	12.751	Pure
2.0	12.813	Very Slightly Impure

All preparations listed above are single phases except for the one with Er at $x = 2.0$. The plots for four systems $\{Nd_{3-y} R_y\} [R_x Ga_{2-x}] (Ga_3)_0_{12}$ with the value of y required for linearity are given in Fig. III - 4. It appears that in the Er case the limiting value of x is lower than 2. Similarly, since y for the Er is 1.1, the dodecahedral ions cause less expansion of the lattice. All attempts to obtain a single-phase composition $\{Nd_{3-y} Er_y\}$

$[\text{Er}_2](\text{Ga}_3)_{0.12}$ by increasing the value of y with x held constant at 2 were unsuccessful probably at least partly because this causes a further decrease in the average size of the dodecahedral ion, and therefore, there is even less enlargement of the octahedral sites.

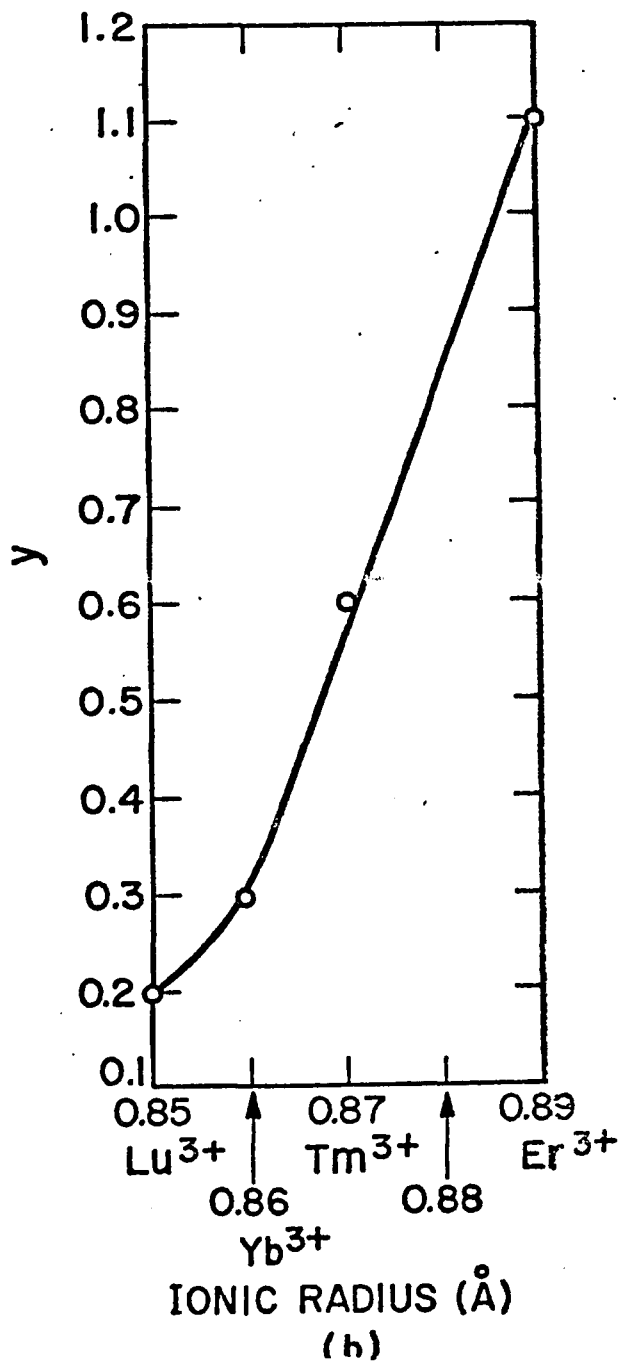
Fig. III - 5 is a plot of the ionic radii vs y values required to satisfy (not saturate) the dodecahedral sites and thus obtain the pure garnets and the straight lines of Fig. III - 4. It should be noted that these "y" values are perhaps not the minimum required for purity at all compositions. For instance, $\{\text{Nd}_3\}[\text{Lu}_2](\text{Ga}_3)_{0.12}$ may be obtained as a single phase material but the y value of 0.2 is required to yield single phase materials throughout the composition range along with a linear relationship between the lattice constant and composition. The extrapolation of the curve in Fig. III - 5 to the radii of Ho^{3+} (0.91A) and Dy^{3+} predicts the y values of 1.65 and 1.9, respectively. In these cases, then, the dodecahedral sites contain more of the small rare earth than Nd ions, and so an assumption can be made that even less of the small rare earth ions can enter the octahedral sites than in the case of Er ions. The limiting values of x for these cases were actually found to be 1.0 for Ho and slightly less than 1.0 for Dy.

Fig. III - 6 is a diagram of the ternary system $\text{Nd}_2\text{O}_3 - \text{Yb}_2\text{O}_3 - \text{Ga}_2\text{O}_3$ but it serves to represent in form, though not in detail, all ternary systems studied. The line representing the pseudobinary system that yielded single phase garnets and the straight line in Fig. III - 3 and III - 4 (i.e. $\{\text{Nd}_{2.7} \text{ Yb}_{0.3}\}[\text{Ga}_2](\text{Ga}_3)_{0.12} - \{\text{Nd}_{2.7} \text{ Yb}_{0.3}\}[\text{Yb}_2](\text{Ga}_3)_{0.12}$) is parallel to the line representing



Lattice constants versus x for $\{Nd_{3-y}R_y\}[R_xGa_{2-x}]$
 $(Ga_3)O_{12}$.

y values required to yield single-phase garnets and straight lines in Figure 4 vs ionic radii of trivalent rare earths, R.



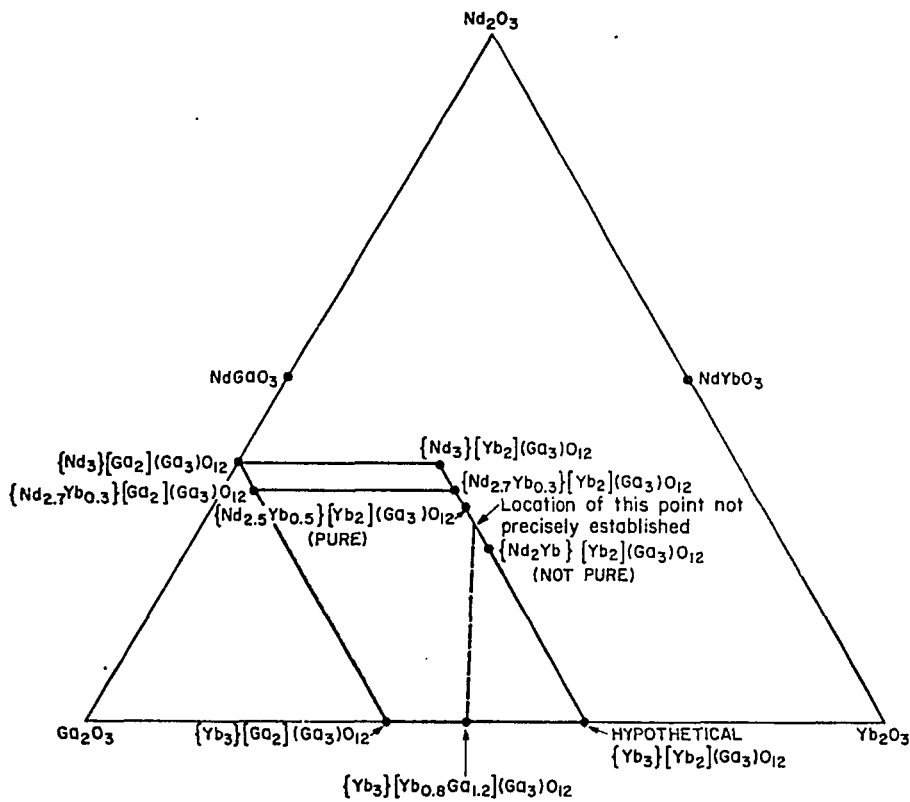


FIG. ■ The ternary system $\text{Nd}_2\text{O}_3\text{-Ga}_2\text{O}_3\text{-Yb}_2\text{O}_3$. Single-phase garnets are found only in the shaded area and along the line between $\{\text{Nd}_3\}\{\text{Ga}_2\}(\text{Ga}_3)\text{O}_{12}$ and $\{\text{Nd}_{2.7}\text{Yb}_{0.3}\}\{\text{Ga}_2\}(\text{Ga}_3)\text{O}_{12}$.

the nominal system $\{Nd_3\}[Ga_2](Ga_3)_{0_{12}} - \{Nd_3\}[Yb_2](Ga_3)_{0_{12}}$, results for which are given in Fig. III - 2. The distance between these parallel lines would probably be different for systems other than the Yb system but generally similar. Single-phase garnets have been found only in the shaded area and along the line between $\{Nd_3\}[Ga_2](Ga_3)_{0_{12}}$ and $\{Nd_{2.7} Yb_{.3}\}[Ga_2](Ga_3)_{0_{12}}$. The solubility limit represented by the point at $\{Yb_3\}[Yb_{.8} Ga_{1.2}](Ga_3)_{0_{12}}$ is from the paper by Schneider, Roth, and Waring (41).

III - 1.2 Praseodymium Systems. These systems are analogous to the materials described above. However, the use of a larger ion (Shannon-Prewitt (64) "IR" radii for coordination number 8: $Pr^{3+} = 1.14 \text{ \AA}$, $Nd^{3+} = 1.12 \text{ \AA}$) on the dodecahedral site might yield further information regarding the relationship between relative sizes of cations in the dodecahedral and the octahedral positions, and the resulting effect on the minimum y value.

At this point, it is desirable to summarize the reasoning that permits assignment of ions to different crystallographic positions. It should be understood that it is possible to make definite assignments only when dealing with single-phase materials of known stoichiometric compositions. Large rare earth ions such as Nd^{3+} or Pr^{3+} can enter only the dodecahedral sites (41). Ga^{3+} ion can enter both tetrahedral and octahedral sites but not the dodecahedral sites. The small rare earth R^{3+} can enter both dodecahedral and octahedral sites but not the tetrahedral sites. If sufficient large rare earth and R^{3+} ions are present to fill both dodecahedral and octahedral

sites, Ga^{3+} ion will enter only the tetrahedral sites. If there is less than enough total rare earth present than needed to fill the dodecahedral and octahedral sites, then the Ga^{3+} ion added over the amount required to fill the tetrahedral sites will enter the octahedral positions. Therefore, in any stoichiometric single phase garnet of the type $\left\{ \text{RE}_{3-y} \text{R}_y \right\} \left[\text{R}_x \text{Ga}_{2-x} \right] (\text{Ga}_3)_0_{12}$ where RE stands for large rare earth ion, the RE^{3+} must be in dodecahedral positions, the tetrahedral positions must be filled with three Ga^{3+} ions, and R^{3+} must be distributed over the dodecahedral and octahedral sites so that there is a total of three ions of RE^{3+} and R^{3+} on the former and two ions of R^{3+} and Ga^{3+} on the latter sites. No other possibility exists.

III - 1.2.1 Preparations. All preparations were made by solid state reaction among the rare earth oxides and Ga_2O_3 . Most of the rare earth oxides employed were sesquioxides but the praseodymium compound was Pr_6O_{11} . It was found that the oxidation state of the Pr in the products was independent of its initial oxidation state in the reactant. The mixtures of oxides were heated 3 hours at 1350°C in open platinum crucibles in a muffle furnace. After that, the samples were reground and reheated for 5 hours under the same conditions. This procedure was found sufficient for equilibrium to be reached in all cases.

III - 1.2.2 Results. As in the case where the large dodecahedral ions were Nd^{3+} , an attempt to prepare $\left\{ \text{Pr}_3 \right\} \left[\text{R}_2 \right] (\text{Ga}_3)_0_{12}$ was made. The results of these attempts are compiled in the following tables.

Table III - 12. System $\{Pr_3\}[Yb_x Ga_{2-x}](Ga_3) O_{12}$

x	a (Å)	Purity
0.0	12.552	Pure
0.4	12.530	Impure
0.5	12.536	Impure
0.8	12.655	Impure
1.0	12.780	Impure
1.2	12.785	Impure
1.5	12.870	Impure
1.6	12.900	Impure
2.0	12.928	Almost Pure

Table III - 13 System $\{Pr_3\}[Tm_x Ga_{2-x}](Ga_3) O_{12}$

x	a (Å)	Purity
0.0	12.552	Pure
0.4	12.505	Impure
0.8	12.655	Impure
1.2	12.798	Impure
1.6	12.867	Impure
2.0	12.904	Almost Pure

Table III - 14 System $\left\{ \text{Pr}_3 \right\} \left[\text{Er}_x \text{Ga}_{2-x} \right] \left(\text{Ga}_3 \right) \text{O}_{12}$

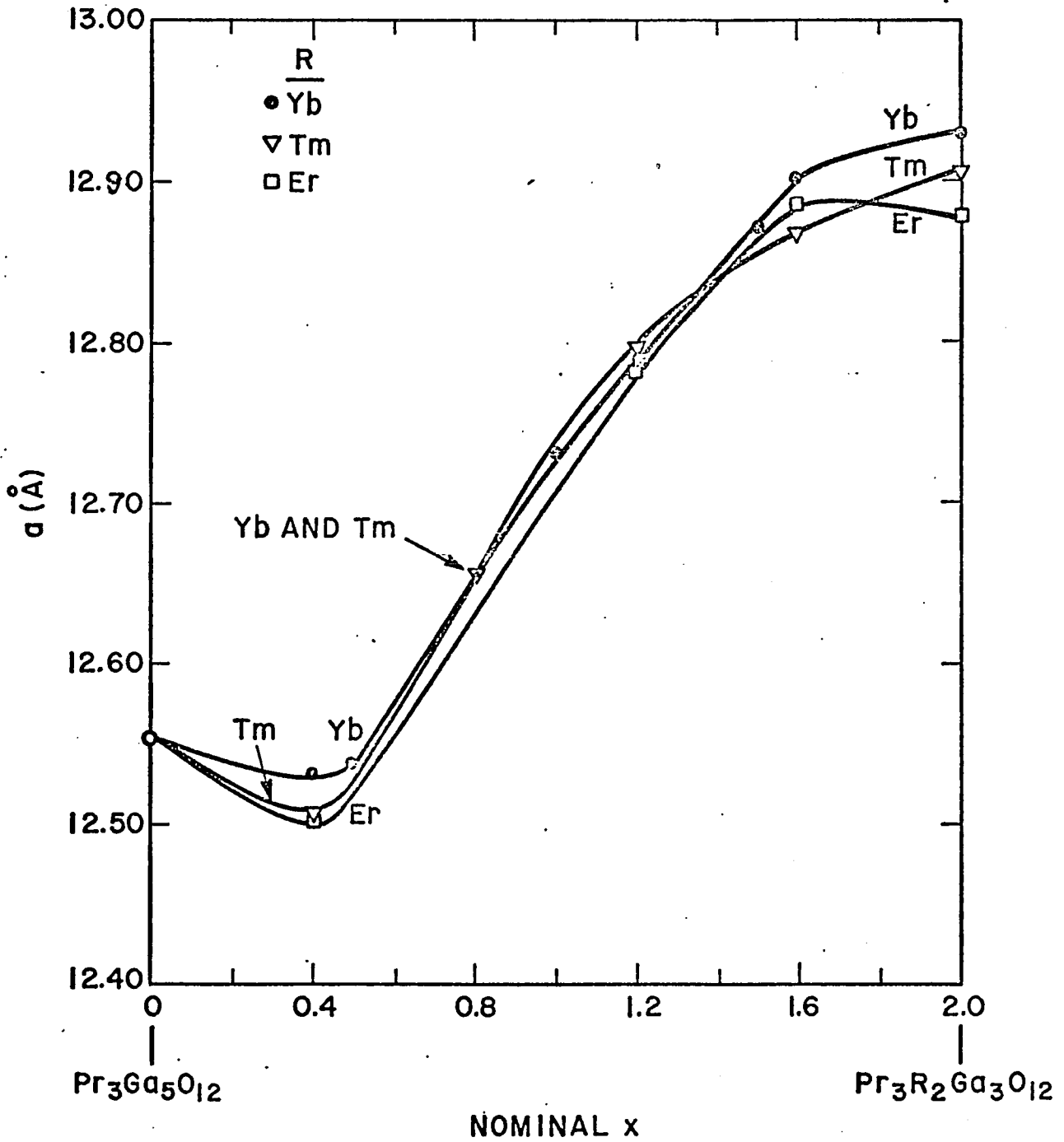
x	a (Å)	Purity
0.0	12.522	Pure
0.4	12.503	Impure
0.8	12.	Very Impure, not measurable
1.2	12.787	Impure
1.6	12.885	Impure
2.0	12.882	Very Impure

III 1.2.3 Discussion of Results. The resulting lattice constants are plotted vs composition in Fig. III - 7. The slopes of the curves in Fig. III - 7 are similar to those of corresponding Nd systems. The segments of different slopes are present but these differences in slopes are even more pronounced than in the former case, suggesting that the small rare earth ion enters the octahedral sites to a greater extent than in the case of Nd^{3+} systems. It was expected that the Pr system would behave similarly to the Nd system, but that there would be some slight differences. It was found that this assumption was correct, and therefore the steps of the experimental procedure chosen were the same as in the system described earlier.

In order to study the effect of y on increasing linearity of the plots of a vs x, two systems have been prepared as listed in following Table III - 15 and Table III - 16, and shown in Fig. III - 8.

FIG. III-7

Lattice constant versus nominal x for nominal $\{Pr_3\}[R_x Ga_{2-x}](Ga_3)O_{12}$



Lattice constant versus nominal x with several values of nominal y for $\{Pr_{3-y} Yb_y\} [Yb_x Ga_{2-x}] (Ga_3) O_{12}$.

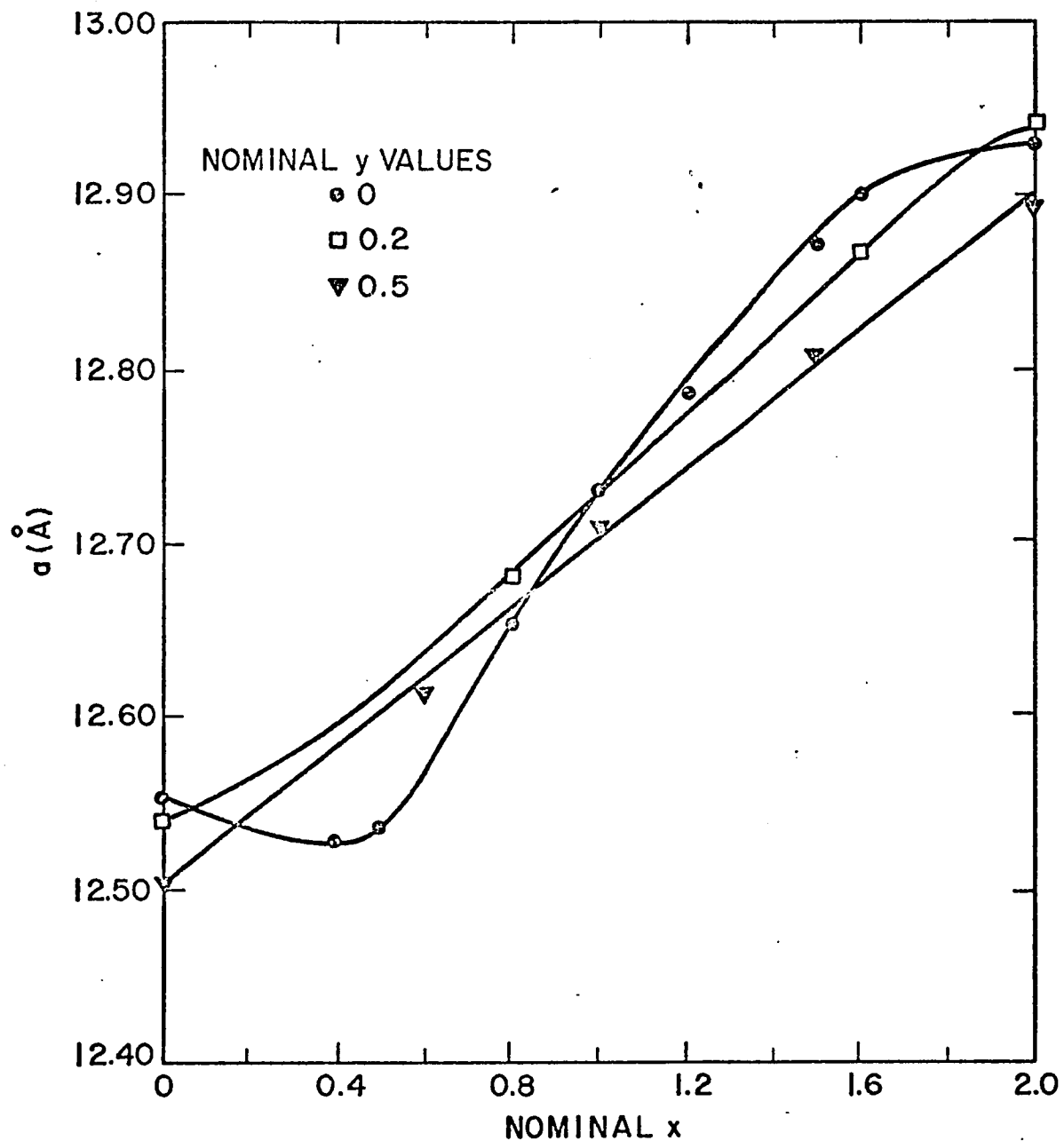


Table III - 15 System $\{Pr_{2.9} Yb_{.2}\} [Yb_x Ga_{2-x}] (Ga_3) O_{12}$
 $y = 0.2$

x	a (Å)	Purity
0.0	12.541	Pure
0.8	12.683	Impure
1.6	12.868	Pure
2.0	12.941	Pure

Table III - 16 System $\{Pr_{2.5} Yb_{.5}\} [Yb_x Ga_{2-x}] (Ga_3) O_{12}$
 $y = 0.5$

x	a (Å)	Purity
0.0	12.505	Pure
0.6	12.610	Pure
1.0	12.710	Pure
1.5	12.810	Pure
2.0	12.890	Pure

The minimum required values of y for Yb, Tm, and Er systems were determined by the same procedure as in the Nd systems, and they were found to be 0.5 for the Yb, 0.8 for the Tm, and 1.15 for the Er systems, respectively. Also the garnet $\{Pr_3\} [Lu_2] (Ga_3) O_{12}$ whose lattice constant is 12.881Å .

Results of these preparations are compiled in Tables III -17 and III - 18, and they are shown graphically in Fig. III - 9.

Table III - 17 System $\{Pr_{2.2} Tm_{.8}\} [Tm_x Ga_{2-x}] (Ga_3) O_{12}$
 $y = 0.8$

x	a (Å)	Purity
0.0	12.480	Pure
0.6	12.590	Pure
1.0	12.670	Pure
1.5	12.770	Pure
2.0	12.882	Pure

Table III - 18 System $\{Pr_{1.85} Er_{1.15}\} [Er_x Ga_{2-x}] (Ga_3) O_{12}$
 $y = 1.15$

x	a (Å)	Purity
0.0	12.433	Pure
0.6	12.564	Pure
1.0	12.652	Pure
1.5	12.770	Pure
1.75	12.823	Pure
2.0	12.860	Slightly Impure

Also as in the Pr system, the minimum required value of y is the value which yields a single-phase material over the entire range of concentrations. However, the end members of the Yb and Tm systems were prepared as single-phase garnets with significantly lower values of y, for example 0.2 for $\{Pr_{3-y} Yb_y\} [Yb_2] (Ga_3) O_{12}$, and 0.3 for $\{Pr_{3-y} Tm_y\} [Tm_2] (Ga_3) O_{12}$. As with the Nd preparations, the maximum possible value of x with $R = Er^{3+}$ was less than 2.

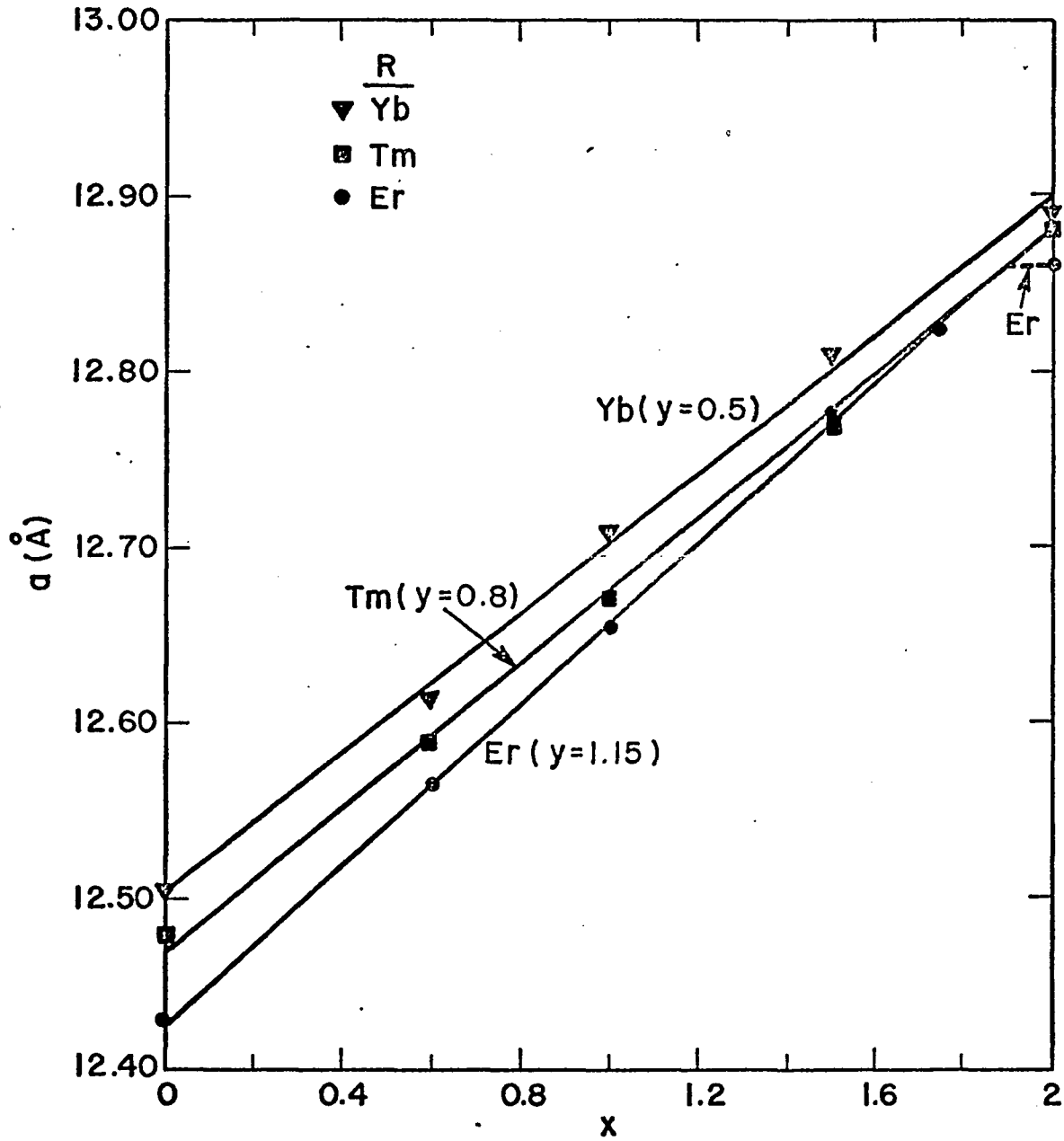
Fig. III 10 contains a plot of the y values required to yield the single-phase Pr garnets and the straight line in Fig. III 9 vs Shannon-Prewitt IR radii for the small rare earth in 8 fold coordination. It also contains a similar plot for the Nd garnets.

In the Nd preparation, it was found that the minimum y value increased with increasing size of the small rare earth ion. The same is true here but it can be seen in addition that the minimum y value for any given small rare earth ion is higher in the Pr materials than in the Nd materials. These results are consistent and may be rationalized on the basis that the radii of both Nd and Pr are somewhat higher than the optimum for such systems. The tendency to reach such an optimum causes some of the smaller rare earth ions to be attracted to the dodecahedral sites in order to decrease the average ionic radius of this site to the optimal value. The smaller the rare earth, R , the smaller amount of it one needs to decrease the average radius to its optimal value. This seems to be true in both Nd and Pr systems.

Therefore, in the case of the larger Pr there is need for a greater value of y than in the Nd system. These values are compared in the following table.

R^{3+}	Nd	Pr		R^{3+}	Nd	Pr
Lu	0.2	--				
Yb	0.3	0.5				
Tm	0.6	0.8				
				Er	1.1	1.15

Lattice constant versus x for $\left\{ \text{Pr}_{3-y} \text{R}_y \right\} \left[\text{R}_x \text{Ga}_{2-x} \right] \left(\text{Ga}_3 \right) \text{O}_{12}$



γ - values required to yield single-phase garnets and straight lines in Fig. 9 (and in Fig. 4) versus ionic radii of trivalent rare earths, R.

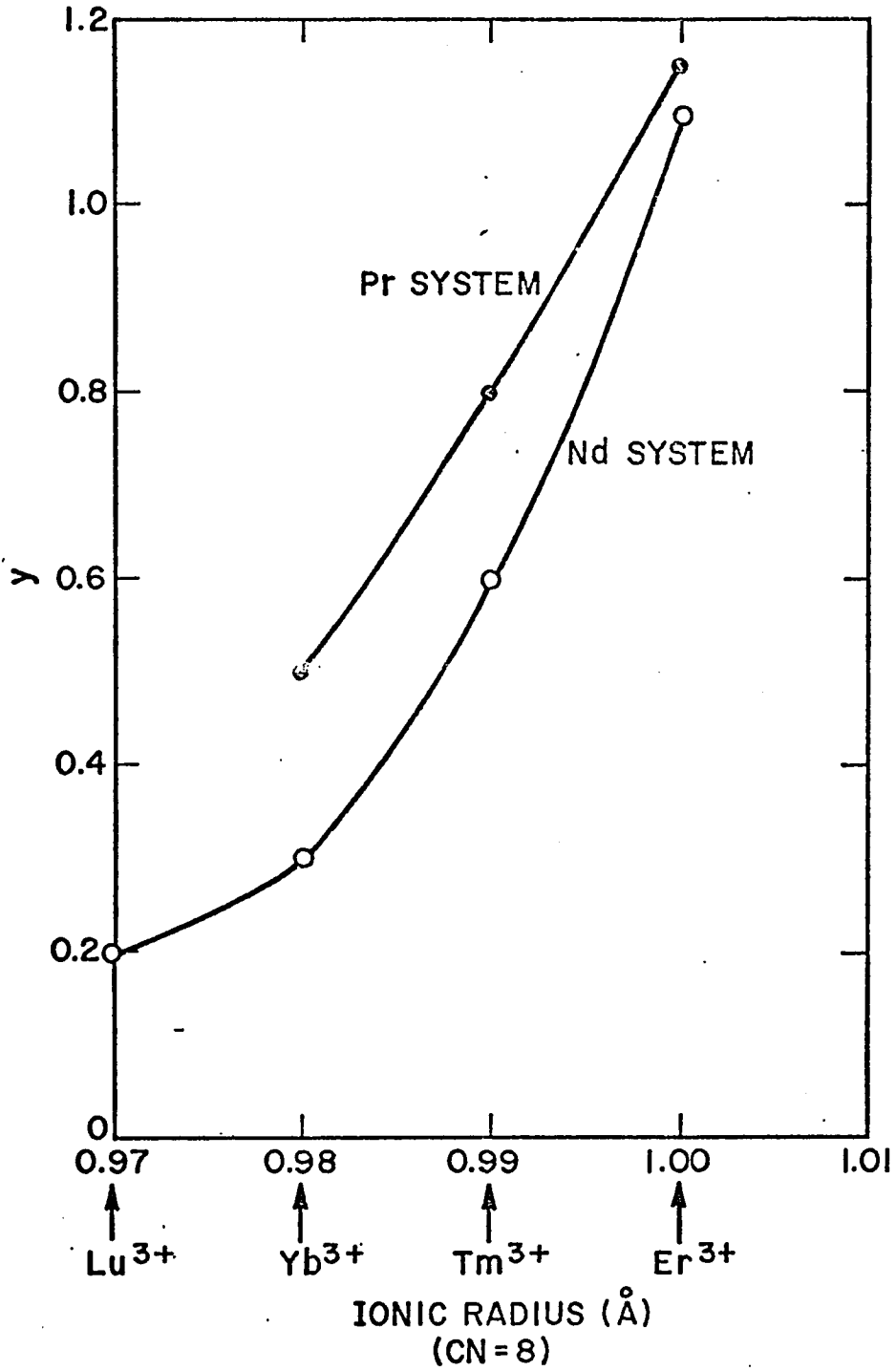


Table III 19 shows the calculated average Shannon-Prewitt (64) "IR" radii for the dodecahedral sites containing Nd^{3+} or Pr^{3+} along with the minimum value of y for various small rare earth ions. The average involving any given small rare earth R are very close for Nd^{3+} and Pr^{3+} but the average decreases slightly as the radius of R^{3+} , which also goes into the octahedral site, increases.

Table III 19. Calculated Average Radii for the Dodecahedral site Containing Nd^{3+} or Pr^{3+} and Minimum y Value Amounts of Small Rare Earth R. Ionic Radii According (64).

R^{3+}	Radius of R^{3+} for Coord. No. 6	Nd^{3+} Compounds	Pr^{3+} Compounds
Yb^{3+}	0.868	1.106	1.114
Tm^{3+}	0.880	1.094	1.100
Er^{3+}	0.890	1.076	1.086

III 2 Rare Earth Iron Garnet with the Octahedral Sites Completely Filled with Nonmagnetic Ions.

As was stated earlier, compounds of this type have attracted the attention of several investigators because such compounds offer possibilities of direct c - d interactions. Loriers and his co-workers (65) studied the systems $\{\text{Gd}_3\} [\text{Sc}_x \text{Fe}_{2-x}] (\text{Fe}_3) \text{O}_{12}$ and $\{\text{Nd}_3\} [\text{Sc}_x \text{Fe}_{2-x}] (\text{Fe}_3) \text{O}_{12}$ but they were not able to prepare compounds with the octahedral sites completely filled with Sc. Geller and his co-workers (60) were not able to prepare garnet $\{\text{Gd}_3\} [\text{Sc}_2] (\text{Fe}_3) \text{O}_{12}$. The only garnet of this group, $\{\text{Gd} \text{Ca}_2\} [\text{Zr}_2] (\text{Fe}_3) \text{O}_{12}$,

was studied by Geller and others (60), and they found that it appeared to be a weak ferromagnet, which was unexpected behavior based on the model of magnetic interactions in the garnet structure. According to this model, the magnetic moments of such compounds should be antiparallel and therefore result in ferrimagnetic interactions.

The behavior of the Nd - Sc - Fe system was reported by Loriers (65, 66). It shows a similarity to systems in the present work in respect to the lattice constant vs, composition plots of similar Ga systems. Because it appeared possible that the concept of simultaneous filling of both dodecahedral and octahedral sites by smaller ions reported in the present work could also be applied to iron systems, the Gd system was studied in some detail, and the end members of similar systems of other rare earth ions were prepared.

III.2.1.1 Preparations. All preparations were made by the same procedure as described for Pr garnets. The only difference was in the heating time periods needed to reach equilibrium. These are listed in the tables for each preparation.

III.2.2.1 Gd - Sc Iron Garnets. The substitution started with the nominal formula for prepared garnet $\{Gd_3\} [Sc_x Fe_{2-x}] (Fe_3) O_{12}$.

III.2.2.2 Results. The results of the preparations are compiled in Table III 20 and shown in Fig. III 11.

Table III 20 System $\{Gd_3\} [Sc_x Fe_{2-x}] (Fe_3) O_{12}$

x	a (Å)	Purity	Heating Time (hrs)
0.0	12.471	Pure	5
0.3	12.488	Pure	5
0.6	12.510	Pure	5
0.9	12.532	Pure	5
1.2	12.563	Slightly Impure	5, 5, 5
1.5	12.594	Slightly Impure	5, 5, 5
1.8	12.600	Impure	5, 5, 5

It was found in Fig. III 11 that the plot of a vs composition follows Vegard's law up to the value of $x = 0.9$. The garnets over this range of compositions are single phases. Above the value $x = 0.9$ the curve is no longer linear but an increase in slope followed by leveling off above the value $x = 1.5$ can be observed. The latter decrease of the slope and leveling off of the curve suggest that some of Sc ions could have entered the dodecahedral sites. The appearance of an impurity phase may be due to Ga ion removed from the dodecahedral sites, and this is consistent with such a suggestion. Several attempts were made to prove this consideration by attaining compounds such as $\{Gd_{3-y} Sc_y\} [Sc_2] (Fe_3) O_{12}$. These attempts were successful at $y = 0.5$, and the single phase garnet $\{Gd_{2.5} Sc_{.5}\} [Sc_2] (Fe_3) O_{12}$ was prepared. Holding the y value constant, the system $\{Gd_{2.5} Sc_{.5}\} [Sc_x Fe_{2-x}] (Fe_3) O_{12}$ was prepared. The results are compiled in Table III 21, and plotted in Fig. III 11.

FIG. III-11.

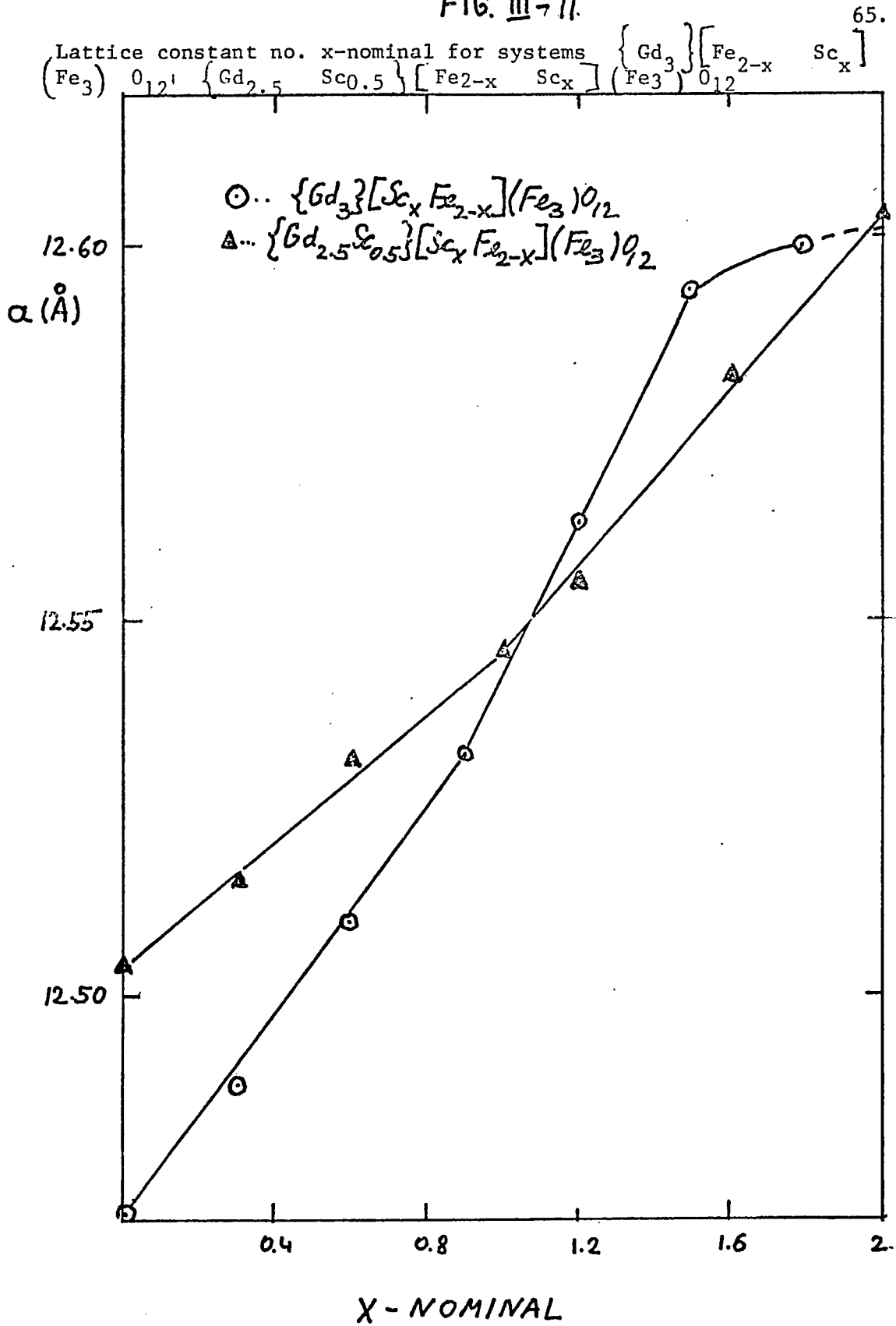


Table III 21 System $\{Gd_{2.5} Sc_{.5}\} [Sc_x Fe_{2-x}] (Fe_3) O_{12}$

x	a (Å)	Purity	Heating Time (Hrs)
0.0	12.504	Slightly Impure	5, 5, 5
0.3	12.515	Slightly Impure	5, 5, 5
0.6	12.532	Slightly Impure	5, 5, 5
1.0	12.546	Slightly Impure	5, 5
1.2	12.555	Pure	5
1.4	12.565	Pure	5
1.6	12.584	Pure	5
2.0	12.604	Pure	5

On inspecting Table III 21 and the plot of the system $\{Gd_{2.5} Sc_{0.5}\} [Sc_x Fe_{2-x}] (Fe_3) O_{12}$ (Fig. III 11), it is found that in this case, the single phase region occurs for values of x larger than .2, and that the plot consists of two linear segments of different slopes. No satisfactory explanation of this behavior can be drawn on the basis of the obtained experimental data.

III 2.3 Related Compounds of General Formula $\{R_{3-y} Sc_y\} [Sc_2] (Fe_3) O_{12}$. Several end members of similar systems with other rare earth ions were prepared and the minimum values of y required to yield a single-phase in the system $\{R_{3-y} Sc_y\} [Sc_2] (Fe_3) O_{12}$ were determined. The resulting compounds are listed in Table III 22.

Table III 22 Compounds $\left\{ R_{3-y} Sc_y \right\} \left[Sc_2 \right] (Fe_3) O_{12}$
 R = Tm, Er, Ho, Dy

Composition	a (Å)	Purity	Heating Time (Hrs.)
$\left\{ Tm_{1.8} Sc_{1.2} \right\} \left[Sc_2 \right] (Fe_3) O_{12}$	--	Pure	5, 5, 5
$\left\{ Er_2 Sc \right\} \left[Sc_2 \right] (Fe_3) O_{12}$	--	Pure	5, 5, 5
$\left\{ Ho_{2.2} Sc_{0.8} \right\} \left[Sc_2 \right] (Fe_3) O_{12}$	12.485	Pure	5, 5, 5
$\left\{ Dy_{2.3} Sc_{0.7} \right\} \left[Sc_2 \right] (Fe_3) O_{12}$	12.520	Pure	5, 5, 5

It is to be noted in Table III 22 that on going along the rare earth series from the lighter ions to the heavier ones the value of y increases. The increase of y value means the decrease of the average ionic radius of the dodecahedral sites. This trend is rather unexpected, and one would certainly expect just the opposite trend because it was shown that the existence of rare earth iron garnets is limited to a certain ionic radius of a rare earth (47, 50). It is possible to prepare iron garnets of all rare earth ions from Sm to Lu but it is impossible to prepare garnets containing only large rare earth ions such as Pr and Nd on the dodecahedral sites. This might suggest the existence of a limit in the value of the lattice constant of the iron garnets, that is, an upper limit for the average ionic radius of the dodecahedral site. The smaller rare earth ions on dodecahedral sites have a smaller y - value to decrease the average ionic size to a proper value for the dodecahedral site.

Substitution of smaller ions on dodecahedral sites makes it possible to prepare single-phase garnet of composition $\left\{ \text{Gd}_{2.5} \text{ Sc}_{0.5} \right\} \left[\text{Sc}_2 \right] \left(\text{Fe}_3 \right) \text{O}_{12}$. According to the above reasoning the garnet with smaller Dy^{3+} on dodecahedral sites should have a y value smaller than 0.5.

The experimental results show that this reasoning is incorrect and the opposite situation is true (see Table III 22). Conditions of the existence of iron garnets depend on factors other than ionic radii alone. When this discrepancy is analysed in terms of differences between ionic radii of ions on dodecahedral and octahedral sites, it is found that the results are consistent with the situation in the systems $\left\{ \text{Nd}_{3-y} \text{ R}_y \right\} \left[\text{R}_x \text{ Ga}_{2-x} \right] \left(\text{Ga}_3 \right) \text{O}_{12}$ and $\left\{ \text{Pr}_{3-y} \text{ R}_y \right\} \left[\text{R}_x \text{ Ga}_{2-x} \right] \left(\text{Ga}_3 \right) \text{O}_{12}$. In the Nd case, the y - value increases when the difference between ionic radius of Nd and R decreases. The same is true for the y - value in Pr systems. In the case of iron garnets with Sc on the octahedral site, the y - value also increases as the difference between ionic radius of Sc and ionic radii of rare earth ions on the dodecahedral site decreases. It is also noteworthy that garnets containing Lu and Yb could not be prepared under the same experimental conditions. More detailed studies would be required in order to explain the irregular behavior of the iron garnet systems. The most helpful one would be structural refinements on single crystals of the above mentioned compositions.

III.2.4 Systems with Large Rare Earth on the Dodecahedral Sites.

III.2.4.1 Neodymium Scandium Iron System. All attempts to prepare the compound $\{Nd_3\}[Sc_2](Fe_3)O_{12}$ have been unsuccessful up to now, and it is also very well known that even $Nd_3 Fe_5 O_{12}$ garnet does not exist. The previous results obtained from gallium garnet systems with rare earth ions on two crystallographic sites, especially the y-values found to be necessary in order to synthesize single phase garnets, encouraged the idea that it might be possible to prepare garnets with large rare earth ions on the dodecahedral sites and Sc ions on the octahedral sites. The approach of distributing Sc ions among the dodecahedral and the octahedral sites proved to be successful in the cases of smaller rare earth on c sites, and it resulted in the preparation of a few new materials.

An attempt to determine the y value in the system $\{Nd_{3-y} Sc_y\}[Sc_2](Fe_3)O_{12}$ was made. The runs were started with $y = 0.1$, and increasing the value of y up to $y = 1.5$, fifteen runs were made. It was found that no single phase resulted nor was any improvement observed toward decreasing the amount of extra phases.

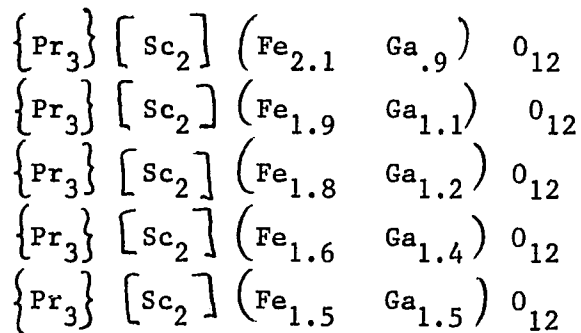
Therefore it was concluded that Nd and Sc do not mix on one type of crystallographic sites. This is probably so because the big difference of ionic radii of Nd^{3+} and Sc^{3+} does not favor solid solution formations.

Because of the failure of the above mentioned approach, a different procedure was tried. It was concluded that in order to decrease the resulting lattice constant the average ionic radius of the tetrahedral sites should be decreased by introducing ions

smaller than Fe^{3+} on the d sites along with Fe^{3+} ions. Attempts to decrease the average ionic radius of the d sites using Al^{3+} ions were not successful either, probably because an AlO_4 tetrahedron would have edges too short to match the Nd^{3+} dodecahedra with which two of them are shared. Therefore, Ga^{3+} ions were chosen for the substitution in d sites because it is known that in the Ga^{3+} case there are no such difficulties.

The formula $\{\text{Nd}_3\}[\text{Sc}_2](\text{Fe}_{3-z} \text{Ga}_z) \text{O}_{12}$ expresses the composition of attempted preparations. The first value of z was 0.1 and it was added in increments of 0.1 until the single-phase garnet was produced. The formula of the single-phase material was found to be $\{\text{Nd}_3\}[\text{Sc}_2](\text{Fe}_{2.2} \text{Ga}_{0.8}) \text{O}_{12}$ with a lattice constant of $a = 12.721 \text{ \AA}$.

III.2.4.2 Praseodymium Scandium Iron System. Following the same procedure as that described in the previous paragraph, several compositions were found to yield single-phase garnets:



III.2.4.3 Discussion of Results. The lattice constants of the new garnets are the main measurable parameters on which any conclusions about ionic distribution are based in the systems

studied. For this reason, it was attempted to predict lattice constants which should result when proposed composition together with proposed ionic distribution is obtained. The calculations were based on the fact that Sc^{3+} ions on the tetrahedral sites cause an increase of 0.14 \AA in the iron garnet lattice when Sc^{3+} fills the a sites completely. The difference between lattice constants of corresponding Fe and Ga garnets is 0.100 \AA . Together with the experimental values of lattice constants of $\{\text{Nd}_3\} \text{Ga}_5 \text{O}_{12}$ and $\{\text{Pr}_3\} \text{Ga}_5 \text{O}_{12}$ these findings allow calculation of the lattice constants for a given composition. Lattice constant calculations are discussed in section IV of this work. In Table III 23, observed values of the lattice constants are compared with values calculated as indicated above.

Table III 23

Composition	a (Å) Observed	a (Å) Cal.	a (Å)
$\{\text{Nd}_3\} [\text{Sc}_2] (\text{Fe}_{2.2} \text{Ga}_{.8}) \text{O}_{12}$	12.721	12.722	-0.001
$\{\text{Pr}_3\} [\text{Sc}_2] (\text{Fe}_{2.1} \text{Ga}_{.9}) \text{O}_{12}$	12.740	12.762	-0.002
$\{\text{Pr}_3\} [\text{Sc}_2] (\text{Fe}_{1.9} \text{Ga}_{1.1}) \text{O}_{12}$	12.748	12.755	-0.007
$\{\text{Pr}_3\} [\text{Sc}_2] (\text{Fe}_{1.8} \text{Ga}_{1.2}) \text{O}_{12}$	12.764	12.752	+0.012
$\{\text{Pr}_3\} [\text{Sc}_2] (\text{Fe}_{1.6} \text{Ga}_{1.4}) \text{O}_{12}$	12.760	12.745	+0.015
$\{\text{Pr}_3\} [\text{Sc}_2] (\text{Fe}_{1.5} \text{Ga}_{1.5}) \text{O}_{12}$	12.759	12.742	+0.017

When Table III 23 is inspected, it is seen that the observed and calculated values of a are in fair agreement except for $\{\text{Pr}_3\}[\text{Sc}_2](\text{Fe}_{2.1} \text{ Ga}_{.9})_{012}$ where the experimental value is lower by 0.02 \AA , and for $\{\text{Pr}_3\}[\text{Sc}_2](\text{Fe}_{1.6} \text{ Ga}_{1.4})_{012}$ and $\{\text{Pr}_3\}[\text{Sc}_2](\text{Fe}_{1.5} \text{ Ga}_{1.5})_{012}$, where the observed values are higher by 0.02 \AA . The lower value of a is a more serious discrepancy because it could indicate that there was not enough Sc_2O_3 used in the original mixture of oxides so that some iron had to enter the octahedral sites, and it resulted in a decrease in the value of the lattice constant. The higher value of a indicates that this calculation is not quite accurate.

III 3 Garnets with Rare Earth on the Octahedral and Dodecahedral Sites Containing Fe Ions on the Tetrahedral Sites.

An attempt was made to replace gallium by iron in systems with Nd and rare earth ions on both octahedral and dodecahedral sites. Such garnets would create a new group of materials employing a - d magnetic interactions of such type have not previously been studied in the garnet system, and it is therefore not known how the octahedrally coordinated rare earth fits the model of the magnetic interactions in the garnet structure. Such studies could not be carried out because there was no known garnet of the required composition, that is with rare earth on a sites and iron on d sites. In order to explore the possibilities of obtaining such compounds, substitution according to the formula $\{\text{Nd}_{2.7} \text{ Yb}_{.3}\}[\text{Yb}_2](\text{Ga}_{3-z} \text{ Fe}_z)_{012}$ was attempted. This system was chosen because c and a sites are completely filled with rare earth ions, and no rare earth ion can

enter d sites. The iron substituted on d sites does not have any place to go except this site, and as long as a single-phase garnet results, the ionic distribution is determined by the composition of the reactant mixture. It was learned later that the amount of Yb on the dodecahedral sites (y value) changes when higher values of z are reached (over $z = 0.8$). Single-phase compounds with a z value greater than 0.8 were obtained by changing values of y in the system $\{Nd_{3-y} Yb_y\} [Yb_2] (Ga_{3-z} Fe_z) O_{12}$. All preparations were made at $1350^\circ C$. It was found that the preparation of single phase garnets with greater z values than 0.8 requires significantly prolonged heating. These compounds were obtained as single phases only after three or four times repeated heating, each at least for twenty-four hours.

Resulting compounds obtained as single phases are compiled in Table III 24. The greatest amount of iron substituted on d sites corresponds to $z = 1.4$. Such a concentration of iron on d sites could be sufficient to provide enough active linkage for magnetic interactions since c and a sites are completely filled with magnetic ions.

Table III 24 System $\{Nd_{3-y} Yb_y\} [Yb_2] (Ga_{3-z} Fe_z) O_{12}$

y	z	a (Å)	Preparation Conditions Firing Time (hrs). (in Separate Periods)
0.3	0.2	12.860	5, 5, 5
0.3	0.4	12.864	5, 5
0.3	0.6	12.864	5, 5
0.3	0.8	12.866	5, 5
0.2	1.0	12.881	3, 5, 24, 24
0.2	1.2	12.881	5, 24, 24, 24
0.35	1.3		24, 24, 24
0.45	1.4		24, 24, 24, 24

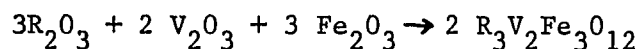
III 4 Garnet Compounds with Trivalent Vanadium.

Decreasing the number of active magnetic linkages (magnetic dilution) is the greatest problem when an attempt to increase net magnetic moment of YIG is made by substitution of nonmagnetic ions on the octahedral sites. The magnetic dilution can be avoided by substitution of suitable magnetic ions with smaller magnetic moment on a sites of the YIG, and thus increasing the net magnetic moment of the iron garnet. The V^{3+} ion with two d - electrons capable of giving a ferrimagnetic moment of $2\mu_B$ seems to be suitable for such substitution. The net magnetic moment of the theoretical compound $\{Y_3\} [V_2] (Fe_3) O_{12}$ should be $11\mu_B$ compared with $5\mu_B$ for YIG. Another reason which supports the choice of V^{3+} is the fact that octahedrally coordinated V^{3+} has the same ionic radius of 0.645 Å as octahedrally coordinated Fe^{3+} ion. The same ionic radii would imply that there should not be any structural restrictions for V^{3+}

entering in place of Fe^{3+} . It was also established (8) that V^{3+} ion does enter the octahedral sites of the garnet structure in compounds like $\text{Ca}_3 \text{V}_2 \text{Si}_3 \text{O}_{12}$ (24) or $\text{Ca}_3 \text{V}_2 \text{Ge}_3 \text{O}_{12}$ (34). But there is no reported garnet compound composed of trivalent cations containing only trivalent vanadium.

III.4.1 Substitution of V^{3+} in Iron Garnets.

III.4.1.2 Preparation. The preparation of the proposed compounds $\text{R}_3 \text{V}_2 \text{Fe}_3 \text{O}_{12}$ was based on solid state reaction among oxides.



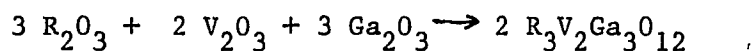
The oxides used for the preparation were 99.9% Fe_2O_3 , 99.9% rare earth oxides, and V_2O_3 prepared by the reduction of 99.9% V_2O_5 by charcoal. The appropriate amounts of oxides were mixed in an agate mortar and sealed in vacuum in fused silica tubes after flushing with argon. The samples were heated for three hours at 400°C , and after that the temperature was increased to 960°C , and after two hours firing the samples were quenched to room temperature by removing them from the furnace.

III.4.1.3 Results and Discussion. The attempted compositions were $\{\text{Sm}_3\}[\text{V}_2](\text{Fe}_3)\text{O}_{12}$ and $\{\text{Gd}_3\}[\text{V}_2](\text{Fe}_3)\text{O}_{12}$. In both cases, the resulting compounds had dark green colors, and x-ray diffraction revealed garnet phases with impurities also present. The x-ray powder patterns had poor back reflections, and therefore lattice constant measurements could not be accomplished. Because of the same ionic radii of V^{3+} and Fe^{3+} on the octahedral sites

in garnets, the lattice constants of proposed compounds should be the same as lattice constants of their iron analogs. Only if the reaction would result in single phase garnet could the conclusion could be drawn that the substitution followed the proposed reaction. However, this was not the case with these preparations, and therefore no conclusion concerning the substitution of V^{3+} on the octahedral sites of the iron garnet could be drawn.

III .4.2 Substitution of V^{3+} in Gallium Garnets.

III.4.2.1 Preparation. The preparations were proposed according to the solid state reaction.

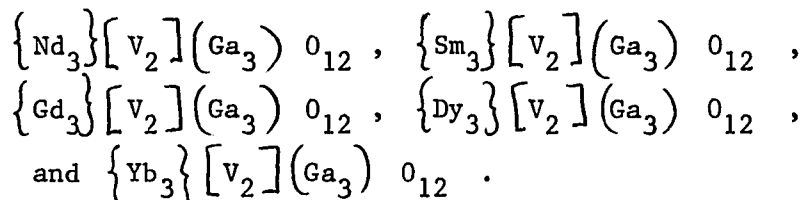


Ga_2O_3 99.9%, rare earth oxides at least 99.9% pure, and V_2O_3 prepared by reducing 99.9% pure V_2O_5 were used. Because it was found, while working with the iron system with fused silica tubes, that silica was visibly attacked by rare earth oxides at elevated temperatures, the runs were done in open Pt crucibles and in graphite crucibles under a nitrogen atmosphere. Weighed amounts of oxides were mixed together in an agate mortar and transferred into crucibles. Each crucible containing a mixture of reactants was placed in a silica tube 5 inches in diameter provided with an insulated stopper and silica tubing for delivery of nitrogen gas. The silica tube was inserted into the furnace and heated to 200° C. Then the temperature was increased to 1100° C. At this temperature, the samples were heated for one hour. After one hour, the furnace was switched off and allowed to cool, while the nitrogen gas was

running through. The cooling took six hours.

III.4.2.2 Results and Discussion. The garnets whose

preparation was attempted were:



All preparations resulted in materials mostly consisting of garnet phases, but some impurities were also present. The extent to which the substitution actually proceeded, can be deduced from the lattice parameter a because the V^{3+} ion is larger than Ga^{3+} and so would increase the size of the unit cell. The difference in lattice constants of $\left\{ \text{R}_3 \right\} \text{Ga}_5 \text{O}_{12}$ and $\left\{ \text{R}_3 \right\} \left[\text{V}_2 \right] \left(\text{Ga}_3 \right) \text{O}_{12}$, calculated from the difference of ionic radii, is 0.04 \AA . Results of these preparations along with the calculated lattice constants appear in Table III 25.

Table III. 25

Nominal Composition	Purity	a (\AA) Exper.	a (\AA) Calc.	a (\AA) of $\text{R}_3\text{Ga}_5\text{O}_{12}$
$\left\{ \text{Nd}_3 \right\} \left[\text{V}_2 \right] \left(\text{Ga}_3 \right) \text{O}_{12}$	Impure	12.524	12.544	12.504
$\left\{ \text{Sm}_3 \right\} \left[\text{V}_2 \right] \left(\text{Ga}_3 \right) \text{O}_{12}$	Impure	12.460	12.480	12.440
$\left\{ \text{Gd}_3 \right\} \left[\text{V}_2 \right] \left(\text{Ga}_3 \right) \text{O}_{12}$	Impure	12.406	12.415	12.375
$\left\{ \text{Dy}_3 \right\} \left[\text{V}_2 \right] \left(\text{Ga}_3 \right) \text{O}_{12}$	Impure	12.348	12.354	12.314
$\left\{ \text{Yb}_3 \right\} \left[\text{V}_2 \right] \left(\text{Ga}_3 \right) \text{O}_{12}$	Slightly Impure	12.248	12.251	12.211

The conclusion can be drawn, based on the increase of lattice constants, that V^{3+} ion enters the octahedral sites of the gallium garnets. The impurity phase was identified as RVO_4 , with the YVO_4 structure. The appearance of vanadates shows that the apparatus was not perfect, and oxidation of some V^{3+} to V^{5+} took place. The studies of these systems were discontinued because of experimental difficulties.

IV. LATTICE CONSTANT CALCULATIONS.

As was mentioned earlier, the assumptions which permitted assignments of ions to different crystallographic sites are derived from the selectivity of the garnet structure with respect to various ions, and from the values of lattice constants. To obtain a single-phase material of known composition is of course a necessary condition. The lattice constant and its variation with composition is of extreme importance in all kinds of such analysis, especially when no other means are easily available for the determination of ionic distribution. Especially in cases when a given ion can enter more than one crystallographic site, the agreement of the experimental value with the calculated value of the lattice constant can confirm the attempted ionic distribution. However, the calculation of the lattice constant of the garnet unit cell cannot be based on simple geometry assumptions because the unit cell is not derived from close packed structures. The analytical solution could be derived from the data supplied by structural refinement measurements.

IV.1 Analytical Calculations.

An attempt was made to derive analytically an expression for lattice constant calculations for rare earth garnets of the type $\left\{ R_3^{3+} \right\} M_5^{3+} O_{12}$. The fraction of the unit cell along the $[001]$ direction where the rare earth dodecahedron shares edges with an M^{3+} tetrahedron, was taken into account. The fraction of the unit cell used for the derivation appears in Fig. IV 1.

Several assumptions were made:

- a) The tetrahedron is distorted and is always stretched along the $[001]$ direction (20). The distortion values were assumed to be constant for all garnets with a given cation on the tetrahedral site.
- b) All ions were assumed to be rigid spheres.
- c) The distances $R - O$ in chains along $[001]$ were assumed to be independent of the type of M^{3+} ions. The notation for these distances is d_{80} .

The geometrical relationship which could be derived from Fig. IV .1, is:

$$\frac{a}{4} = (R_t + R_0) \cos\theta_1 + d_{80} \cos\theta_2 \quad (\text{IV} - 1)$$

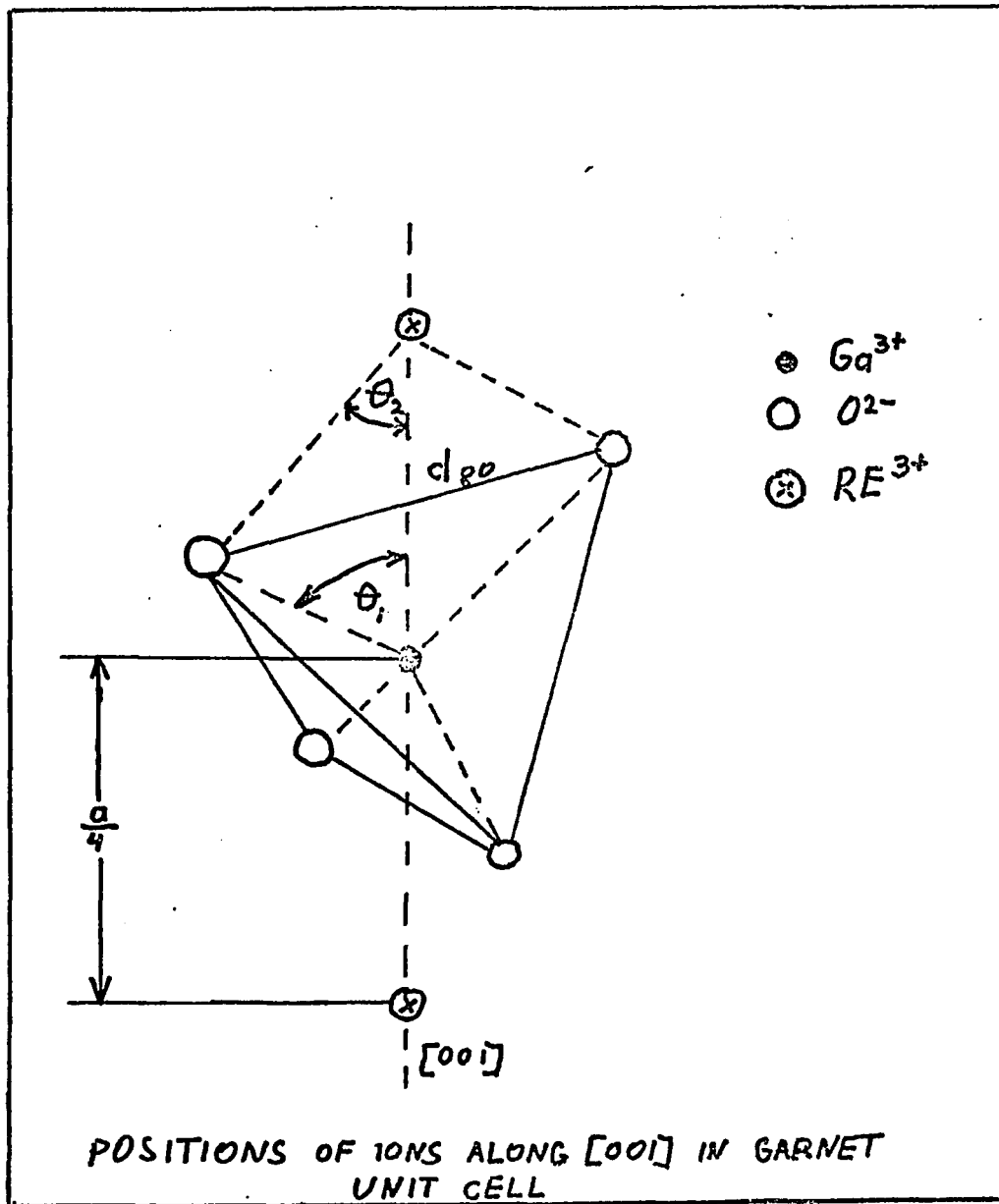
$$(R_t + R_0) \sin\theta_1 = d_{80} \sin\theta_2 \quad (\text{IV} - 2)$$

where R_t is ionic radius of the tetrahedral ion, and R_0 is the radius of oxygen.

The structural refinement of YIG was used to calculate θ_1 for iron garnet (12) using expressions IV 1 and IV 2. Then the set of d_{80} distances was calculated for the whole series of rare earth ions using the set of ionic radii given in (64) and reported values of lattice constants of rare earth iron garnets. These values can be applied in the expression for calculating lattice constants of rare earth garnets of the type $R_3 M_5 O_{12}$. This expression was derived from IV 1 and IV 2.

$$a = 4 \left[(R_t + R_0) \cos\theta_1 + \sqrt{d_{80}^2 - (R_t + R_0)^2 \sin^2\theta_1} \right] \quad (\text{IV} 3)$$

FIG. IV-1



Detail of garnet structure along $[001]$ direction.

The only unknown in this expression is the angle θ_1 . Its variation actually is the measure of the stretching of the given tetrahedron along 001 direction. According to assumption a above, this angle can be calculated from the knowledge of the lattice constant of one garnet in the given group, using the expression IV 3.

The values of d_{80}° calculated for rare earth ions appear in Table IV 1.

Table IV 1

Ion	d_{80}° (Å)	Radii of rare earth ions CN = 8
Pr ³⁺	2.414	1.14
Nd ³⁺	2.405	1.12
Sm ³⁺	2.390	1.09
Eu ³⁺	2.384	1.07
Gd ³⁺	2.380	1.06
Dy ³⁺	2.366	1.03
Ho ³⁺	2.360	1.02
Er ³⁺	2.354	1.00
Tm ³⁺	2.349	0.99
Yb ³⁺	2.345	0.98

For gallium garnets, $\cos\theta_1 = 0.641$ for the GaO_4 tetrahedron was calculated from the experimental a of $\text{Yb}_3\text{Ga}_5\text{O}_{12}$. Using IV 1, the lattice constants of gallium rare earth garnets were calculated and compared to the experimental value. The results appear in Table IV 2.

Table IV 2.

Composition	a (Å) Exper.	a (Å) Calc.
$\text{Yb}_3\text{Ga}_5\text{O}_{12}$	12.211	12.209
$\text{Tm}_3\text{Ga}_5\text{O}_{12}$	12.229	12.229
$\text{Er}_3\text{Ga}_5\text{O}_{12}$	12.255	12.254
$\text{Ho}_3\text{Ga}_5\text{O}_{12}$	12.282	12.284
$\text{Dy}_3\text{Ga}_5\text{O}_{12}$	12.314	12.314
$\text{Gd}_3\text{Ga}_5\text{O}_{12}$	12.375	12.384
$\text{Eu}_3\text{Ga}_5\text{O}_{12}$	12.405	12.404
$\text{Sm}_3\text{Ga}_5\text{O}_{12}$	12.440	12.434
$\text{Nd}_3\text{Ga}_5\text{O}_{12}$	12.504	12.508
$\text{Pr}_3\text{Ga}_5\text{O}_{12}$	12.552	12.553

The agreement in the above table is fair in spite of the fact that the above mentioned assumptions are not perfectly correct, but unfortunately equation IV 3 holds only for simple compounds such as $\text{R}_3\text{M}_5\text{O}_{12}$ and is therefore of rather restricted use. To make a similar derivation for more complex compounds is not possible because there are no available data of structural refinements of such compounds.

IV 2 Empirical Calculation.

The problem of prediction of the lattice constants had to be approached on a more empirical basis using lattice constants collected from experimental work and conclusions were drawn from the distribution of ions on different sites. When an ion enters one of the sublattices in the garnet structure the resulting effect on the lattice constant depends on the change of the average ionic radius of ions which occupy the site in question. As the average radius of ions on the given site decreases, the lattice constant should also decrease. Similarly, the lattice constant should increase as the average radius of ions on the given site increases. Employing these assumptions, a formula was developed for calculating lattice constants of new garnets (67). The increase or decrease of the lattice constant of a garnet is proportional to the increase or decrease of the average ionic radius caused by substitution. Therefore, the change in the lattice constant is given by the difference between the ionic radius of an ion in a new garnet and the ionic radius of the ion in a reference garnet multiplied by a proportionality constant. It was found that the proportionality constant is different for different sublattices. Proportionality constants for gallium garnets were determined in the following way:

$$K_{\text{DOD}} \frac{\Delta a}{\Delta r_{\text{DOD}}} = \frac{a(\text{Nd}_3 \text{Ga}_5 \text{O}_{12}) - a(\text{Yb}_3 \text{Ga}_5 \text{O}_{12})}{r_{\text{Nd}^{3+}} - r_{\text{Yb}^{3+}}} = 2.15$$

$$K_{\text{Oct}} \frac{\Delta a}{\Delta r_{\text{Oct}}} = \frac{a(\text{Nd}_3 \text{Lu}_2 \text{Ga}_3 \text{O}_{12}) - a(\text{Nd}_3 \text{Ga}_5 \text{O}_{12})}{r_{\text{Lu}^{3+}} - r_{\text{Ga}^{3+}}} = 1.56$$

Using these constants, the formula for calculation of constants of gallium garnets can be written:

$$a_{\text{calc}} = (\text{average } r_{\text{DOD}} - r_{\text{Nd}^{3+}}) \times K_{\text{DOD}} + (\text{average } r_{\text{oct}} - r_{\text{Ga}^{3+}}) \times K_{\text{oct}} + a_{\text{Nd}_3\text{Ga}_5\text{O}_{12}} \quad (\text{IV } 1)$$

or

$$a_{\text{calc}} = (\text{average } r_{\text{DOD}} - 1.12) \times (2.15) + (\text{average } r_{\text{oct}} - 0.620) \times (1.56) + 12.504 \quad (\text{IV } 2)$$

where r_{DOD} and r_{oct} represent radii of ions on the dodecahedral and the octahedral sites, respectively. Observed and calculated lattice constants of prepared garnets (using Shannon-Prewitt IR radii (64)) are listed in Tables IV 3-5.

Table IV 3 Observed and Calculated Lattice Constants of
Neodymium-Gallium Garnets

Compound or Solid Solution	Observed a (Å)	Calculated a (Å)
$\{Nd_3\} [Ga_2] (Ga_3)_{0_{12}}$	12.50 ₄	a
$\{Yb_3\} [Ga_2] (Ga_3)_{0_{12}}$	12.20 ₃	a
$\{Nd_3\} [Lu_2] (Ga_3)_{0_{12}}$	12.88 ₁	a
$\{Nd_3\} [Yb_2] (Ga_3)_{0_{12}}$	12.89 ₀ ⁶	12.89
$\{Nd_3\} [Tm_2] (Ga_3)_{0_{12}}$	12.88 ₂ ^b	12.91
$\{Nd_3\} [Er_2] (Ga_3)_{0_{12}}$	12.83 ₁ ^b	12.93
$\{Nd_3\} [Ho_2] (Ga_3)_{0_{12}}$	12.65 ₂ ^b	12.94
$\{Nd_3\} [Dy_2] (Ga_3)_{0_{12}}$	12.51 ₀ ^b	12.96
$\{Nd_{2.8} Lu_{.2}\} [Lu_2] (Ga_3)_{0_{12}}$	12.86 _b	12.86
$\{Nd_{2.7} Yb_{.3}\} [Yb_2] (Ga_3)_{0_{12}}$	12.86 ₄	12.86
$\{Nd_{2.5} Yb_{.5}\} [Yb_2] (Ga_3)_{0_{12}}$	12.85 ₅	12.84
$\{Nd_{2.4} Tm_{.6}\} [Tm_2] (Ga_3)_{0_{12}}$	12.85 ₄	12.85
$\{Nd_{1.9} Er_{1.1}\} [Er_2] (Ga_3)_{0_{12}}$	12.81 ₃ ^b	12.83

a - calculation based on these

b - from nominal compositions

c - note that this preparation contains more Yb (y = 0.5) on the dodecahedral site than the minimum (y = 0.3) required to obtain a single phase-garnet.

Table IV 4 Observed and Calculated Lattice Constants of Some
Other Rare Earth Gallium Garnets.

Compound	Observed a (Å)	Calculated a (Å)
$\{\text{Tm}_3\} [\text{Ga}_2] (\text{Ga}_3)_{0_{12}}$	12.22	12.22
$\{\text{Er}_3\} [\text{Ga}_2] (\text{Ga}_3)_{0_{12}}$	12.25	12.25
$\{\text{Ho}_3\} [\text{Ga}_2] (\text{Ga}_3)_{0_{12}}$	12.28	12.29
$\{\text{Dy}_3\} [\text{Ga}_2] (\text{Ga}_3)_{0_{12}}$	12.31	12.31

The correspondence of calculated and observed values from Table IV 2, and Table IV 3 is good in cases where prepared compounds were single-phases. In addition, it can be observed that in the case of neodymium systems the agreement is better than in the case of praseodymium preparations. This might be due to the fact that calculation of proportionality constants for Eq.IV.1 were based on neodymium preparations and any experimental error in determination of lattice constants of these preparations is reflected in the other systems. Improvement of these calculations could be obtained by employing high precision measurement of lattice constants. However, calculations made as shown here serve their purpose satisfactorily especially if one is aware fo the source of the error and its value.

Table IV 5 Observed and Calculated Lattice Constants of
Praseodymium-Gallium Garnets.

Composition	Observed a (Å)	Calculated a (Å)
$\{\text{Pr}_3\} [\text{Ga}_2] (\text{Ga}_3)_{0_{12}}$	12.55 ₂	12.55
$\{\text{Pr}_3\} [\text{Lu}_2] (\text{Ga}_3)_{0_{12}}$	12.94 ₂	12.92
$\{\text{Pr}_3\} [\text{Yb}_2] (\text{Ga}_3)_{0_{12}}$	12.928 ^a	12.93
$\{\text{Pr}_{2.5} \text{ Yb}_{.5}\} [\text{Ga}_2] (\text{Ga}_3)_{0_{12}}$	12.50 ₅	12.49
$\{\text{Pr}_{2.5} \text{ Yb}_{.5}\} [\text{Yb Ga}] (\text{Ga}_3)_{0_{12}}$	12.70 ₆	12.68
$\{\text{Pr}_{2.5} \text{ Yb}_{.5}\} [\text{Yb}_2] (\text{Ga}_3)_{0_{12}}$	12.89	12.88
$\{\text{Pr}_3\} [\text{Tm}_2] (\text{Ga}_3)_{0_{12}}$	12.90 ₄ ^b	12.95
$\{\text{Pr}_{2.2} \text{ Tm}_{.8}\} [\text{Ga}_2] (\text{Ga}_3)_{0_{12}}$	12.48	12.46
$\{\text{Pr}_{2.2} \text{ Tm}_{.8}\} [\text{Tm Ga}] (\text{Ga}_3)_{0_{12}}$	12.67	12.66
$\{\text{Pr}_{2.2} \text{ Tm}_{.8}\} [\text{Tm}_2] (\text{Ga}_3)_{0_{12}}$	12.88 ₂	12.87
$\{\text{Pr}_3\} [\text{Er}_2] (\text{Ga}_3)_{0_{12}}$	12.88 ₂	12.97
$\{\text{Pr}_{1.85} \text{ Er}_{1.15}\} [\text{Ga}_2] (\text{Ga}_3)_{0_{12}}$	12.43	12.43
$\{\text{Pr}_{1.85} \text{ Er}_{1.15}\} [\text{Er}_{1.75} \text{ Ga}_{.25}] (\text{Ga}_3)_{0_{12}}$	12.82 ₃	12.80
$\{\text{Pr}_{1.85} \text{ Er}_{1.15}\} [\text{Er}_2] (\text{Ga}_3)_{0_{12}}$	12.86 ^a	12.85

a - almost single-phase

b - nominal composition

V. RESULTS OF MAGNETIC MEASUREMENTS

V.1 Preliminary Measurements

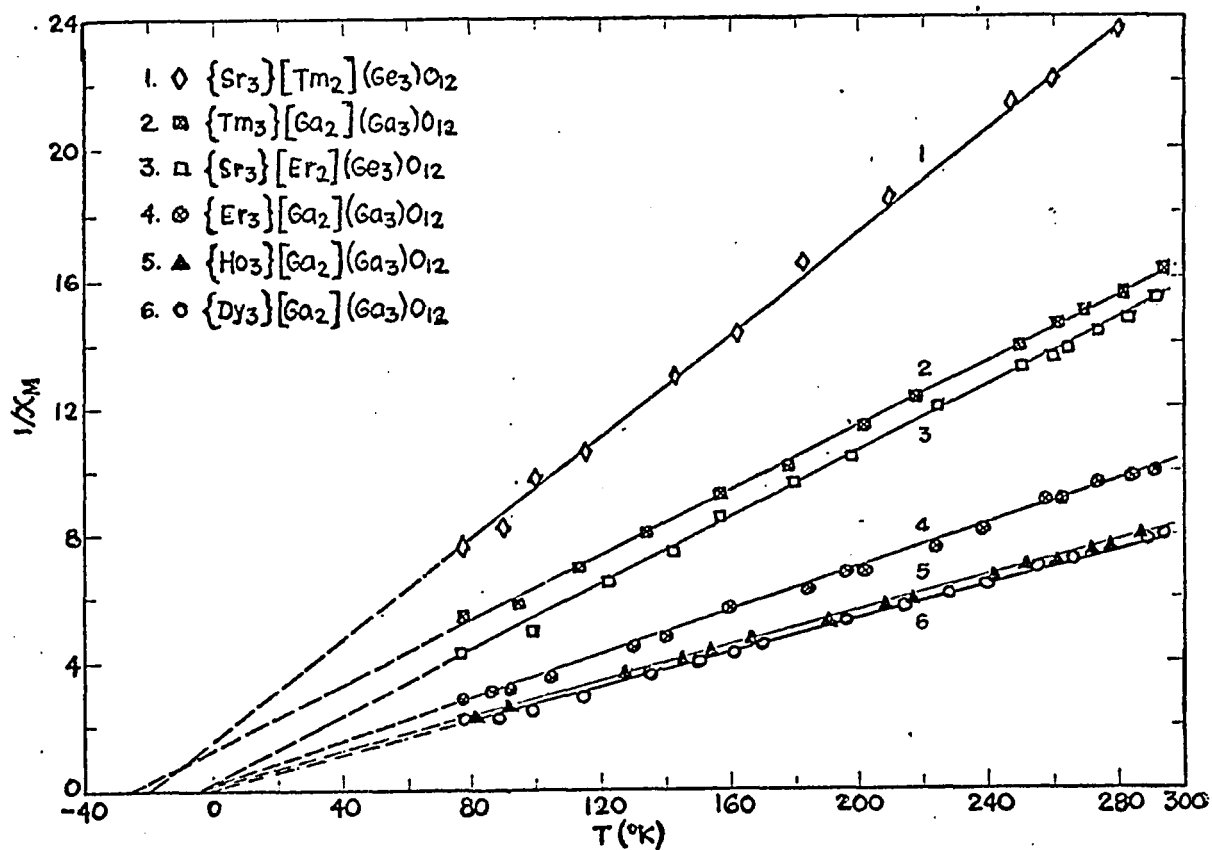
Before making magnetic measurements on the preparations with which this work deals, garnet compounds containing pertinent rare earth ions only on the octahedral sites (in germanates) and only on the dodecahedral sites (in gallates) were prepared and their magnetic susceptibilities measured at temperatures from 78°K to 300°K. The obtained data were put into the form of $\frac{1}{\chi_M}$ vs T plots, and Curie constants determined from the slopes of the resulting straight line portions. Molar Curie constants (C_M) were obtained, and the individual gram - atom Curie constants (C_M) for the rare earth ions were calculated from them. The magnetic properties of these compounds had been earlier reported in the literature (by Belov et al. (68)) but it was thought necessary to repeat the work with the same apparatus and under the same conditions employed for the measurements on new materials. The data are plotted in Figs. V 1 and V 2, where the compounds and solid solutions are grouped according to their magnetic susceptibilities rather than their composition. The materials are all paramagnetic and they obey the Curie - Weiss law, at least over the temperature range 78 - 300°K. The dashed line portions are extrapolated to $\frac{1}{\chi_M} = 0$ in order to indicate the magnitudes of the Weiss constants.

The molar Curie constants (C_M) obtained from 78 - 300°K portions of the plot are given in Table V 1 along with those calculated from theoretical values. Table V 2 gives the individual

gram - atom Curie constants (C_M) for the pertinent rare earth ions as calculated from experimental values in Table V 1 and from the theoretical magnetic moments given by Kern and Raccah (69).

The low experimental values found in this temperature range for C_M (Table V 1) and $C_{M(ind)}$ (Table V 2) were not unexpected. Values lower than theoretical were observed not only by Belov et al, (68) but also by Aleonard and Pauthenet (70) who measured the magnetic susceptibilities of rare earth gallium garnets with the rare earth only on the dodecahedral sites. The lower than theoretical values are attributed to partial quenching of the magnetic moment (70, 71). Experimental values which appear in Tables V 1 and V 2 are therefore consistent with the values in the literature. The data indicate little or no dependence on site in the cases of Tm^{3+} and Er^{3+} , but the difference appears to be significant for Yb^{3+} .

Reciprocal Molar Susceptibility vs Absolute Temperature for Garnet Compounds with Trivalent Rare Earth Ions on Either Dodecahedral or Octahedral Sites.



Reciprocal Molar Susceptibilities vs Absolute Temperature for Garnet Compounds and Solid Solutions with Trivalent Rare Earth Ions on either Dodecahedral or Octahedral Sites.

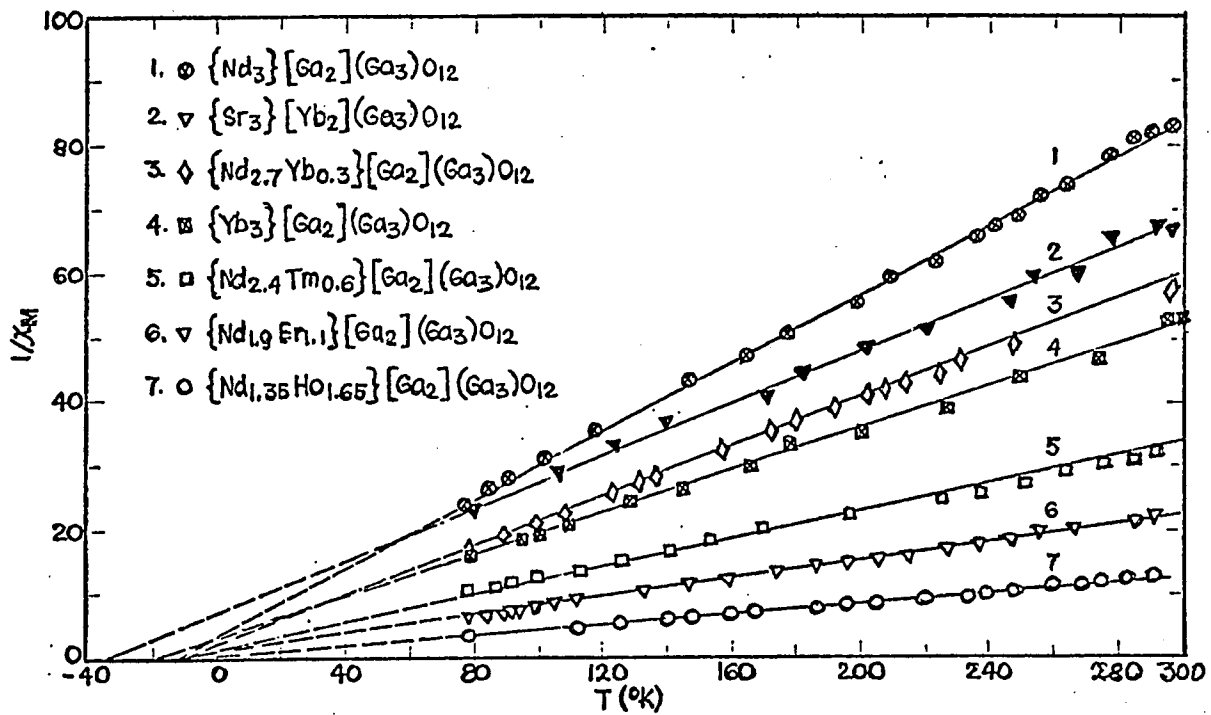


Table V 1 Experimental and Calculated Molar Curie Constants (C_M)
of Garnets with Trivalent Rare Earth Ions on Either
Dodecahedral or Octahedral Sites.

Compound	Experimental C_M	C_M Calculated From Theoretical Values *
$\{Sr_3\} [Yb_2] (Ge_3) O_{12}$	4.92	5.12
$\{Sr_3\} [Tm_2] (Ge_3) O_{12}$	12.64	12.18
$\{Sr_3\} [Er_2] (Ge_3) O_{12}$	19.24	22.76
$\{Yb_3\} [Ga_2] (Ga_3) O_{12}$	6.03	7.68
$\{Tm_3\} [Ga_2] (Ga_3) O_{12}$	19.74	21.27
$\{Er_3\} [Ga_2] (Ga_3) O_{12}$	29.41	34.14
$\{Ho_3\} [Ga_2] (Ga_3) O_{12}$	36.53	41.82
$\{Dy_3\} [Ga_2] (Ga_3) O_{12}$	37.91	42.18
$\{Nd_3\} [Ga_2] (Ga_3) O_{12}$	3.74	4.86
$\{Pr_3\} [Ga_2] (Ga_3) O_{12}$	4.72	4.77

* in column 3 of Table V 2.

Table V 2 Individual Gram - atom Curie Constants (C_{ind})

Ion	From Experimental C_M Values in Table V 1		Calculated from Theoretical Magn. Moments in Ref. (69)
	Dodecahedral Site	Octahedral Site	
Yb ³⁺	2.01	2.46	2.56
Tm ³⁺	6.58	6.32	7.09
Er ³⁺	9.80	9.62	11.38
Ho ³⁺	12.18	a	13.94
Dy ³⁺	12.64	a	14.06
Nd ³⁺	1.25	b	1.62
Pr ³⁺	1.57	b	1.59

a - We were unable to prepare single-phase Sr or Ca germanate garnets with these rare earth ions on the octahedral sites by solid state reaction of the oxides at 1350°C.

b - Nd³⁺ and Pr³⁺ do not enter the octahedral sites.

V .2 Measurements on Neodymium-Small Rare Earth Gallium Garnets.

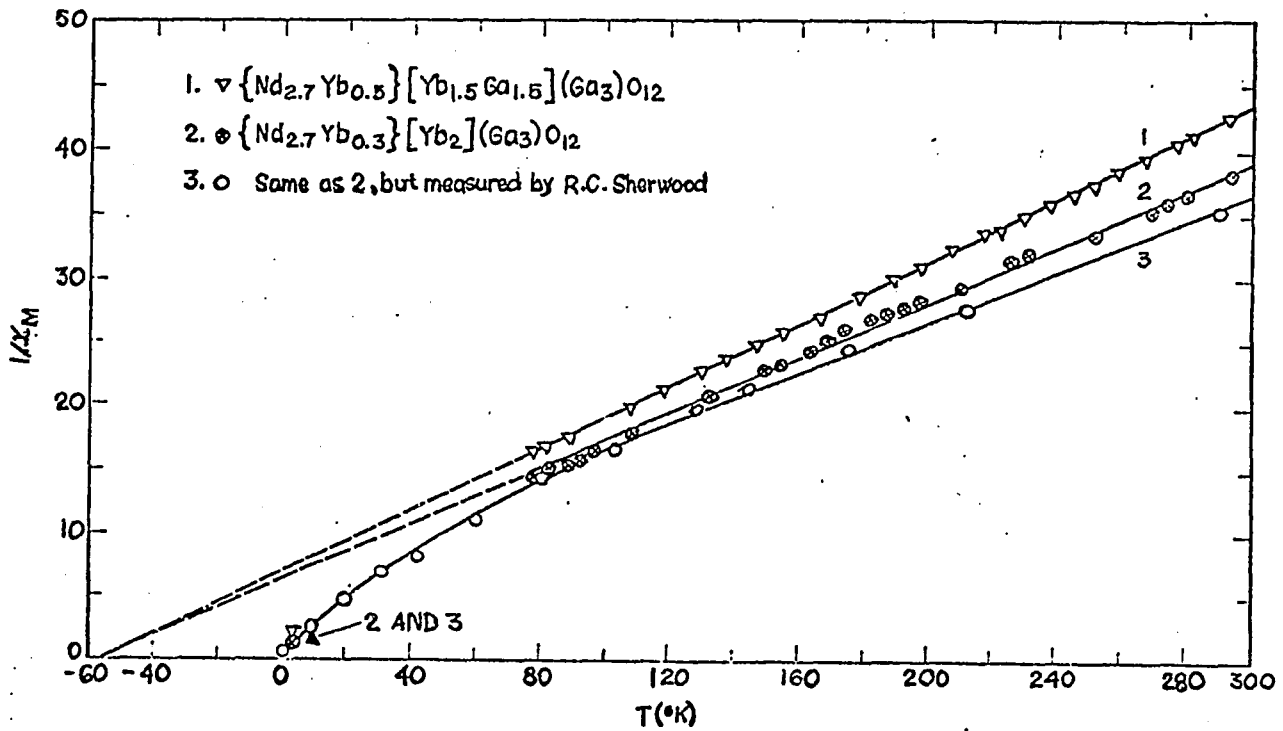
New materials of this type were subjected to measurements at temperatures from 78 - 300°K. Five of them, those with high concentration of rare earth ions on the octahedral sites, were also measured at 4.2°K with a vibrating sample magnetometer (field strength about 7.8KG) in the laboratory of Professor A. Wold at Brown University, Providence, R.I., and two samples were checked

at temperatures down to 1.6° K with a pendulum magnetometer (field strength 15.2 KG) in the laboratory of R.C. Sherwood at Bell Telephone Laboratories. The data were again put into the form of $\frac{1}{\chi_M}$ vs T plots and Curie constants, C_M , were determined. The magnetic data obtained from these measurements are given in Figs. V 3, V 4, and V 5. As can be seen from these figures, the Curie-Weiss law is observed, at least over the $78 - 300^{\circ}$ K range, and the dashed line portions are extrapolations to indicate the magnitudes of the Weiss constants.

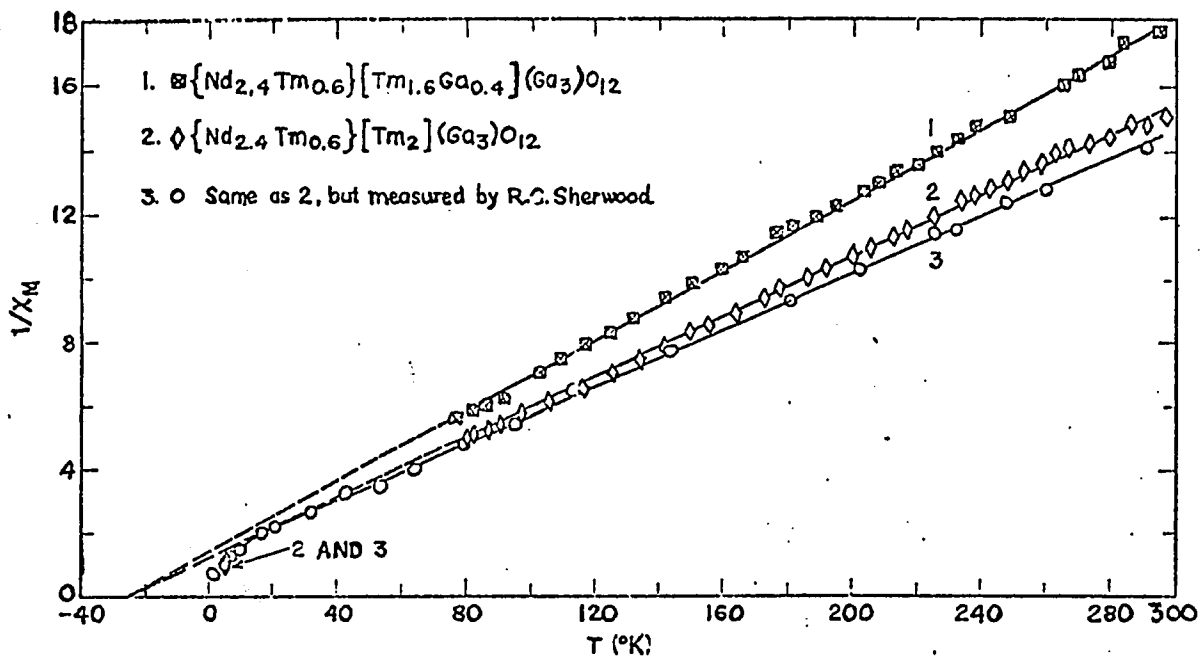
The 4.2° K points fall on these extrapolations in some cases but in other cases the graphs show changes in slopes downward toward the T axis. The experimental Curie constant values, those calculated from theoretical values, and those calculated primarily from experimental values for ions on the dodecahedral and octahedral sites are given in Table V 3.

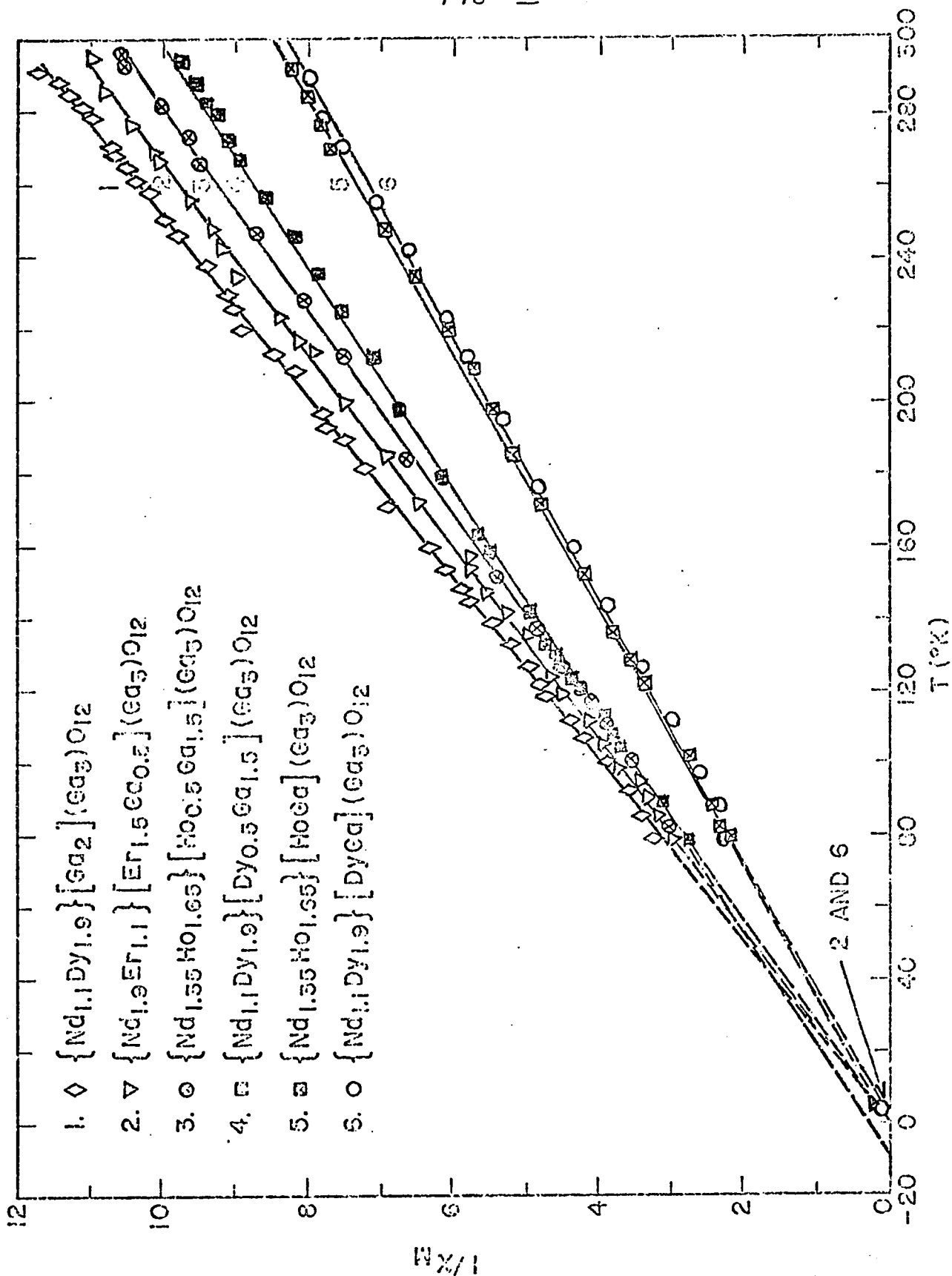
Inspecting Table V 3 and comparing experimental values of C_M with those calculated from experimental values for ions on one site only, a trend in quenching of paramagnetic moments can be seen. The presence of heavier small rare earth ions along with Nd seems to remove some or all of the quenching. This tendency decreases as the small rare earth ion becomes lighter and in the case of the lightest ion used, Dy, there is even a little more quenching than would be expected from the calculation from experimental values. It is difficult to be certain that this trend is real because the Curie constants measurements are reliable only to about 5%. In order to determine the extent of a change of quenching phenomenon, more detailed studies on a larger set of compounds would be required.

Reciprocal Molar Susceptibility vs Absolute Temperature for Garnets with Trivalent Rare Earth Ions on both Dodecahedral and Octahedral Sites (R = Yb).



Reciprocal Molar Susceptibility vs Absolute Temperature for Garnets with Trivalent Rare Earth Ions on Both Dodecahedral and Octahedral Sites (R = Tm).





Reciprocal Molar Susceptibility vs Absolute Temperature for Garnet with Trivalent Rare Earth Ions on Both Dodecahedral and Octahedral Sites (R = Er, Ho, Dy).

Table V 3 Experimental and Calculated Molar Curie Constants, C_M
of Garnets with Two Rare Earth Ions on Dodecahedral
Sites and Ga and/or Rare Earth Ions on Octahedral Sites.

Composition	C_M		
	Experimental	Calculated from Theoretical values (Column 3 in Table V 2)	Calculated from Calc. Values for ions on Dod. and Oct. Sites (Column 2 in Table V 2)
$\{Nd_{2.7} Yb_{0.3}\} [Ga_2] (Ga_3)_{0_{12}}$	5.18	5.14	3.98
$\{Nd_{2.7} Yb_{0.3}\} [Yb_{1.5} Ga_{0.5}] (Ga_3)_{0_{12}}$	8.19	8.98	7.67
$\{Nd_{2.7} Yb_{0.3}\} [Yb_2] (Ga_3)_{0_{12}}$	9.33, (10.0)*	10.3	8.90
$\{Nd_{2.4} Tm_{0.6}\} [Ga_2] (Ga_3)_{0_{12}}$	8.69	8.14	6.95
$\{Nd_{2.4} Tm_{0.6}\} [Tm_{1.6} Ga_{0.4}] (Ga_3)_{0_{12}}$	18.2	19.5	17.1
$\{Nd_{2.4} Tm_{0.6}\} [Tm_2] (Ga_3)_{0_{12}}$	21.2, (22.2)*	22.3	19.6
$\{Nd_{1.9} Er_{1.1}\} [Ga_2] (Ga_3)_{0_{12}}$	14.1	15.6	13.2
$\{Nd_{1.9} Er_{1.1}\} [Er_{1.5} Ga_{0.5}] (Ga_3)_{0_{12}}$	26.9	32.7	27.6
$\{Nd_{1.35} Ho_{1.65}\} [Ga_2] (Ga_3)_{0_{12}}$	23.4	25.2	21.8
$\{Nd_{1.35} Ho_{1.65}\} [Ho_{0.5} Ga_{1.5}] (Ga_3)_{0_{12}}$	28.1	32.2	28.0
$\{Nd_{1.35} Ho_{1.65}\} [Ho Ga] (Ga_3)_{0_{12}}$	35.0	39.1	34.2
$\{Nd_{1.1} Dy_{1.9}\} [Ga_2] (Ga_3)_{0_{12}}$	25.0	28.5	25.4
$\{Nd_{1.1} Dy_{1.9}\} [Dy_{0.5} Ga_{1.8}] (Ga_3)_{0_{12}}$	30.5	35.5	31.6
$\{Nd_{1.1} Dy_{1.9}\} [Dy Ga] (Ga_3)_{0_{12}}$	36.0	42.6	37.9

* Value obtained from measurements of R. C. Sherwood at Bell Telephone Laboratories.

From the graphs, no evidence was found of ferromagnetic, ferrimagnetic, or antiferromagnetic ordering. Ferromagnetism can be ruled out on the basis of the absence of positive Weiss constants. In the case of antiferromagnetism, $\frac{1}{\chi_M}$ should decrease with decreasing temperature above the Neel point and then rise again below the Neel point. In other words, the slope changes sign at the Neel temperature. Above the Neel temperature paramagnetic behavior is to be expected. In no case is such change of slope observed here.

Ferrimagnetism cannot be ruled out on the basis of these measurements because the $\frac{1}{\chi_M}$ value at 4.2°K might not be much lower in the case of ferrimagnetism than for paramagnetism, and downward changes of direction of the $\frac{1}{\chi_M}$ vs T curve were indicated by 4.2°K measurements. For this reason, measurements over the range 1.6°K were carried out on two compounds,

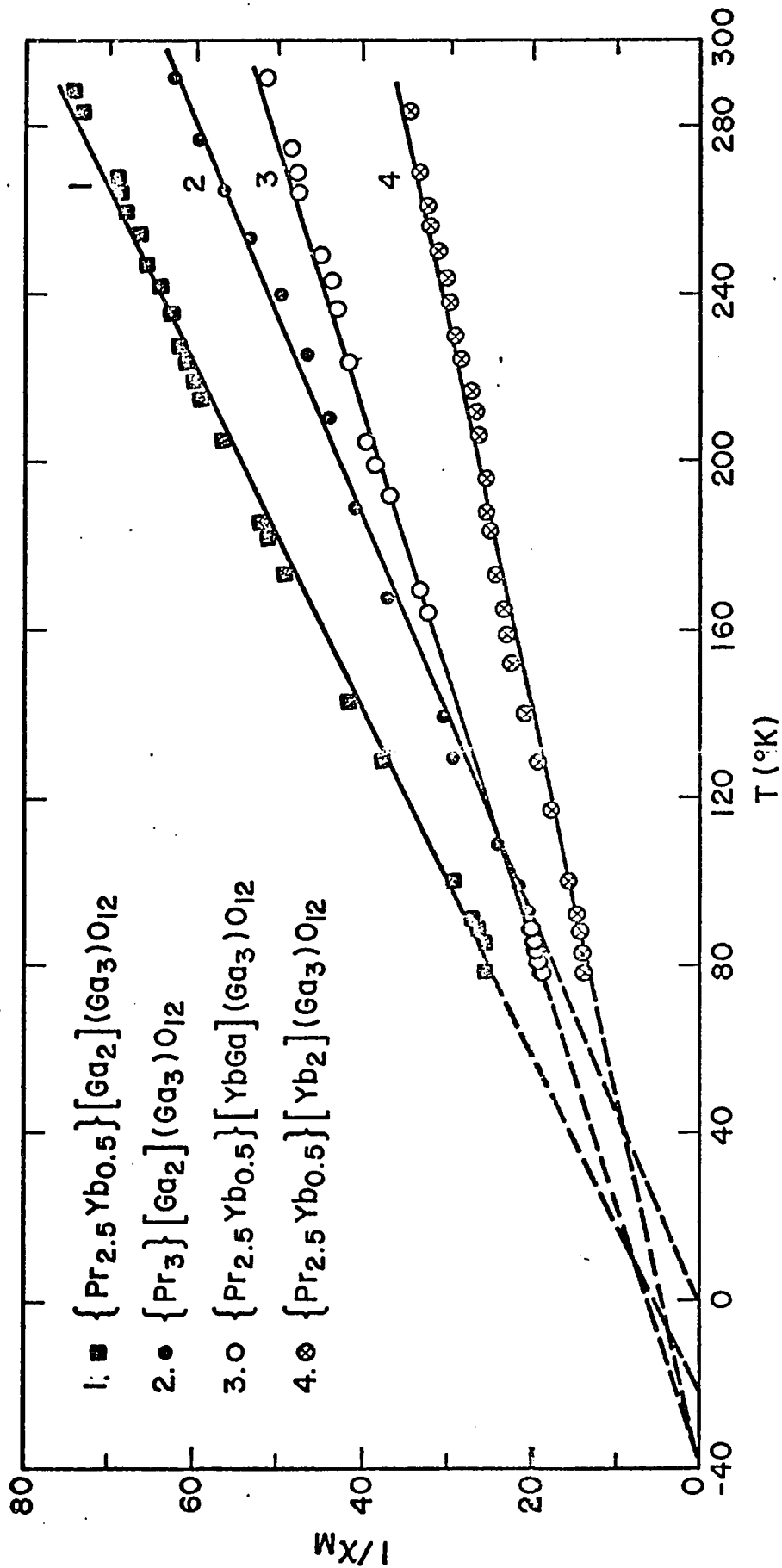
$\{\text{Nd}_{2.7} \text{ Yb}_{0.3}\} [\text{Yb}_2] (\text{Ga}_3)_{0.12}$ and $\{\text{Nd}_{2.4} \text{ Tm}_{0.6}\} [\text{Tm}_2] (\text{Ga}_3)_{0.12}$. These two measurements confirmed the departure from linearity of the $\frac{1}{\chi_M}$ vs T curve at low temperatures but they did not reveal any positive intercepts of these curves with the T axis. In addition, measurements of magnetic moment of several samples at 4.2°K as a function of decreasing field (over the range $7.8 - 0.0 \text{ KG}$) were made but no evidence was found for any magnetic remanance which one might expect if ferrimagnetic ordering exists in the compound. Neither did the two samples measured at 1.6°K show any sign of hysteresis on changing the applied magnetic field over the range $0.0 - 15.2 - 0.0 \text{ KG}$. However, all measurements were made in relatively weak magnetic fields, and repeating these measurements in stronger

fields of the order of 20 - 40 KG might be worth trying. From the above described results, it can be stated that no long-range ordering exists at temperatures over 1.6°K and under applied fields up to 15.2 KG in these compounds.

V 3 Measurements on Praseodymium Small Rare Earth Gallium Garnets.

The compounds which appear in Table V 4 were subjected to magnetic measurements at temperatures over the range $78 - 300^{\circ}\text{K}$. The magnetic data obtained were treated as in the case of neodymium compounds; that is, the molar Curie constants, C_M , were calculated from the slopes of the $\frac{1}{\chi_M}$ vs T curves and compared with values calculated from theoretical values and from experimental values (for ions on the octahedral and dodecahedral sites) of the individual gram - atom Curie constants C_{ind} . The magnetic data plotted in the form of $\frac{1}{\chi_M}$ vs T appear in Fig. V 6, V 7, and V 8. No 4.2°K or other low temperature (i.e. below 78°K) measurements were made on these compounds. From these plots, there is no evidence that would suggest ferrimagnetic, ferromagnetic, or antiferromagnetic ordering. Therefore, it can be stated that all these compounds are paramagnetic under the conditions at which the measurements were carried out. The paramagnetic C_M values obtained experimentally are in all cases closer to those calculated from values calculated for ions on the dodecahedral and octahedral sites than to theoretical values. In fact, they are lower than those calculated from experimental values, unlike the values for most of the corresponding Nd - small rarer earth garnets (72). This suggests that quenching in Pr garnet solid solutions is greater than in Nd garnet solid solutions. However,

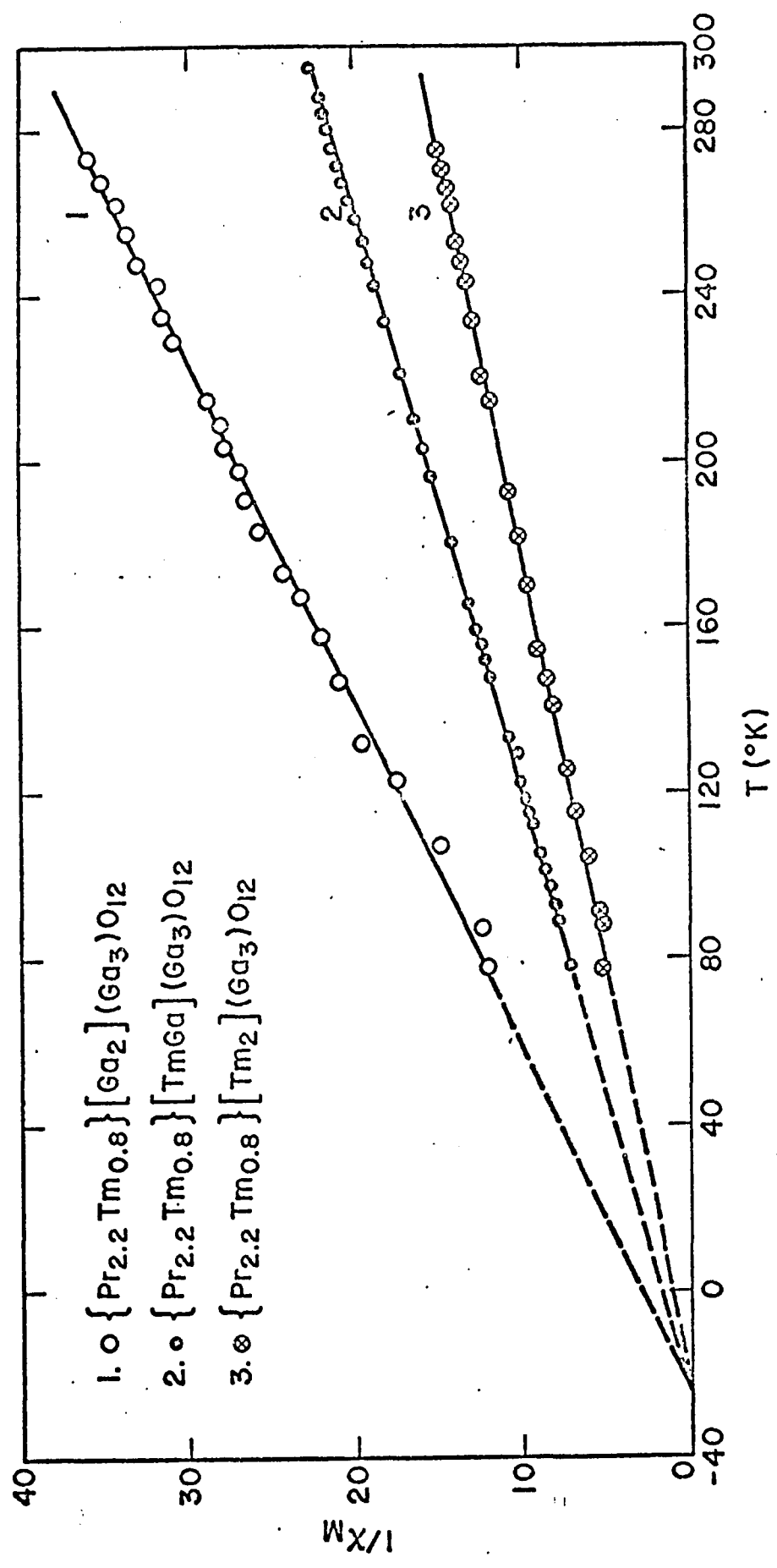
FIG. V-6



Reciprocal Molar Susceptibility vs Absolute Temperature for Garnet with Rare Earth Ions

on Both Sites with $r = Yb$.

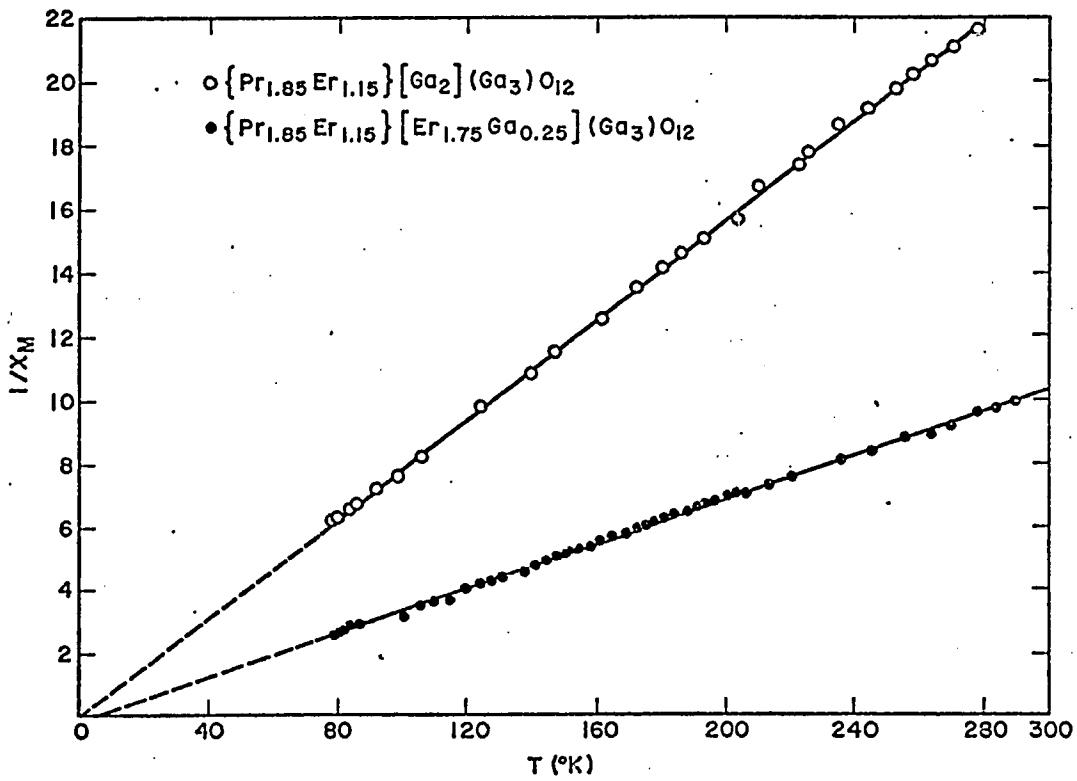
FIG. V-7



Reciprocal Molar Susceptibility vs Absolute Temperature for Garnet with Rare Earth

Ions on Both Sites with R = Tm.

Reciprocal Molar Susceptibility vs Absolute Temperature for Garnets with Rare Earth Ions on Both Dodecahedral and Octahedral Sites with R = Er.



there is a possibility that an oxidation - reduction process would yield small amounts of Pr^{4+} along with R^{2+} ions.

Such an oxidation - reduction process would be probable in the case where $\text{R} = \text{Yb}$. There is some optical evidence that small amounts of these ionic species are present when $\text{R} = \text{Yb}$, such as a change of color from yellowish green to tan in the case of $\left\{ \text{Pr}_{2.5} \text{Yb}_{0.5} \right\} \left[\text{Yb}_2 \right] (\text{Ga}_3)_{0.12}$ ($\text{Pr}_6 \text{O}_{11}$ is dark brown). Reflectance spectra have been measured by R. Mondegarian (73).

Table V 4 Experimental and Calculated Molar Curie Constants, C_M , of Pr - Small Rare Earth Garnet Solid Solutions.

Composition	C_M		
	Experimental	Theo - retical	Calculated from Experimental C_M values given in Table V 2 Column 2
$\left\{ \text{Pr}_{2.5} \text{Yb}_{0.5} \right\} \left[\text{Ga}_2 \right] (\text{Ga}_3)_{0.12}$	4.10	5.26	4.93
$\left\{ \text{Pr}_{2.5} \text{Yb}_{0.5} \right\} \left[\text{Yb Ga} \right] (\text{Ga}_3)_{0.12}$	6.23	7.82	7.39
$\left\{ \text{Pr}_{2.5} \text{Yb}_{0.5} \right\} \left[\text{Yb}_2 \right] (\text{Ga}_3)_{0.12}$	9.27	10.4	9.85
$\left\{ \text{Pr}_{2.2} \text{Tm}_{0.8} \right\} \left[\text{Ga}_2 \right] (\text{Ga}_3)_{0.12}$	8.28	9.17	8.72
$\left\{ \text{Pr}_{2.2} \text{Tm}_{0.8} \right\} \left[\text{Tm Ga} \right] (\text{Ga}_3)_{0.12}$	14.2	16.3	15.0
$\left\{ \text{Pr}_{2.2} \text{Tm}_{0.8} \right\} \left[\text{Tm}_2 \right] (\text{Ga}_3)_{0.12}$	19.4	23.4	21.4
$\left\{ \text{Pr}_{1.85} \text{Er}_{1.15} \right\} \left[\text{Ga}_2 \right] (\text{Ga}_3)_{0.12}$	12.8	16.0	14.2
$\left\{ \text{Pr}_{1.85} \text{Er}_{1.15} \right\} \left[\text{Er}_{1.75} \text{Ga}_{.25} \right] (\text{Ga}_3)_{0.12}$	28.6	35.9	31.0

V.4 Magnetic Measurements on Iron - Containing Garnets.

V.4.1 Magnetic Behavior of the Compounds $\{R_{3-y} Sc_y\} [Sc_2] (Fe_3) O_{12}$. The R in these systems corresponds to Gd, Dy, Ho, Er, and Tm. The compounds containing rare earth on the dodecahedral sites and iron on the tetrahedral sites while the octahedral sites are occupied by nonmagnetic ions should behave, according to the model of magnetic interactions and the results obtained from measurements on $R_3 Fe_5 O_{12}$ garnets, as ferrimagnets provided that interactions are strong enough. Fig. V 9 shows the results of susceptibility measurements over the range of temperatures 78 - 300°K. In the case of $\{Gd_{2.5} Sc_{.5}\} [Sc_2] (Fe_3) O_{12}$, the plot of $\frac{1}{\chi_M}$ vs T shows only paramagnetic behavior giving $C_M = 26.3$ compared with the theoretical value for $C_M = 30.8$. The difference can be attributed to quenching of paramagnetic moment as in preceding cases.

Different behavior is indicated by plots of $\frac{1}{\chi_M}$ vs T for the compounds containing Dy, Ho, Er, and Tm on the dodecahedral sites. The $\frac{1}{\chi_M}$ vs T plots are not straight lines as they should be for the case of paramagnetism, and also the values of $\frac{1}{\chi_M}$ at low temperatures are smaller than they should be in the case of paramagnetism, indicating greater than paramagnetic moments. Also plot of molar susceptibilities vs T in Fig. V 10 shows that χ_M is considerably greater than in the case of paramagnetism and increases along the Rare Earth serie as it goes to heavier rare earth elements involved. The magnetic data over the temperature range 78 - 300°K are not sufficient to draw any definite conclusions about the type of

magnetic behavior. The only conclusion about the type of magnetic behavior. The only conclusion which can be stated is that these compounds do not behave paramagnetically, and additional detailed magnetic studies would be required.

V.4.2 Magnetic Measurements on System $\{R_3\}[Sc_2](Ga_{3-z}Fe_z)O_{12}$.

R in these systems stands for Nd^{3+} or Pr^{3+} ions. According to the model of magnetic interactions in the garnet structure, net moments of Nd or Pr on the dodecahedral sites should be aligned parallel to the magnetic moment of the tetrahedral sublattice, thus resulting in ferromagnetism. Magnetic data over the range 78 - 300°K for several compounds are shown in Fig. V 1. The dashed portion of curves $\frac{1}{\chi_M}$ vs T are extrapolations to the temperature axis in order to determine Weiss constants. As these plots indicate, the intercepts of $\frac{1}{\chi_M}$ vs T are positive on the temperature axis. The positive Weiss constants can perhaps indicate ferromagnetic interactions below these temperatures, but the dashed portions should be confirmed by low temperature measurements. Table V 4 contains experimental molar Curie constants, C_M , and Weiss constants obtained by extrapolation.

Reciprocal Susceptibility vs Temperature for Garnets of the Type

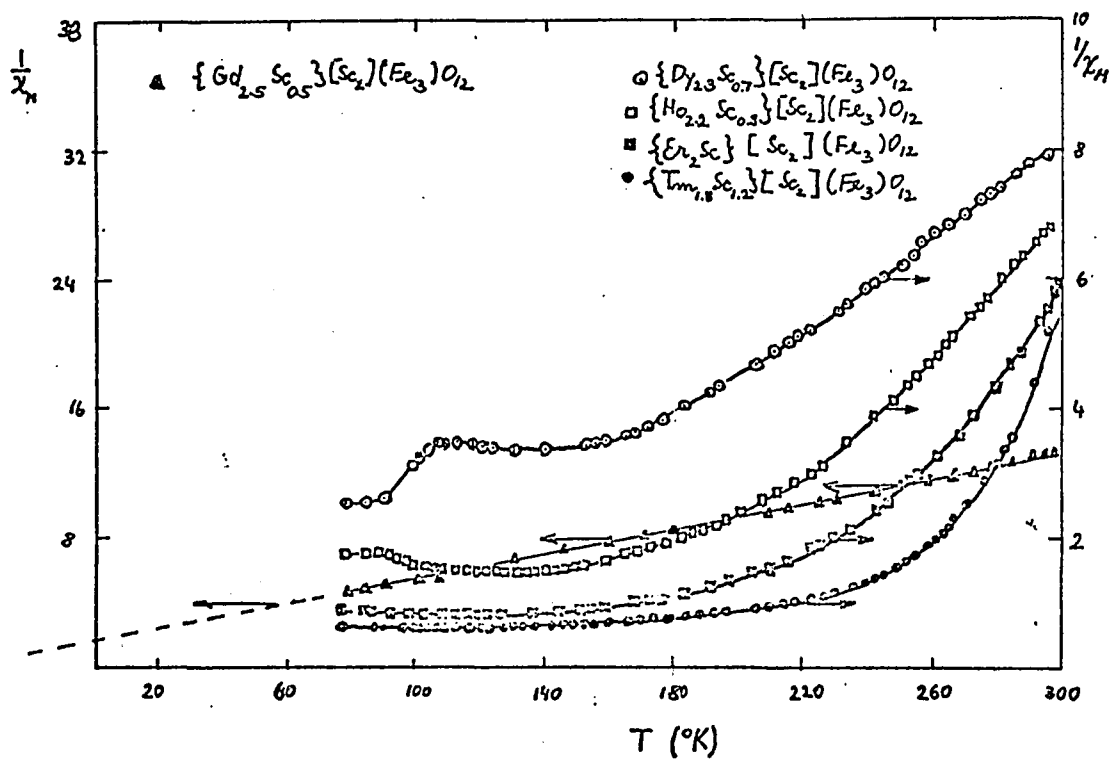
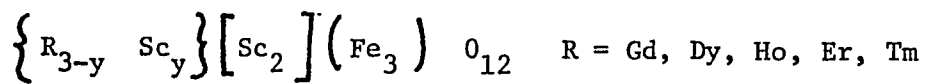


FIG. V-10.

Molar susceptibility χ_M vs absolute temperature T for garnets of the type $\{R_{3-y} Sc_y\} [Sc_2] (Fe_3) O_{12}$ R = Gd, Dy, Ho, Er, Tm

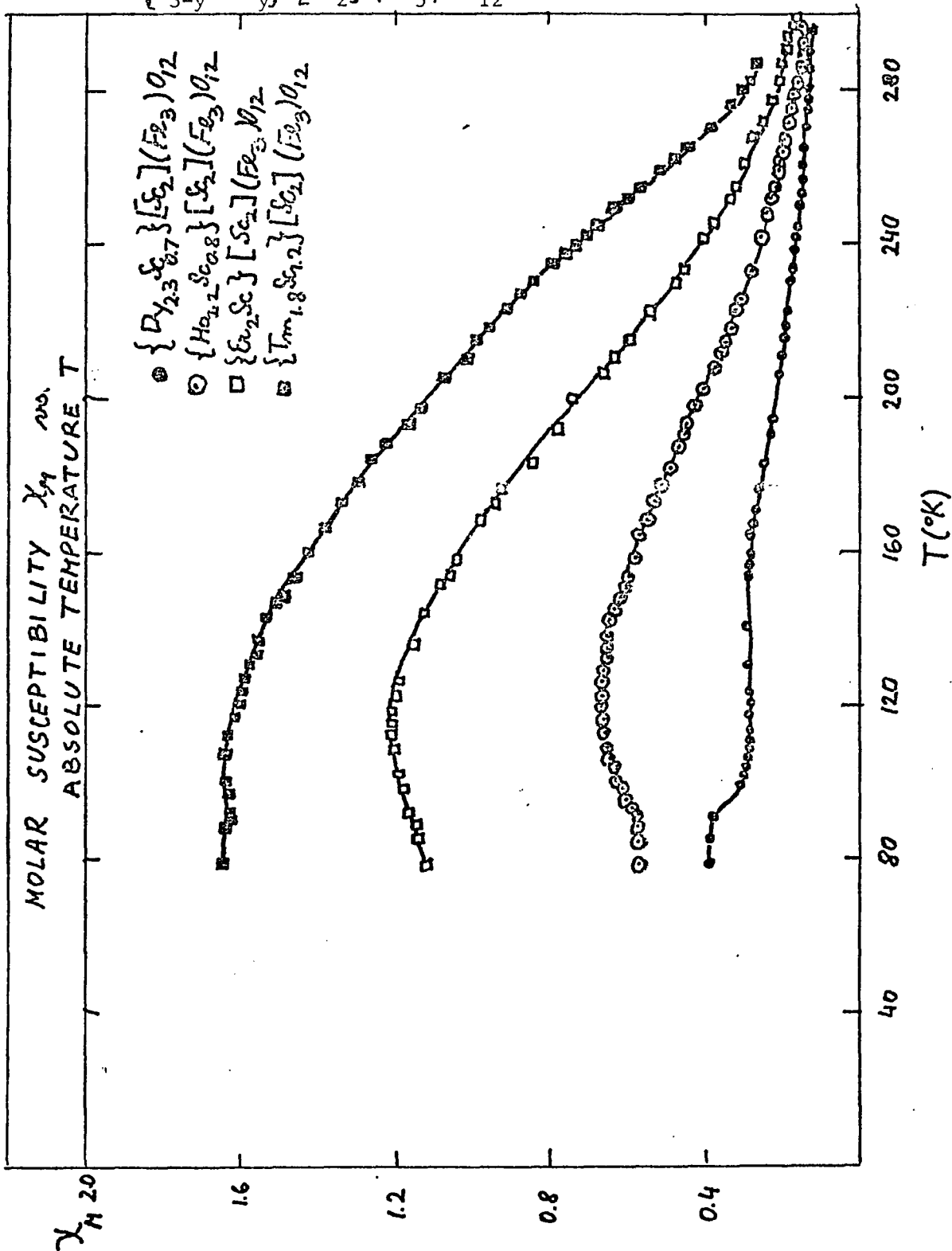


Table V 5 Experimental and Theoretical Curie Constants and Weiss
Constants Obtained by Extrapolation of $\frac{1}{\chi}$.

Composition					C_M Exp.	C_M Theor.	Extrapolated Weiss Constant
Nd ₂	Sc ₂	Fe _{2.2}	Ga _{.8}	O ₁₂	11.6	13.2	32°K
Pr ₃	Sc ₂	Fe _{1.5}	Ga _{1.5}	O ₁₂	8.4	10.39	6°K
Pr ₃	Sc ₂	Fe _{1.6}	Ga _{1.4}	O ₁₂	9.7	10.77	8°K
Pr ₃	Sc ₂	Fe _{1.8}	Ga _{1.2}	O ₁₂	9.1	11.52	18°K

V.4.3 Magnetic Measurements on Garnets $\left\{ \begin{matrix} \text{Nd}_{3-y} & \text{Yb}_y \end{matrix} \right\} \left[\text{Yb}_2 \right]$
 $\left(\text{Ga}_{3-z} \text{Fe}_z \right) \text{O}_{12}$. Magnetic data obtained from measurements over the temperature range 78 - 300°K of various compositions of this system were treated as in the preceding cases, i.e. plotted in the form $\frac{1}{\chi_M}$ vs T, and molar Curie constants were determined from the slopes of these curves. Also, extrpolations were made in order to determine the values of Weiss constants.

Magnetic data for three compounds of this system appear in Fig. V 12. Experimental values of molar Curie constants compared with theoretical values and Weiss constants obtained by extrapolation are given in Table V 5.

FIG. V-11

Reciprocal Molar Susceptibilities vs Absolute Temperature for

Garnets $\{R_3\}[Sc_2](Ga_{3-z}Fe_z)O_{12}$ where R = Nd, Pr

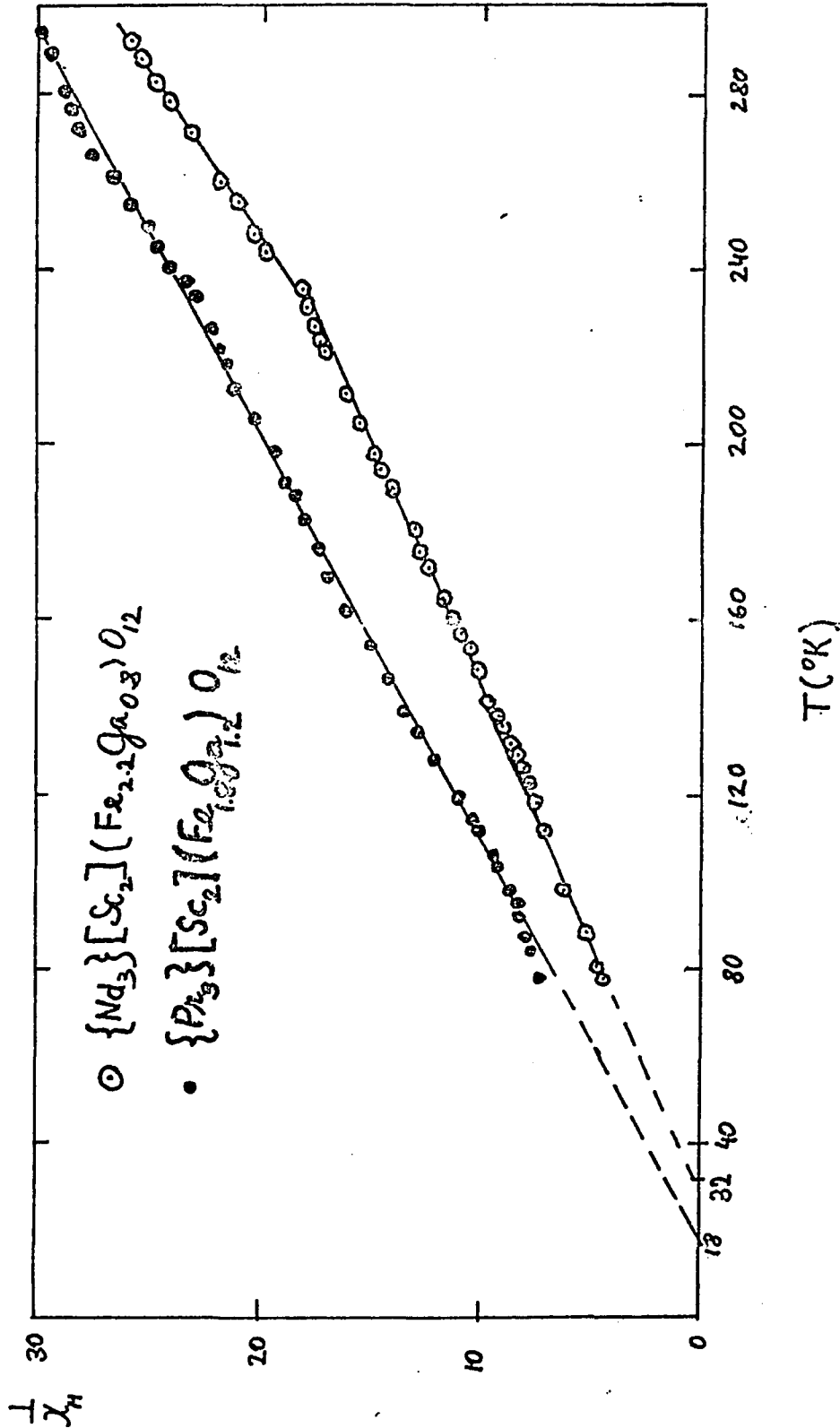
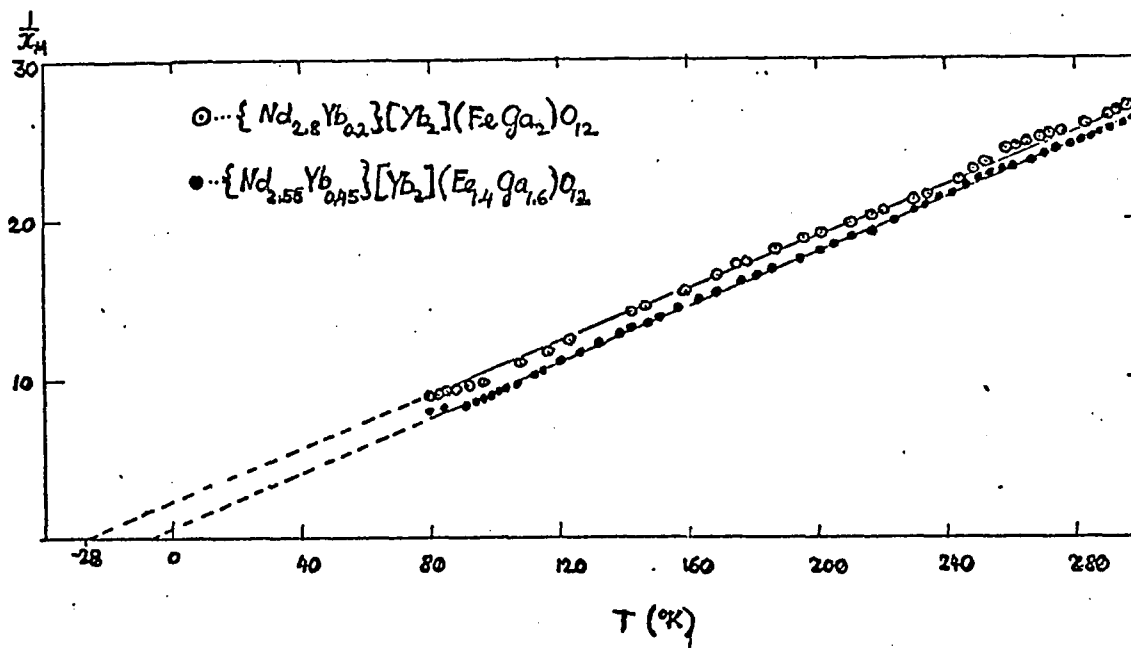
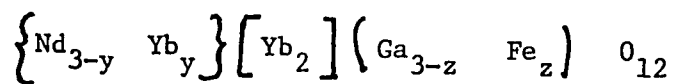


Table V 6 Experimental and Theoretical C_M and Weiss Constants for Garnet Compounds, $\left\{ \text{Nd}_{3-y} \text{ Yb}_y \right\} \left[\text{Yb}_2 \right] \left(\text{Ga}_{3-z} \text{ Fe}_z \right) \text{O}_{12}$.

Composition		Weiss Constant		
y	z	C_M Exp.	C_M Theor.	(by Extrapol.)
0.2	1.0	12.0	13.92	- 28° K
0.35	1.3	12.31	15.18	- 22° K
0.45	1.4	11.43	15.65	- 6° K

As magnetic data show these compounds appear to be paramagnetic over the temperature range 78 - 300°K displaying also a considerable quenching of paramagnetic moments. However, from the high concentration of magnetic ions, one might expect long range ordering at least at low temperatures.

Reciprocal Susceptibility vs Absolute Temperature for Garnets



VI. CRITICAL EVALUATIONS AND RECOMMENDATIONS

VI.1 Compounds with Rare Earth Ions on Both Dodecahedral and Octahedral Sites.

Attempts to prepare garnet compounds with rare earth ions on two crystallographic sites (dodecahedral and octahedral) were successful. The assumption that the presence of a large rare earth ion on the dodecahedral site "opens" the crystal structure so that the smaller rare earth ion may enter the octahedral site was confirmed by these studies. Several facts which might be considered as contributions to the crystal chemistry of garnets were discovered during the course of this investigation.

First of all, rather important is the fact that the smaller ion also simultaneously enters the dodecahedral site to a certain extent when being substituted in the octahedral site. Secondly, it was found that there does not exist one "maximum average ionic radius" on the dodecahedral site, but the average ionic radius on the dodecahedral site depends on the composition of the garnet and is decreased when a larger ion is substituted on the octahedral site. Experimental data also suggest the existence of a maximum lattice constant for a given system, such as $\left\{ \text{Nd}_{3-y} \text{ R}_y \right\} \left[\text{R}_x \text{ Ga}_{2-x} \right] (\text{Ga}_3)$ O_{12} . It was found that values of such maximum lattice constants are different for different systems. When Pr is used instead of Nd, the value of the maximum lattice constant was found to be larger.

The studies of magnetic properties of these compounds revealed only paramagnetic behavior. An attempt to grow single crystals

with composition suggested by the present work would be most desirable for further work.

VI. 2 Compounds with Nonmagnetic Ions on Octahedral Sites.

Attempts to prepare garnets with rare earth ions on the dodecahedral sites, iron on the tetrahedral sites, and nonmagnetic ions on the octahedral sites were successful. A number of compounds of this type was prepared. The idea of simultaneous placement of small ions on both sites (dodecahedral and octahedral) proved to be successful in yielding single-phase compounds in many cases. However, it would be desirable to study these systems in more detail in order to determine the conditions of their existence (e.g. the ranges of composition).

The preliminary studies of magnetic behavior of these compounds showed that many of them were more than just paramagnetic. Further more detailed magnetic studies at low temperature might reveal interesting results. There is no doubt that these compounds show signs of long-range magnetic order. However, the determination of the nature of magnetic interaction is beyond the limits of the present equipment employed for magnetic studies described earlier.

VI. 3 Garnet Compounds with Rare Earth on Dodecahedral and Octahedral Sites and with Iron on the Tetrahedral Site.

A representative of this group was prepared. As was said earlier, the role of rare earth ions occupying octahedral sites in garnets has not previously been studied for ferrimagnetic interaction.

The prepared material, $\left\{ \text{Nd}_{2.55} \text{ Yb}_{0.45} \right\} \left[\text{Yb}_2 \right] \left(\text{Fe}_{1.4} \text{ Ga}_{1.6} \right) \text{O}_{12}$,

probably contains enough iron on the tetrahedral site to yield at least weak interactions. However, no signs of such interactions were found in preliminary measurements. Therefore, it is believed that magnetic measurements at low temperatures (4.2°K) might uncover such interactions.

Also, a preparation of other compounds of this type containing Pr, Tm, and probably Er, followed by detailed magnetic measurements could contribute to the task of finding the role of octahedrally coordinated rare earth ions on ferrimagnetic interactions of garnets.

REFERENCES

- (1) International Tables for X-ray Crystallography, Kynoch Press, Birmingham, 1952.
- (2) E. F. Bertaut, R. Nathouse, S.J. Pichart, G. T. Rado, Magnetism, III. Acad. Press, New York. London, 1963.
- (3) A. I. Shubnikov, Symmetria i Antisymmetria Konecnych Figure, Science Academy USSR Press, Moscow, 1951.
- (4) S. Krupicka, Physics of Ferrites and Related Magnetic Oxides, Academia, Czech Academy of Science Press, Prague, 1969
- (5) G. Menzer, Centralbl. Min. A 1925, 344 - 345; Z. Kristallogr. 63, 157 -158, 1926.
- (6) G. Menzer, Z. Kristallogr. 69, 300 - 396, 1928.
- (7) L. Neel, Annales Physique, Paris 3, 137 - 198, 1948.
- (8) S. Geller, Z. Kristallogr. 125, 1 - 6, 1967.
- (9) S. Geller, H. J. Williams, G. P. Espinosa, R. C. Sherwood, Bell System Technical Journal, Vol. 43, 565 - 623, 1964.
- (10) S. Geller, J. Appl. Phys., Vol. 31, 305 - 375, 1960.
- (11) F. Bertaut et F. Forrat, C. R. Acad. Science Paris, 243, 392 - 384, 1956.
- (12) S. Geller and M. A. Gilleo, Acta Crystallogr. 10, 239. 1957.
- (13) J. E. Geusic, H. M. Marcos and L. G. Van Wiertert, Appl. Phys. Letters 4 , 182 - 184, 1964.
- (14) B. Cockayne, D. B. Gasson, D. Findlay, D. W. Goodwin and R. A. Clay, J. Phys. Chem. Solids 29, 905, 1968.
- (15) M. Kestigian and W. W. Holloway Jr., J. Crystal Growth 3, 4, 455, 1968.
- (16) Proc. of 19th Conference on Magnetism and Magnetic Materials, Chicago in Press, 1972.
- (17) S. C. Abrahams and S. Geller, Acta Cryst. 11. 437 - 441, 1958.

REFERENCES (Continued)

- (18) A. Zemann and J. Zemann, Acta Cryst. 14., 835 - 837, 1961.
- (19) G. V. Gibbs and J. V. Smith, Amer. Mineral. 50., 2023 - 2039, 1965.
- (20) F. Euler and J. A. Bruce, Acta Cryst. 19., 971 - 978, 1965.
- (21) W. Prandl, Z. Kristallogr. 123., 81 - 116, 1966.
- (22) L. Coes, J. Amer. Ceram. Soc. 38., 298, 1955.
- (23) B. J. Skinner, Amer. Mineral 41., 428 - 436, 1956.
- (24) B. V. Mill, Dokl. Akad. Nauk USSR, 156., 814 - 816, 1964.
- (25) R. G. Strens, Amer. Mineral. 50., 260, 1965.
- (26) H. E. Swanson, M.I. Cook, E.H. Evans and J. H. de Groot, Standard X-ray Diffraction Patterns, NBS Circular 539, Vol. 10, 17 - 18, 1960.
- (27) H.E. Swanson, M.I. Cook, t. Isaacs and E.H. Evans, NBS Circular 539, Vol. 9, 22 - 23, 1960.
- (28) B.V. Mill, Zhur. Neorg. Khim., 1533 -1538, 1966.
- (29) S. Geller and C. E. Miller, Amer. Mineral. 44., 1115 - 1120, 1959.
- (30) S. Geller and E.C. Miller, Amer. Mineral. 44., 665 - 667, 1959.
- (31) J. A. Kohn and D.W. Eckart, Amer. Mineral. 47., 1422 - 1230, 1962.
- (32) A. L. Gentile and R. Roy, Amer. Mineral. 45., 701 - 711, 1960.
- (33) S. Geller and C. E. Miller, Amer. Mineral. 44., 445 - 446, 1959.
- (34) B. V. Mill, Dokl. Akad. Nauk USSR 165, 555 - 558, 1965.
- (35) S. Geller, C. E. Miller and R. G. Treuting, Acta Cryst. 13., 179 - 186, 1960.

REFERENCES (Continued)

- (36) A. Tauber, C. G. Whineray and E. Banks, J. Phys. Chem. Solids 21., 25 - 32, 1961.
- (37) A. Tauber, E. Banks and H. Kedesdy, Acta Crystallogr. 11., 893 - 894, 1958.
- (38) B. V. Mill, Zhur. Strukt. Khim. 6., 471 - 473, 1965.
- (39) H. S. Yoder and M. L. Keith, Amer. Mineral 36., 519 - 533, 1951.
- (40) M. L. Keith and R. Roy, Amer. Mineral 39., 1 - 23, 1954.
- (41) S. J. Schneider, R. S. Roth and J. L. Waring, J. Res. Nat. Bur. Standarts, 65 A., 345 - 371, 1961.
- (42) F. Bertaut and F. Forrat, Compt. Rend. Acad. Sci. (Paris) 243, 1219 - 1222, 1956.
- (43) M. A. Gilleo and S. Geller, Phys. Rev. 10., 73 - 78, 1958.
- (44) C. B. Rubenstein and R. L. Barns, Amer. Mineral 50., 782 - 785, 1965.
- (45) C. B. Rubenstein and R. L. Barns, Amer. Mineral 49., 1489 - 1490, 1964.
- (46) F. Bertaut and F. Forrat, Compt. Rend. Acad. Sci. (Paris) 244., 96 - 99, 1957.
- (47) G. P. Espinosa, J. Chem. Phys. 37., 2344 - 2347, 1962.
- (48) S. Geller, H. J. Williams and R. C. Sherwood, Phys. Rev. 123., 1692 - 1699, 1961.
- (49) S. Geller and D. W. Mitchell, Acta Crystallogr. 12., 936, 1959.
- (50) G. P. Espinosa, Inorg. Chem. 3, 848 - 850, 1964.
- (51) H. A. Kramers, Physica 1., 182, 1934.
- (52) M. A. Gilleo, J. Phys. Chem. Solids 13., 33, 1960.
- (53) Y. Yafet and L. C. Kittel, Phys. Rev. 87., 290, 1952.
- (54) P. W. Anderson, Phys. Rev. 79., 350, 1950.
- (55) P. W. Anderson, Phys. Rev. 115., 2, 1959.

REFERENCES (Continued)

- (56) R. M. Bozorth and S. Geller, J. Phys. Chem. Solids 11., 263, 1959.
- (57) A. Tauber, E. Banks and H. Kedesdy, J. Appl. Phys. 29., 385, 1958.
- (58) M. D. Lind, S. Geller, Z. Kristall. 129., 427 - 434, 1969.
- (59) M. A. Gilleo and S. Geller, J. Phys. Chem. Solids 10., 187, 1959.
- (60) S. Geller, H. J. Williams, R. C. Sherwood and G. P. Espinosa, J. Appl. Phys. 36, 87, 1963.
- (61) Summary of such Work may be Found in "Experimental Magnetochemistry" by M. M. Schieber, Published by North Holland Publishing Co., Amsterdam, 1967.
- (62) B. N. Figgis, and R. S. Nyholm, J. Chem. Soc. London, 4190, 1958.
- (63) L. Suchow, A. Ando, J. Solid State Chemistry 2, 156 - 159, 1970., Also A Ando, Master's Thesis, NCE, 1969.
- (64) R. D. Shannon and C. T. Prewitt, Acta Cryst. B25, Part 5, 925 - 946, 1969, Acta Cryst. B26, Part 7, 1046 - 8, 1970.
- (65) J. Loriers, G. Villers, F. Clerc and F. Lacour, C.R. Acad. Sc. Paris, 268., 1553 - 1556, 1969.
- (66) J. Loriers, M. Vichr and H. Makram, J. Cryst. Growth 8., 69 - 72, 1971.
- (67) L. Suchow, M. Kokta and V. J. Flynn, J. Solid State Chem. 2., 137 - 143, 1970.
- (68) K. P. Below, B. V. Mill, V. I. Sokolov and Than Dyk Chien, Fiz. Metal Metalloved, 27., 4, 610, 1969.
- (69) S. Kern and P. M. Raccah, J. Phys. Chem. Solids 26., 1625 - 1628 1965.
- (70) R. Aleonard and R. Pauthenet, Comptes Rendus des Seances, Academie des Sciences 255., 2727 - 2729, 1962.
- (71) R. Pauthenet, Le Journal de Physique et Le Radium 20., 388 - 392, 1959.

REFERENCES (Continued)

- (72) L. Suchow and M. Kokta, J. Solid State Chem. in press.
- (73) R. Mondegarian, Master's Thesis, NCE, June 1972.
- (74) Schieber, M., and L. Holmes, J. Appl. Phys. 36., 1159, 1965.
- (75) Nat. Bur. Standards (V.S.) Mono, 25, Sec. 1, 1961.

VITA

Name MILAN KOKTA

Education: CHEMISTRY INDUSTRIAL HIGH SCHOOL

1955-1959, Pardubice, Czechoslovakia

Date of graduation: June, 1959

ENGINEER OF CHEMISTRY (equivalent to M.S.)

1962-1968, Institute of Chemical Technology

and Chemistry, Pardubice, Czechoslovakia

Master Thesis:

" PURIFICATION OF CHEMICAL COMPOUNDS

BY MEANS OF CRYSTALLIZATION

FROM MOLTEN PHASE "

Date of graduation: June, 1968